Identification of Block Cascade Models Of Nonlinear Systems

by

Jameel Hasan Talaq

A Thesis Presented to the

FACULTY OF THE COLLEGE OF GRADUATE STUDIES

KING FAHD UNIVERSITY OF PETROLEUM & MINERALS

DHAHRAN, SAUDI ARABIA

In Partial Fulfillment of the
Requirements for the Degree of

MASTER OF SCIENCE

In

MECHANICAL ENGINEERING

June, 1994

Order Number 1360410

Identification of block cascade models of nonlinear systems

Talaq, Jaleel Hasan, M.S.

King Fahd University of Petroleum and Minerals (Saudi Arabia), 1994

U·M·I
300 N. Zeeb Rd.
Ann Arbor, MI 48106

IDENTIFICATION OF BLOCK CASCADE MODELS OF NONLINEAR SYSTEMS

BY

JALEEL HASAN TALAQ

A Thesis Presented to the
FACULTY OF THE COLLAGE OF GRADUATE STUDIES

KING FAHD UNIVERSITY OF PETROLEUM & MINERALS
DHAHRAN, SAUDI ARABIA

In Partial Fulfillment of the
Requirements for the Degree of

MASTER OF SCIENCE
In

MECHANICAL ENGINEERING

JUNE, 1994

KING FAHD UNIVERSITY OF PETROLEUM & MINERALS
DHAHRAN, SAUDI ARABIA

COLLAGE OF GRADUATE STUDIES

This thesis, written by ***JALEEL HASAN TALAQ*** under the direction of his thesis Advisor and approved by his thesis committee, has been presented to and accepted by the Dean of Collage of Graduate Studies, in partial fulfillment of the requirements for the degree of ***MASTER OF SCIENCE in MECHANICAL ENGINEERING.***

THESIS COMMITTEE

11/6/1994
Dr. Kamal A.F. Moustafa

11/6/94
Dr. Hosam E. Emara-Shabaik

11/6/94
Dr. Yehia Khulief

15/6/94
Dr. Ahmed, M.S.

Department Chairman

15.6.94
Dean, Collage of Graduate Studies

IN THE NAME OF GOD, THE MOST GRACIOUS AND MERCIFUL

To My Father and Mother

To My Wife, FATIMA

and

My Family

With Love

ACKNOWLEDGMENTS

My grateful thanks are for my advisor Dr. Kamal Moustafa and my co-advisor Dr. Hosam Shabaik for all their supervision and guidance. Also I would like to thank my examining committees for their helpful comments.

TABLE OF CONTENTS

GLOSSARY OF SYMBOLS

$E[\ ]$	Expected value of $[\ ]$
ω	Angular frequency (rad/s)
$F.T.[\ ]$	Fourier transform of $[\ ]$
$G_{xx}(\omega)$	Autospectral density function (one-sided)
$G_{xy}(\omega)$	Cross-spectral density function (one-sided)
$h(\tau)$	Linear weighting function (Impulse response)
$H(\omega)$	Linear frequency response function (Transfer function)
$H_o(\omega)$	Optimum linear frequency response function
$p(x)$	Probability density function
$R_{xx}(\tau)$	Autocorrelation function
$R_{xy}(\tau)$	Cross-correlation function
$S_{xx}(\omega)$	Autospectral density function (two-sided)
$S_{xy}(\omega)$	Cross-spectral density function (two-sided)
$P(\omega)$	Power spectrum
$B_y(\omega_1,\omega_2)$	Bispectrum
$b_y(\omega_1,\omega_2)$	Bicoherence function
t	Time variable
T	Record length
$x(t), y(t)$	Time-dependent real-valued records
$X(\omega), Y(\omega)$	Fourier transforms of $x(t), y(t)$
$\lvert[\ ]\rvert$	Absolute value of
$\delta()$	Delta function
μ	Mean value
σ	Standard deviation
σ^2	Variance
τ	Time shift
$\phi(\omega)$	System phase factor

LIST OF EXAMPLES

LIST OF FIGURES

ABSTRACT

NAME OF STUDENT : JALEEL HASAN TALAQ

TITLE OF STUDY : IDENTIFICATION OF BLOCK CASCADE MODELS OF NONLINEAR SYSTEMS

MAJOR FIELD : SYSTEM IDENTIFICATION

DATE OF DEGREE : June, 1994

In this thesis, the structure identification problem of block cascade models composed of linear dynamic and static nonlinear blocks is addressed. Two main approaches are considered, the structure identification in the time domain and the structure identification in the frequency domain.

In the time domain analysis, cross-correlation techniques are used for the structure identification of nonlinear systems when the input to these systems is a white Gaussian signal. The nonlinear systems considered in this part are those that can be described by a model consisting of a linear dynamic block in cascade with a static nonlinear element followed by another linear dynamic block. This model is referred to as a Wiener-Hammerstein model. Two cross-correlation functions, named as the linear and nonlinear cross-correlation functions, were used to identify the structure of this model. From these two functions, a structure identification criterion that covers all the subclasses of the Wiener-Hammerstein model is presented.

In the frequency domain analysis, the structure identification of the Wiener-Hammerstein model is performed utilizing the bispectrum of the system output. Using a zero-mean stationary white Gaussian process as an input to this model, a structure identification criterion based on the bispectrum of the output

sequence only is presented and applied to the above Wiener-Hammerstein model as well as to a more general class of nonlinear systems that can be represented by parallel branches of block cascades in parallel with a linear system. The case treated here is for branches of the same type. The mixed type branches case, however, needs further investigation. It is found from the simulation results that the structure identification criterion is still effective in characterizing the system structure in both situations.

The last part of the thesis treats the impulse response identification of the linear blocks in the system structure. Simulation examples are given to illustrate the results and findings of the present research.

الخلاصة

اسم الطالب : جليل حسن طلاق
عنوان الرسالة : التعرف على بنية النماذج ذات القوالب المتوالية للأنظمة الغير خطية.
التخصص : هندسة ميكانيكية
تاريخ الشهادة : محرم ١٤١٥ هـ.

تتناول هذه الأطروحة مسألة تحديد البنية للأنظمة المكونة من دوال ديناميكية خطية ودوال ساكنة غير خطية . هناك طريقتان رئيسيتان لتناول هذه المسألة ؛ تحديد البنية في المجال الزمني و تحديد البنية في المجال الترددي.

في التحليل في المجال الزمني , تستخدم تقنيات العلاقة المتبادلة لتحديد بنية الأنظمة الغير خطية عندما تكون الإشارة الداخلة لهذه الأنظمة عبارة عن إشارة جوسينية بيضاء . الأنظمة الغير خطية المعتبرة في هذا التحليل عبارة عن تلك التي يمكن التعبير عنها بنموذج وينرهامرشتاين . هناك نوعان من معادلات العلاقة المتبادلة (الخطية و غير الخطية) استخدما للتعرف على بنية نموذخ وينرهامرشتاين . تكون هاتان المعادلتان معيارا لتحديد بنية كل النماذج الجزئية التي يمكن تكوينها من نموذج وينرهامرشتاين .

في التحليل في المجال الترددي , تعالج مسألة تحديد البنية لنموذج وينرهامرشتاين بالأستفادة من قوة الطيف الثنائية لناتج هذا النموذج . باستخدام اشارة جوسينية بيضاء صفرية المتوسط , يتم تشكيل معيار تحديد البنية على أساس قوة الطيف الثنائية لناتج النموذج فقط حيث يتم تطبيق هذا المعيارعلى نموذج وينرهامرشتاين و على نموذج اكثر عمومية مكون من فروع متوازية من قوالب متوالية التي بدورها تكون متوازية مع نموذج خطي . الفروع المتوازية في النموذج العام تكون من نفس النوع . في المقابل , تحتاج مسألة الفروع المختلطة الى تحقيق اضافي. لقد وجد من النتائج الحسابية بأن معيار تحديد البنية أبدى فعالية في تحديد البنية في كلا النموذجين.

الجزء الأخير من الأطروحة يعالج مسألة التعرف على الدوال الخطية في بنية النظام. سوف تعطى بعض الأمثلة الحسابية لتوضيح نتائج البحث الحالي.

درجة الماجستير في العلوم
جامعة الملك فهد للبترول و المعادن
الظهران–المملكة العربية السعودية
محرم ١٤١٥ هـ.

CHAPTER 1

INTRODUCTION

System identification can be generally defined as the determination of a mathematical model for a system or a process by observing its input-output relationships. In most practical systems, such as industrial processes, engineers need to obtain better knowledge about their plants for improved control. In order to obtain this lacking knowledge, they have to perform experiments on their systems. So in control problems, the purpose of the identification is to design control strategies for a particular system. In some situations, however, analyzing the properties of a system is the primary purpose of the identification. Also, in other situations, identification is performed to determine specific parameter values *[1]*.

In practice, most processes are nonlinear and dynamic. Because of this, researchers came up with different methods to represent nonlinear systems. A well established method that can represent a wide class of nonlinear systems is the well known Volterra series expansion. In some particular cases, nonlinear systems can be separated into linear subsystems that include zero-memory nonlinearities in various combinations.

In most engineering systems and industrial processes encountered in practice, some basic characteristics of the system, such as linearity and bandwidth, are assumed to be known. In other words, the structure of the system is assumed to be known. So it becomes possible to derive a specific mathematical model of the system dynamics. As a result of that, what is left to be determined is a set of parameters in the model equation. Thus, the identification problem is reduced to

that of parameter estimation in this case. Hence, there is always a need to perform a structure identification method on the system as a first stage. In this stage of identification, the system is also tested for the existence of any nonlinearity. After that, the parameter estimation problem is solved to determine the parameters of the model.

Methods for system identification are classified into two main categories named as parametric and nonparametric methods. Parametric methods are those whose resulting models are parametrized by a finite-dimensional parameter vector. An example of such methods is the Least Square (LS) method. Nonparametric methods are those whose resulting models are curves or functions *[42]*.

1.1 LITERATURE REVIEW

Generally, any nonlinear system can be represented using the Volterra series representation *[2,30,39]* as follows:

$$y(t)=\sum_{n=1}^{\infty} H_n[x(t)] \qquad (1.1)$$

where the n-th order Volterra operator, $H_n[x(t)]$, is given by

$$H_n[x(t)]=\int_{-\infty}^{\infty}\cdots\int_{-\infty}^{\infty} h_n(\tau_1,\ldots,\tau_n)x(t-\tau_1)\ldots x(t-\tau_n)d\tau_1\ldots d\tau_n \qquad (1.2)$$

and

$y(t)$ = the output time function

$x(t)$ = the input time function

H_n = the n-th order Volterra operator

$h_n(\tau_1,\ldots,\tau_n)$ = the n-th order Volterra kernel.

Fig. 1.1 is a schematic representation of Eq.(1.1), where the total output is obtained as the sum of the outputs of the boxes with the operators $H_n[x(t)]$.

In the above representation, $H_n[x(t)]$ is a homogeneous Volterra functional because $H_n[cx(t)] = c^n H_n[x(t)]$, in which c is a constant. Homogeneity of $H_n[x(t)]$ means that any change in the amplitude of the input results in a change of the output amplitude only but not in the output waveform. If this condition is not satisfied, the functional is called a nonhomogeneous Volterra functional. The

representation of nonlinear systems using nonhomogeneous functionals is called a Wiener series representation. Palm and Poggio *[38]* discussed the representation of nonlinear systems by Volterra and Wiener series. They also derived sufficient conditions to provide a connection between the two representations.

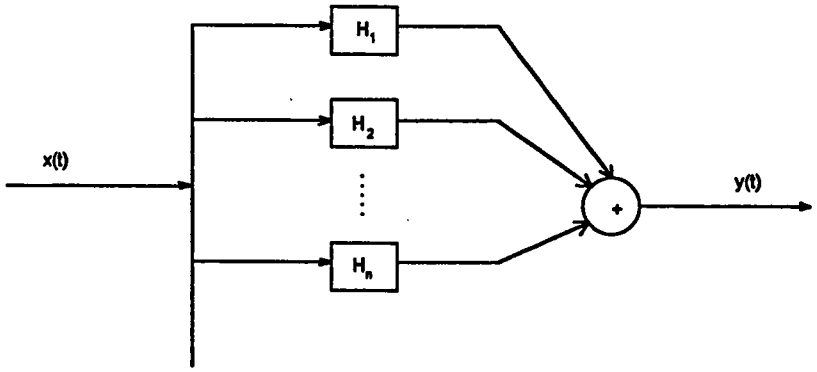

Fig. 1.1 *Schematic Representation of a Nonlinear System in terms of Volterra Series.*

It is known that a wide class of nonlinear systems can be modeled by interconnected memoryless nonlinear gains and linear dynamic subsystems. Several researchers have studied the general class of nonlinear systems comprising static nonlinear elements and dynamic linear elements in various combinations. As shown in Fig. 1.2, three basic configurations of such models are given *[22]*: the Wiener model, the Hammerstein model, and the Wiener-Hammerstein model. These models, known also as block-cascade models, can be used to model many practical systems such as mechanical systems, power plants, bridges and offshore structures such as vertical piles and oil and gas platforms *[2]*. For example, the wave forces on structures can be modeled using linear and nonlinear blocks as shown in Fig. 1.3 in which the output wave force $y(t)$ due to the input wave velocity $x(t)$ consists of three components; a linear inertia force $m(t)$, a nonlinear drag force $d(t)$ and an extraneous noise $n(t)$. This model will be treated in more details later on.

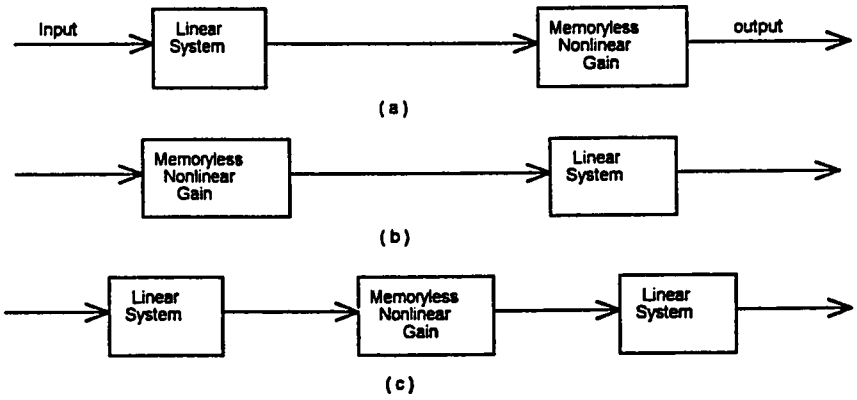

Fig. 1.2 *Three Types of Nonlinear Models:*
(a) Wiener Model (b) Hammerstein Model (c) Wiener-Hammerstein Model

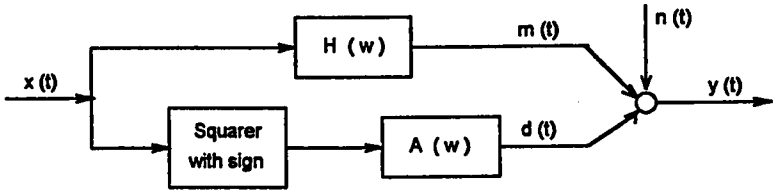

Fig. 1.3 *Nonlinear wave force model with parallel linear and nonlinear systems.*

Narendra and Gallman *[32]* suggested a particular form of Hammerstein model to describe nonlinear systems. They assumed the nonlinearity in this model to be of the polynomial form. Using this model, they suggested an iterative procedure for the identification of nonlinear systems. Hsia *[21]*,on the other hand, developed a noniterative method to estimate the parameters of the nonlinear element of the above model for the case where the linear pulse transfer function has no zeros. Then, Chang and Luss *[12]* extended this method to the general case where the transfer function may have zeros. They showed that the computation time for their method is considerably less than that for the iterative procedure proposed by Narendra and Gallman *[32]* while the accuracy of the estimates is comparable. Later on, Daist, Chang and Luss *[13]* developed a single iterative technique for the estimation of parameters in a Hammerstein model for the class of systems where noise in the output data is correlated.

Palm *[36]* characterized a wide class of systems which can be represented by cascades of linear systems and zero-memory nonlinearities and developed connections between such a representation and the Volterra series representation. Using branches of such cascades in parallel give what he refers to as a "sandwich" system. Palm later discussed representation of nonlinear systems by thin sandwiches *[37]*. These thin sandwiches represent parallel branches in which each branch contains a memoryless nonlinearity embedded between two linear systems (LNL branches).

Parallel LNL cascades procedure is capable of representing a wide variety of nonlinear systems. Korenberg *[5,27,28,29,30]* described a method of obtaining a parallel cascade representation for any nonlinear system having a Wiener functional expansion. Each individual cascade is identified at a time. He has shown that, for the procedure to be general, it is sufficient that each cascade path comprises a dynamic linear system followed by a static nonlinearity. This parallel cascade identification method *[5,27,28,29,30]* does not require use of a Gaussian input. Moreover, it handles those systems with high order nonlinearities and lengthy memories.

Non-linearity detection and characterization in dynamic systems is a fundamental step in nonlinear system identification which should precede any structure and parameter identification. Moustafa and Emara-Shabaik *[25]* treated this problem using the perturbation technique and developed a criterion for the detection of even non-linearities in terms of the third-order cumulant of the system output. Using a probabilistic approach, Emara-Shabaik and Moustafa *[24,44]* then showed that the third and fourth order cumulants of the system output can be

used to detect and characterize systems nonlinearities in its general form e.g. even and/or odd.

The concept of the theory of separability of processes is presented in Billings and Fakhouri *[6,7]*. They considered a model consisting of a linear system in cascade with a nonlinear element followed by another linear system (i.e., the linear and zero-memory nonlinear elements are separable). Based on this, the identification procedure for this class of nonlinear systems is decoupled into two distinct steps when the input is white Gaussian , namely, identification of the linear subsystems and characterization of the nonlinear element. They used cross-correlation techniques to identify both the linear and nonlinear elements.

Haber *[15,16]* introduced the two-step identification method of least-square parameter estimation based on correlation functions for nonlinear dynamic systems with linear parameters. The method is so called because first, correlation analysis is used to identify the structure of the system and then the least-square (LS) method is used to determine the parameters of the process. This identification method was originally introduced for linear single-input/single-output (SISO) systems by Isermann *[23]*. Upon choosing suitable multipliers, this method could be extended to the identification of multi-input/single-output (MISO) nonlinear dynamic systems by Haber *[15,16]*. In these two papers, new correlation functions which were derived from nonlinear functions of the input and output signals were introduced. Such nonlinear correlation functions also give a simple linearity/nonlinearity detection test. This identification method is valid both in open-loop and closed-loop systems.

Haber *[17]* used the Volterra Series to identify the structure of block-oriented models. As a special case Haber *[18]* considered the quadratic block-oriented

models and used the estimated Volterra Kernels to identify the structure of quadratic block-oriented models. In his paper, the quadratic nonlinear block-oriented models were summarized for the Hammerstein, Wiener and Wiener-Hammerstein cascade models. For the structural identification, he used a graphical procedure in addition to the analytical procedure.

Structure identification of block-oriented models, cascade models, and other models were reviewed by Haber *[20]*. These identification methods were summarized based on step and impulse tests, frequency response measurements, correlation analysis, repeated reproducible tests and normal operating data.

A survey paper regarding the general class of nonlinear systems comprising static nonlinear elements and dynamic linear elements in various combinations is given by Billings *[10]*. Billings and Fakhouri *[6]* treated the identification of a single Hammerstein branch with correlated noise and with the nonlinearity expressed as a polynomial. Billings and Fakhouri *[7,11]* included work on parallel systems (i.e., parallel branches) in which each branch comprises a nonlinear element embedded between two linear elements. As a special case, Falkner *[13]* discussed identification of systems comprising parallel Hammerstein branches in which a dynamic linear element follows a static nonlinear element in each branch. In this paper, methods of identification were developed and results were reported for both noise-free and noisy systems.

Michael J. Korenberg *[29]* considered the representation and identification of nonlinear systems via parallel cascades of alternating dynamic linear and static nonlinear elements. In his paper, he showed that any discrete-time finite-memory nonlinear system having a finite-order Volterra series representation can be represented by a finite number of parallel linear/nonlinear (LN) cascade branches.

He provided an upper bound for the number of parallel LN branches required to represent a discrete-time finite-memory nonlinear system with a given order of Volterra functionals. Moreover, he showed how to obtain a parallel cascade representation of a nonlinear system from a single input-output record.

More recently, Emara-Shabaik and Moustafa *[26]* considered the structure identification of nonlinear models that are composed of cascades of linear and static nonlinear blocks i.e., the generalized Wiener-Hammerstein models. They studied the bispectrum of the generalized Wiener-Hammerstein models and showed that bispectrum analysis can effectively be used to identify the structure of a nonlinear dynamic system in terms of block cascade models. This approach requires only measurements of the system output and is robust as regarding measurements noise effects.

Shi and Sun *[40]* have considered the use of parallel cascades to represent nonlinear systems. They point out that the number of branches in parallel and the number of nonlinear elements in a single branch of the structure are finite if the system is a discrete-time, finite-memory, finite-order Volterra series. They later developed a new algorithm to identify a cascaded block model consisting of cascaded blocks of dynamic linear (L), static nonlinear (N), and dynamic linear (L) subsystems *[41]*. Their algorithm is based strictly on the input-output relationship and does not require a priori knowledge of the system and also does not restrict the type of input signals. Two linear subsystems were decoupled from the nonlinear subsystem based on a series of multilevel input and then the predictor-corrector algorithm was used to obtain the parameters of the subsystems.

1.2 RESEARCH OBJECTIVE

In this thesis the attention will be on the representation of nonlinear systems using branches of cascaded blocks of dynamic linear (L), static nonlinear (N), and dynamic linear (L) subsystems. The three basic configurations of Wiener, Hammerstein and Wiener-Hammerstein models, will be studied in more detail, as they form the basis for developing more general structure (i.e. parallel block cascades). The purpose of the present research is to consider the following three aspects:

(1) The structure identification criterion developed by Emara-Shabaik and Moustafa *[26]*, which handles a single branch model, is to be extended to handle models of parallel branches by simulation. This criterion uses the output bispectrum to identify the model structure as a Wiener model (LN), Hammerstein model (NL), or Wiener-Hammerstein model (LNL).

(2) The structure identification criterion using the bispectrum approach will be compared with another structure identification criterion that uses correlation techniques by simulating various examples. The correlation approach utilizes two types of correlation functions, named as the linear and nonlinear cross-correlation functions, to identify the structure of the Wiener-Hammerstein model.

(3) The spectral analysis approach is used to identify the impulse responses of the linear blocks within nonlinear models, and it will be demonstrated by simulation.

The outline of this thesis will be as follows:

Chapter 1 presents an introduction and literature review about nonlinear systems.

Chapter 2 discusses the structure identification problem in the time domain using correlation analysis.

Chapter 3 handles the structure identification problem in the frequency domain using the bispectrum approach.

Chapter 4 presents the spectral analysis approach to identify the impulse responses of the linear blocks within nonlinear models.

Chapter 5 provides simulation examples which support the theoretical results.

Chapter 6 states the conclusions of the research.

CHAPTER 2

STRUCTURE IDENTIFICATION VIA CORRELATION FUNCTIONS

2.1 INTRODUCTION

In this chapter, the structure identification problem will be studied in the time domain using correlation analysis in which the input is taken as a white noise signal. Second order correlation functions will be used for the structure determination of a certain class of nonlinear systems.

The class of nonlinear systems that will be studied in this work is of the cascade systems type which is composed of a linear (L) system with impulse response $h_1(t)$ in cascade with a nonlinear (N) zero-memory element followed by another linear (L) system with impulse response $h_2(t)$ as illustrated in Fig. 2.1. The input is considered to be a white-noise process. Correlation functions are to be used to identify the linear and nonlinear subsystems.

Two types of correlation functions, named as the linear and nonlinear cross-correlation functions, will be employed in this regard. This amounts to finding all the various combinations that can be formed from the general model shown in Fig. 2.1. The general model of this figure is known as the Wiener-Hammerstein (LNL) model. Combinations which can be formed from this general

model are the Wiener model (LN), the Hammerstein model (NL), the linear model (L), and the static model (N).

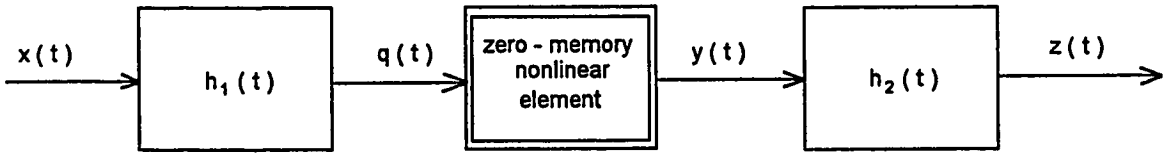

Fig. 2.1 *A Class of nonlinear systems*

2.2 PROBLEM FORMULATION

A class of nonlinear systems which consists of a linear system with impulse response $h_1(t)$ in cascade with a nonlinear zero-memory element followed by another linear system with impulse response $h_2(t)$ is considered as shown in Fig. 2.1. The nonlinear zero-memory element is assumed to be represented by a finite polynomial of degree M, i.e.,

$$y(t) = c_1 q(t) + c_2 q_2(t) + \ldots + c_M q^M(t) \qquad (2.1)$$

The output $q(t)$ of the first linear system is given by the convolution integral as

$$q(t) = \int_{-\infty}^{\infty} h_1(\tau) x(t-\tau) d\tau \qquad (2.2)$$

The output $y(t)$ of the nonlinear element can be expressed in terms of the input $x(t)$ by substituting Eq. (2.2) into Eq. (2.1) as

$$y(t)=c_1\int_{-\infty}^{\infty}h_1(\tau_1)x(t-\tau_1)d\tau_1$$
$$+c_2\int_{-\infty}^{\infty}\int_{-\infty}^{\infty}h_1(\tau_1)h_1(\tau_2)x(t-\tau_1)x(t-\tau_2)d\tau_1d\tau_2$$
$$+...$$
$$+c_M\int_{-\infty}^{\infty}...\int_{-\infty}^{\infty}h_1(\tau_1)...h_1(\tau_M)x(t-\tau_1)...x(t-\tau_M)d\tau_1...d\tau_M \qquad (2.3)$$

The total output $z(t)$ is found by the convolution integral as

$$z(t)=\int_{-\infty}^{\infty}h_2(\tau)y(t-\tau)d\tau \qquad (2.4)$$

Substituting Eq.(2.3) into Eq. (2.4) yields

$$z(t)=c_1\int_{-\infty}^{\infty}\int_{-\infty}^{\infty}h_1(\tau_1)h_2(\tau_2)x(t-\tau_1-\tau_2)d\tau_1d\tau_2$$
$$+c_2\int_{-\infty}^{\infty}\int_{-\infty}^{\infty}\int_{-\infty}^{\infty}h_1(\tau_1)h_1(\tau_2)h_2(\tau_3)x(t-\tau_1-\tau_3)x(t-\tau_2-\tau_3)d\tau_1d\tau_2d\tau_3$$
$$+...$$
$$+c_M\int_{-\infty}^{\infty}...\int_{-\infty}^{\infty}h_1(\tau_1)...h_1(\tau_M)h_2(\tau_{M+1})x(t-\tau_1-\tau_{M+1})...x(t-\tau_M-\tau_{M+1})d\tau_1...d\tau_{M+1} \qquad (2.5)$$

In the remaining of this chapter, all the possible combinations that can be formed from the Wiener-Hammerstein model shown in Fig. 2.1 will be identified by comparing two kinds of correlation functions. The first one correlates the system output $z(t)$ with the system input $x(t)$ and is called the linear cross-correlation function. The second one correlates the system output $z(t)$ with the

square of the system input $x^2(t)$ and is called the nonlinear cross-correlation function.

2.3 CORRELATION ANALYSIS OF THE GENERAL MODEL

If the input signal $x(t)$ is a zero-mean white Gaussian process with a spectral density of unity, then its ith dimensional autocorrelation function is given by *[6]*

$$E[x(t_1)x(t_2)\ldots x(t_i)] = \begin{cases} \sum\prod_{i-1\ n\neq m} \delta(t_n - t_m) & \text{for even } i \\ 0 & \text{for odd } i \end{cases} \tag{2.6}$$

For example

$$E[x(t)] = 0 \tag{2.7}$$

$$E[x(t_1)x(t_2)] = \delta(t_2-t_1) \tag{2.8}$$

$$E[x(t_1)x(t_2)x(t_3)] = 0 \tag{2.9}$$

$$E[x(t_1)x(t_2)x(t_3)x(t_4)] = \delta(t_1-t_2)\delta(t_3-t_4) + \delta(t_1-t_3)\delta(t_2-t_4) + \delta(t_1-t_4)\delta(t_2-t_3) \tag{2.10}$$

Eq. (2.5) can be rewritten as

$$z(t) = w_1(t) + w_2(t) + \ldots + w_M(t) \tag{2.11}$$

where w_i , $i=1,2,...,M$ are given by

$$w_i = c_i \int_{-\infty}^{\infty} \cdots \int_{-\infty}^{\infty} h_1(\tau_1) \cdots h_1(\tau_i) h_2(\tau_{i+1}) x(t-\tau_1-\tau_{i+1}) \cdots x(t-\tau_i-\tau_{i+1}) d\tau_1 \cdots d\tau_{i+1} \qquad (2.12)$$

Define the following terms

$$z'(t) = z(t) - E[z(t)] \qquad (2.13)$$

$$w'_i(t) = w_i(t) - E[w_i(t)] \qquad (2.14)$$

It is clear that when i is odd, then $E[w_i(t)]$ is zero from Eq. (2.6).

2.3.1 Linear cross-correlation Function

The linear cross-correlation function is defined as the correlation function between the output $z(t)$ and the input $x(t)$ with the mean values removed from them. In our analysis here, $x(t)$ is already of a zero-mean value. Therefore, the linear cross-correlation function is given by

$$R_{xz'}(\tau) = E[x(t-\tau)z'(t)] \qquad (2.15)$$

Substituting Eq. (2.13) into the above equation and using Eq. (2.11) yield

$$R_{xz'}(\tau) = E[x(t-\tau)w'_1(t)] + E[x(t-\tau)w'_2(t)] + \ldots + E[x(t-\tau)w'_M(t)] \qquad (2.16)$$

The first term of Eq. (2.16) can be evaluated using Eq.s (2.12), (2.14) and (2.7) as follows

$$\begin{aligned} E[x(t-\tau)w'_1(t)] &= E[x(t-\tau)w_1(t)] \\ &= E[c_1 x(t-\tau)\int_{-\infty}^{\infty}\int h_1(\tau_1)h_2(\tau_2)x(t-\tau_1-\tau_2)d\tau_1 d\tau_2] \\ &= c_1\int_{-\infty}^{\infty}\int h_1(\tau_1)h_2(\tau_2)E[x(t-\tau)x(t-\tau_1-\tau_2)]d\tau_1 d\tau_2 \\ &= c_1\int_{-\infty}^{\infty}\int h_1(\tau_1)h_2(\tau_2)\delta(\tau-\tau_1-\tau_2)d\tau_1 d\tau_2 \\ &= c_1\int_{-\infty}^{\infty} h_1(\tau_1)h_2(\tau-\tau_1)d\tau_1 \end{aligned} \qquad (2.17)$$

The second term of Eq. (2.16) can be evaluated in a similar manner as

$$\begin{aligned} E[x(t-\tau)w'_2(t)] &= E[x(t-\tau)w_2(t)] \\ &= c_2\int_{-\infty}^{\infty}\int\int h_1(\tau_1)h_1(\tau_2)h_2(\tau_3)E[x(t-\tau)x(t-\tau_1-\tau_3)x(t-\tau_2-\tau_3)]d\tau_1 d\tau_2 d\tau_3 \end{aligned}$$

Since the third moment of $x(t)$ is zero for all shifting times (see Eq.(2.9)), it follows from the above equation that

$$E[x(t-\tau)w'_2(t)] = 0 \qquad (2.18)$$

and hence, all even terms of Eq. (2.16) are also zero.

The third term of Eq. (2.16) can be evaluated as follows

$$
\begin{aligned}
E[x(t-\tau)w'_3(t)] &= E[x(t-\tau)w_3(t)] \\
&= E[c_3 x(t-\tau)\int_{-\infty}^{\infty}\int_{-\infty}^{\infty}\int_{-\infty}^{\infty}\int_{-\infty}^{\infty}h_1(\tau_1)h_1(\tau_2)h_1(\tau_3)h_2(\tau_4)x(t-\tau_1-\tau_4)* \\
&\qquad x(t-\tau_2-\tau_4)x(t-\tau_3-\tau_4)]d\tau_1 d\tau_2 d\tau_3 d\tau_4 \\
&= c_3\int_{-\infty}^{\infty}\int_{-\infty}^{\infty}\int_{-\infty}^{\infty}\int_{-\infty}^{\infty}h_1(\tau_1)h_1(\tau_2)h_1(\tau_3)h_2(\tau_4)E[x(t-\tau)x(t-\tau_1-\tau_4)* \\
&\qquad x(t-\tau_2-\tau_4)x(t-\tau_3-\tau_4)]d\tau_1 d\tau_2 d\tau_3 d\tau_4 \\
&= c_3\int_{-\infty}^{\infty}\int_{-\infty}^{\infty}\int_{-\infty}^{\infty}\int_{-\infty}^{\infty}h_1(\tau_1)h_1(\tau_2)h_1(\tau_3)h_2(\tau_4)\{\delta(\tau-\tau_1-\tau_4)\delta(\tau_2-\tau_3)+ \\
&\qquad \delta(\tau-\tau_2-\tau_4)\delta(\tau_1-\tau_3)+\delta(\tau-\tau_3-\tau_4)\delta(\tau_1-\tau_2)\}d\tau_1 d\tau_2 d\tau_3 d\tau_4 \\
&= 3c_3\int_{-\infty}^{\infty}\int_{-\infty}^{\infty}h_1(\tau_1)h_1^2(\tau_2)h_2(\tau-\tau_1)d\tau_1 d\tau_2 \\
&= \int_{-\infty}^{\infty}h_1(\tau_1)h_2(\tau-\tau_1)d\tau_1\{3c_3\int_{-\infty}^{\infty}h_1^2(\tau_2)d\tau_2\}
\end{aligned}
\qquad (2.19)
$$

Higher order terms can be evaluated in a similar manner. Substituting Eq.s (2.17), (2.18) and (2.19) into Eq. (2.16) yields

$$
R_{xw'}(\tau) = \int_{-\infty}^{\infty}h_1(\tau_1)h_2(\tau-\tau_1)d\tau_1\{c_1+0+3c_3\int_{-\infty}^{\infty}h_1^2(\tau_2)d\tau_2+0+\ldots\} \qquad (2.20)
$$

If the linear subsystems of Fig. 2.1 are stable, then the terms enclosed in square brackets in Eq. (2.20) are finite (See Eq. (A.36) in Appendix A). Since those terms do not depend on τ, then they can be replaced by a constant and thus the linear cross-correlation function can be expressed as

$$
R_{xw'}(\tau) = \beta\int_{-\infty}^{\infty}h_1(\tau_1)h_2(\tau-\tau_1)d\tau_1 \qquad (2.21)
$$

where the constant β is given by

$$\beta = c_1 + 0 + 3c_3 \int_{-\infty}^{\infty} h_1^2(\tau_2) d\tau_2 + 0 + \ldots \qquad (2.22)$$

So, the linear cross-correlation function $R_{xz}(\tau)$ is given by the convolution integral between the impulse response $h_1(\tau)$ of the first linear system and the impulse response $h_2(\tau)$ of the second linear system.

2.3.2 Nonlinear Cross-Correlation Function

The nonlinear cross-correlation function is defined as the correlation function between the output $z(t)$ and the square of the input $x(t)$ after the mean values of both $z(t)$ and $x(t)$ are removed from them. So, the nonlinear cross-correlation function is given by

$$R_{x^2z}(\tau) = E[x^2(t-\tau)z'(t)] \qquad (2.23)$$

Substituting Eq. (2.13) into the above equation and using Eq. (2.11) yield

$$R_{x^2z}(\tau) = E[x^2(t-\tau)w'_1(t)] + E[x^2(t-\tau)w'_2(t)] + \ldots + E[x^2(t-\tau)w'_M(t)] \qquad (2.24)$$

The first term of Eq. (2.24) can be evaluated using Eq.s (2.12), (2.14) and (2.7) as follows

$$\begin{aligned} E[x^2(t-\tau)w'_1(t)] &= E[x^2(t-\tau)w_1(t) - x^2(t-\tau)E[w_1(t)]] \\ &= E[x^2(t-\tau)w_1(t)] - E[x^2(t-\tau)]E[w_1(t)] \\ &= E[x^2(t-\tau)w_1(t)] - 1 * E[w_1(t)] \\ &= E[c_1 x^2(t-\tau) \int_{-\infty}^{\infty}\int_{-\infty}^{\infty} h_1(\tau_1)h_2(\tau_2)x(t-\tau_1-\tau_2)d\tau_1 d\tau_2] - 0 \\ &= c_1 \int_{-\infty}^{\infty}\int_{-\infty}^{\infty} h_1(\tau_1)h_2(\tau_2)E[x^2(t-\tau)x(t-\tau_1-\tau_2)]d\tau_1 d\tau_2 \end{aligned}$$

Using Eq.(2.9), it follows that

$$E[x^2(t-\tau)w'_1(t)] = 0 \tag{2.25}$$

Similarly all odd terms of Eq. (2.24) are zero.

The second term of Eq. (2.23) can be evaluated as follows

$$\begin{aligned}
E[x^2(t-\tau)w'_2(t)] &= E[x^2(t-\tau)w_2(t) - x^2(t-\tau)E[w_2(t)]] \\
&= E[x^2(t-\tau)w_2(t)] - E[x^2(t-\tau)]E[w_2(t)] \\
&= c_2 \int_{-\infty}^{\infty}\int_{-\infty}^{\infty}\int_{-\infty}^{\infty} h_1(\tau_1)h_1(\tau_2)h_2(\tau_3)E[x^2(t-\tau)x(t-\tau_1-\tau_3)x(t-\tau_2-\tau_3)]d\tau_1 d\tau_2 d\tau_3 \\
&\qquad - c_2 \int_{-\infty}^{\infty}\int_{-\infty}^{\infty}\int_{-\infty}^{\infty} h_1(\tau_1)h_1(\tau_2)h_2(\tau_3)E[x(t-\tau_1-\tau_3)x(t-\tau_2-\tau_3)]d\tau_1 d\tau_2 d\tau_3 \\
&= c_2 \int_{-\infty}^{\infty}\int_{-\infty}^{\infty} h_1(\tau_1)h_1(\tau_1)h_2(\tau_3)d\tau_1 d\tau_3 + 2c_2 \int_{-\infty}^{\infty} h_1(\tau-\tau_3)h_1(\tau-\tau_3)h_2(\tau_3)d\tau_3 \\
&\qquad - c_2 \int_{-\infty}^{\infty}\int_{-\infty}^{\infty} h_1(\tau_1)h_1(\tau_1)h_2(\tau_3)d\tau_1 d\tau_3 \\
&= 2c_2 \int_{-\infty}^{\infty} h_1^2(\tau-\tau_3)h_2(\tau_3)d\tau_3
\end{aligned} \tag{2.26}$$

The fourth term of Eq. (2.24) can be evaluated in a similar manner as follows

$$\begin{aligned}
E[x^2(t-\tau)w'_4(t)] &= E[x^2(t-\tau)w_4(t) - x^2(t-\tau)E[w_4(t)]] \\
&= E[x^2(t-\tau)w_4(t) - E[x^2(t-\tau)]E[w_4(t)] \\
&= c_4 \int_{-\infty}^{\infty}\int_{-\infty}^{\infty}\int_{-\infty}^{\infty}\int_{-\infty}^{\infty}\int_{-\infty}^{\infty} h_1(\tau_1)h_1(\tau_2)h_1(\tau_3)h_1(\tau_4)h_2(\tau_5)* \\
&\quad [\delta(0)\{\delta(\tau_1-\tau_2)\delta(\tau_3-\tau_4)+\delta(\tau_1-\tau_3)\delta(\tau_2-\tau_4)+\delta(\tau_1-\tau_4)\delta(\tau_2-\tau_3)\} \\
&\quad +\delta(\tau-\tau_1-\tau_5)\{\delta(\tau-\tau_2-\tau_5)\delta(\tau_3-\tau_4)+\delta(\tau-\tau_3-\tau_5)\delta(\tau_2-\tau_4)+\delta(\tau-\tau_4-\tau_5)\delta(\tau_2-\tau_3)\} \\
&\quad +\delta(\tau-\tau_2-\tau_5)\{\delta(\tau-\tau_1-\tau_5)\delta(\tau_3-\tau_4)+\delta(\tau-\tau_3-\tau_5)\delta(\tau_1-\tau_4)+\delta(\tau-\tau_4-\tau_5)\delta(\tau_1-\tau_3)\} \\
&\quad +\delta(\tau-\tau_3-\tau_5)\{\delta(\tau-\tau_1-\tau_5)\delta(\tau_2-\tau_4)+\delta(\tau-\tau_2-\tau_5)\delta(\tau_1-\tau_4)+\delta(\tau-\tau_4-\tau_5)\delta(\tau_1-\tau_2)\} \\
&\quad +\delta(\tau-\tau_4-\tau_5)\{\delta(\tau-\tau_1-\tau_5)\delta(\tau_2-\tau_3)+\delta(\tau-\tau_2-\tau_5)\delta(\tau_1-\tau_3)+\delta(\tau-\tau_3-\tau_5)\delta(\tau_1-\tau_3)\}] \\
&\qquad d\tau_1 d\tau_2 d\tau_3 d\tau_4 d\tau_5
\end{aligned}$$

$$-1\cdot c_4\int_{-\infty}\int_{-\infty}\int_{-\infty}\int_{-\infty}\int_{-\infty}h_1(\tau_1)h_1(\tau_2)h_1(\tau_3)h_1(\tau_4)h_2(\tau_5)\{\delta(\tau_1-\tau_2)\delta(\tau_3-\tau_4)+$$
$$\delta(\tau_1-\tau_3)\delta(\tau_2-\tau_4)+\delta(\tau_1-\tau_4)\delta(\tau_2-\tau_3)\}d\tau_1 d\tau_2 d\tau_3 d\tau_4 d\tau_5$$
$$=4c_4\int_{-\infty}\int_{-\infty}h_1(\tau-\tau_5)h_1(\tau-\tau_5)h_1(\tau_4)h_1(\tau_4)h_2(\tau_5)d\tau_4 d\tau_5$$
$$=\int_{-\infty}h_1^2(\tau-\tau_5)h_2(\tau_5)d\tau_5\{4c_4\int_{-\infty}h_1^2(\tau_4)d\tau_4\} \qquad (2.27)$$

Higher order terms can be evaluated in a similar manner. Substituting Eq.s. (2.25), (2.26) and (2.27) into Eq. (2.24) yields

$$R_{x^2z'}(\tau)=\int_{-\infty}h_1^2(\tau-\tau_1)h_2(\tau_1)d\tau_1+\{0+2c_2+0+4c_4\int_{-\infty}h_1^2(\tau_2)d\tau_2+0+\ldots\} \qquad (2.28)$$

If the linear subsystems of Fig. 2.1 are stable, then the terms enclosed in square brackets are finite *[6,7]*. Since those terms do not depend on τ, then they can be replaced by a constant and thus the nonlinear cross-correlation function can be expressed as

$$R_{x^2z'}(\tau)=\alpha\int_{-\infty}h_1^2(\tau-\tau_1)h_2(\tau_1)d\tau_1 \qquad (2.29)$$

where the constant α is given by

$$\alpha=\{0+2c_2+0+4c_4\int_{-\infty}h_1^2(\tau_2)d\tau_2+0+\ldots\} \qquad (2.30)$$

So, the nonlinear cross-correlation function $R_{x^2z'}(\tau)$ is given by the convolution integral between the square of the impulse response $h_1(\tau)$ of the first linear system and the impulse response $h_2(\tau)$ of the second linear system with the convolution integral multiplied by the constant α.

2.4 NONLINEAR STRUCTURE IDENTIFICATION

The results derived in section 2.3 will be applied in this section to identify the structure of the general model of Fig. 2.1. Since input and output data of practical systems are collected using digital computers, then the results obtained in section 2.3 need to be descretized. In reality, $h_1(\tau)$ and $h_2(\tau)$ are considered to be zero when τ is negative. Therefore, Eq.s (2.21) and (2.29) can be expressed in discrete form, respectively, as follows

$$R_{xz'}(\tau)=\beta \sum_{\tau_1=0}^{\tau_1=\tau} h_1(\tau_1)\, h_2(\tau-\tau_1) \qquad (2.31)$$

$$R_{x^2z}(\tau)=\alpha \sum_{\tau_1=0}^{\tau_1=\tau} h_1^2(\tau_1)\, h_2(\tau-\tau_1) \qquad (2.32)$$

where $\tau=0,1,2,...N$ and N is the length of the the data record. Note also that in this section the variable t will be refered to as a discrete varaible.

If the zero-memory nonlinear element of Fig. 2.1 has odd nonlinearity only, then the nonlinear cross-correlation function $R_{x^2z}(\tau)$ is zero from Eq.s (2.24) and (2.25). On the other hand, if the nonlinear element has even nonlinearity only, then the linear cross-correlation function $R_{xz'}(\tau)$ is zero from Eq.s (2.16) and (2.18). Therefore

$$R_{xz'}(\tau) = 0 \quad \textit{for even nonlinearity only} \qquad (2.33)$$

$$R_{x^2z}(\tau) = 0 \quad \textit{for odd nonlinearity only} \qquad (2.34)$$

The above two equations will be used in later developments.

2.4.1 Wiener Model

The Wiener model consists of a linear system followed by a zero-memory nonlinearity as shown in Fig. 2.2. It can be obtained from Fig. 2.1 by setting

$$h_2(t) = \delta(t) \tag{2.35}$$

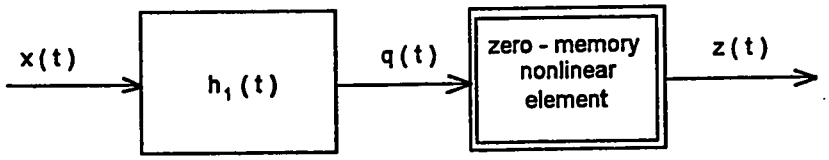

Fig. 2.2 *Wiener model*

Substituting Eq. (2.35) into Eq.s (2.31) and (2.32) , respectively , yields

$$R_{xz}(\tau) = \beta\, h_1(\tau) \tag{2.36}$$

$$R_{x^2z}(\tau) = \alpha\, h_1^2(\tau) \tag{2.37}$$

where the constants β and α are given respectively by Eq.s (2.22) and (2.30).

Thus, for a Wiener model the linear cross-correlation function $R_{xz}(\tau)$ is directly proportional to the impulse response $h_1(\tau)$ of the linear system and the nonlinear cross-correlation function $R_{x^2z}(\tau)$ is proportional to the square of $h_1(\tau)$. Therefore, the nonlinear cross-correlation function of a Wiener model is proportional to the square of the linear cross-correlation.

2.4.2 Hammerstein Model

The Hammerstein model consists of a zero-memory nonlinearity followed by a linear system. This is shown in Fig. 2.3 which can be obtained from Fig. 2.1 bt setting

$$h_1(t) = \delta(t) \tag{2.38}$$

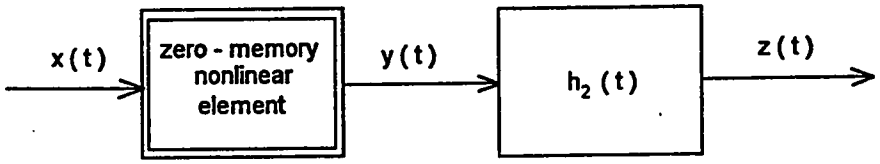

Fig. 2.3 *Hammerstein model*

Substituting the above equation into Eq.s (2.31) and (2.32) ,respectively, yields

$$R_{xz}(\tau) = \beta \sum_{\tau_1=0}^{\tau_1=\tau} \delta(\tau_1) h_2(\tau - \tau_1) = \beta h_2(\tau) \tag{2.39}$$

$$R_{x^2z}(\tau) = \alpha \sum_{\tau_1=0}^{\tau_1=\tau} \delta^2(\tau_1) h_2(\tau - \tau_1) = \alpha h_2(\tau) \tag{2.40}$$

Thus, for a Hammerstein model, the linear cross-correlation function $R_{xz}(\tau)$ and the nonlinear cross-correlation function $R_{x^2z}(\tau)$ are directly proportional to the impulse response of the second linear system $h_2(\tau)$. Therefore, the linear cross-correlation function $R_{xz}(\tau)$ and the nonlinear cross-correlation function $R_{x^2z}(\tau)$ of a Hammerstein model are directly proportional to each other.

2.4.3 Linear Model

A linear system can be obtained from Fig. 2.1 by letting

$$c_1 = 1$$
$$c_i = 0 \ , \ i = 2,3,...,M \qquad (2.41)$$

and is shown in Fig. 2.4.

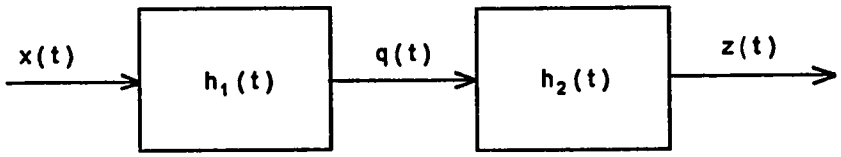

Fig. 2.4 *Linear model*

Substituting the above equation into Eq.s (2.31) and (2.32) ,respectively, yields

$$R_{xz}(\tau) = \sum_{\tau_1=0}^{\tau_1=\tau} h_1(\tau_1) h_2(\tau - \tau_1) \qquad (2.42)$$

$$R_{x^2z}(\tau) = 0 \qquad (2.43)$$

Thus for a linear system, the nonlinear cross-correlation function is zero for all shifting times and hence it can be used as convenient test for linearity.

2.4.4 Static Model

For the static model shown in Fig. 2.5 the weighting functions of the linear subsystems are

$$h_1(t) = h_2(t) = \delta(t) \tag{2.44}$$

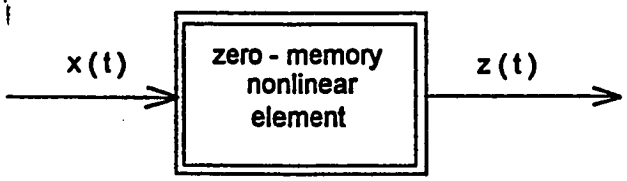

Fig. 2.5 *Static model*

Substituting Eq. (2.44) into Eq.s (2.31) and (2.32) ,respectively, yields

$$R_{xz}(\tau) = \beta\delta(\tau) \tag{2.45}$$

$$R_{x^2z}(\tau) = \alpha\delta(\tau) \tag{2.46}$$

Thus, for a static model with general nonlinearity, the linear cross-correlation function $R_{xz}(\tau)$ and nonlinear cross-correlation function $R_{x^2z}(\tau)$ are both zero for all shifting times except for zero shifting time.

2.4.5 Structure Identification Criterion

The results derived in above provide a convenient test for the structure identification of the class of nonlinear systems shown in Fig. 2.1 by using the linear and the nonlinear cross-correlation functions only. The results can be summarized as follows:

1. *Static Model*

Both linear and nonlinear cross-correlation functions are zero for all shifting times except for zero shifting time. If the linear cross-correlation function is always zero, then the nonlinearity of the static element is even only. On the other hand, if the nonlinear cross-correlation function is always zero, then the nonlinearity of the static element is odd only.

2. *Linear Model*

The nonlinear cross-correlation function is zero for all shifting times.

2. *Hammerstein Model*

The linear and nonlinear cross-correlation functions are proportional to each other.

4. *Wiener Model*

The nonlinear cross-correlation function is proportional to the square of the linear one.

5. *Wiener-Hammerstein Model*

If none of the above four results holds.

Simulation examples will be provided in chapter 5 to demonstrate the above criterion in identifying the structure of nonlinear systems using correlation techniques.

CHAPTER 3

STRUCTURE IDENTIFICATION VIA BISPECTRUM

3.1 INTRODUCTION

In this chapter, the structure identification of nonlinear systems utilizing the bispectrum of the system output is considered. The considered class of nonlinear systems is the same as that considered in chapter 2 (see Fig. 2.1). Using a zero-mean stationary white Gaussian process as an input to such model, Emara-Shabaik and Moustafa *[26]* developed a structure identification criterion based on the bispectrum of the output sequence. Their structure identification criterion requires only measurements of the output sequence. Moreover, it is robust as regarding the effects of the output noise. The extension of this structure testing criterion to parallel branch models is considered in this chapter.

3.2 ANALYSIS OF THE WIENER-HAMMERSTEIN MODEL

In order to present the structure identification criterion developed in *[26]* one should consider the following block cascade model of Fig. 3.1.

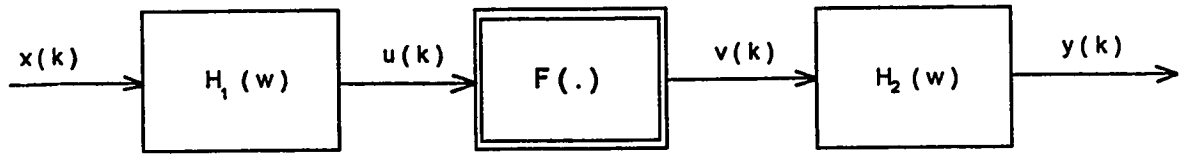

Fig. 3.1 *Wiener-Hammerstein model*

Let the input to the system $x(k)$ be a stationary zero-mean white Gaussian random sequence, then the second and third order cumulants of $x(k)$ are given, respectively, by *[26]*

$$C_2(\tau) = Q\delta(\tau) \tag{3.1}$$

$$C_3(\tau_1, \tau_2) = 0 \tag{3.2}$$

where Q is the mean square value of the input $x(k)$ which equals the variance of $x(k)$ in this case because $x(k)$ has a zero mean value. It follows from Appendix A that $x(k)$ has a flat power spectrum and zero bispectrum. That is

$$P_x(\omega) = P_x \quad , \quad \forall \omega \tag{3.3}$$

$$B_x(\omega_1, \omega_2) = 0 \quad , \quad \forall \omega_1, \omega_2 \tag{3.4}$$

Since the first block is linear and driven by Gaussian input, its output $u(k)$ is a stationary zero mean non-white Gaussian random sequence. The power spectrum and the bispectrum of the output of the first linear block $u(k)$ can be obtained, respectively, as *[33]*

$$P_u(\omega) = |H_1(\omega)|^2 P_x(\omega) \tag{3.5}$$

$$B_u(\omega_1, \omega_2) = H_1(\omega_1)H_1(\omega_2)H_1^*(\omega_1+\omega_2)B_x(\omega_1, \omega_2) \tag{3.6}$$

where $*$ stands for the conjugate transpose.

Substituting Eq. (3.3) into Eq. (3.5) and Eq. (3.4) into Eq. (3.6) yields the following results

$$P_u(\omega) = P_x |H_1(\omega)|^2 \tag{3.7}$$

$$B_u(\omega_1, \omega_2) = 0 \quad , \quad \forall\, \omega_1, \omega_2 \tag{3.8}$$

which means that if a linear block is excited by a stationary zero-mean white Gaussian random sequence, then the power spectrum of its output is always real and the bispectrum of its output is identically zero.

Since the nonlinear block has no memory, then its output power spectrum is a function of the input power spectrum and its output bispectrum is a function of both the power spectrum and bispectrum of the input. Therefore, the power spectrum $P_v(\omega)$ and the bispectrum $B_v(\omega_1, \omega_2)$ of the output of the nonlinear block $v(k)$ are both real-valued for all values of ω, ω_1 and ω_2 because both $P_u(\omega)$ and $B_u(\omega_1, \omega_2)$ are real *[2,4,33]*.

The output $y(k)$ of the second linear block has the following polyspectra

$$P_y(\omega) = |H_2(\omega)|^2 P_v(\omega) \tag{3.9}$$

$$B_y(\omega_1, \omega_2) = H_2(\omega_1)H_2(\omega_2)H_2^*(\omega_1+\omega_2)B_v(\omega_1, \omega_2) \tag{3.10}$$

It is thus clear that the power spectrum of the system output is real because $P_v(\omega)$ is real. However, the bispectrum of the system output $B_y(\omega_1, \omega_2)$ is not generally real but it depends on the second linear block $H_2(\omega)$. The magnitude and the phase angle of the system output bispectrum $B_y(\omega_1, \omega_2)$ are given ,respectively, as

$$|By(\omega_1, \omega_2)| = |H_2(\omega_1)||H_2(\omega_2)||H_2^*(\omega_1+\omega_2)||B_v(\omega_1, \omega_2)| \tag{3.11}$$

$$\phi y(\omega_1, \omega_2) = \phi_2(\omega_1) + \phi_2(\omega_1) + \phi_2(\omega_1+\omega_2) \tag{3.12}$$

where $|H_2(\omega)|$ and $\phi_2(\omega)$ are, respectively, the magnitude and the phase angle of $H_2(\omega)$.

3.2.1 Wiener Model

As mentioned previously in section 2.4.1, the Wiener model is characterized by a linear dynamic system followed by a static nonlinearity. So, it can be obtained from the general model as a special case by setting $H_2(\omega) = 1$. Therefore,

$$\phi_2(\omega) = 0 \tag{3.13}$$

Substituting Eq. (3.13) into Eq. (3.12) yields

$$\phi_y(\omega_1, \omega_2) = 0 \qquad (3.14)$$

It follows that for a Wiener model, the bispectrum of its output is real for all values of ω_1 and ω_2.

3.2.2 Hammerstein Model

The Hammerstein model is characterized by a static nonlinearity followed by a linear dynamic system. So, it can be obtained as a special case of the general model by setting $H_1(\omega) = 1$ and it follows that $u(k) = x(k)$. Since the input $x(t)$ has a flat power spectrum and a zero bispectrum (i.e., constant values), then both the power spectrum $P_v(\omega)$ and the bispectrum $B_v(\omega_1, \omega_2)$ of $v(k)$ are constants. Therefore,

$$P_v(\omega) = P_v \quad , \quad \forall \omega \qquad (3.15)$$

$$B_v(\omega_1, \omega_2) = B_v \quad , \quad \forall \omega_1, \omega_2 \qquad (3.16)$$

Using the above two equations, the power spectrum and the bispectrum of the output $y(k)$ can be obtained, respectively, from Eq.s (3.9) and (3.10) as

$$Py(\omega) = |H_2(\omega)|^2 P_v \qquad (3.17)$$

$$By(\omega_1, \omega_2) = H_2(\omega_1)H_2(\omega_2)H_2^*(\omega_1+\omega_2)B_v \qquad (3.18)$$

To differentiate between the Hammerstein model and the Wiener-Hammerstein model, one can use the bicoherence function which is defined as *[26]*

$$b_y(\omega_1,\omega_2)=\frac{\left|B_y(\omega_1,\omega_2)\right|}{\sqrt{\left|P_y(\omega_1)\right|\left|P_y(\omega_2)\right|\left|P_y(\omega_1+\omega_2)\right|}} \qquad (3.19)$$

substituting Eq.s (3.17) and (3.18) into Eq. (3.19) yields

$$b_y(\omega_1,\omega_2)=\frac{B_v}{P_v\sqrt{P_v}} \qquad (3.20)$$

which means that for a Hammerstein model, the bicoherence function $b_y(\omega_1,\omega_2)$ of the output is constant for all values of ω_1 and ω_2.

3.2.3 Linear Model

If the nonlinear block in Fig. 3.1 contains a constant value only, then the system is linear and results similar to Eq.s (3.7) and (3.8) are obtained. Therefore,

$$Py(\omega) = |cH_1(\omega)H_2(\omega)|^2 P_x \qquad (3.21)$$

$$By(\omega_1,\omega_2) = 0 \quad , \quad \forall\, \omega_1,\omega_2 \qquad (3.22)$$

which implies that if the system is linear, then its output bispectrum is always zero.

3.2.4 Static Nonlinear Model

The system of Fig. 3.1 is static if $H_1(\omega) = H_2(\omega) = 1$. In this case the output of the system will be the output of the nonlinear block and hence similar results to Eq.s (3.15) and (3.16) are obtained. Therefore

$$P_y(\omega) = P_y \quad , \quad \forall \omega \tag{3.23}$$

$$B_y(\omega_1, \omega_2) = B_y \quad , \quad \forall \omega_1, \omega_2 \tag{3.24}$$

which show that if the system is static, then both the power spectrum and the bispectrum of the system output are constants.

3.2.5 Structure Identification Criterion

The results derived in sections 3.2.1 - 3.2.4 can be used to identify the structure of nonlinear systems that are represented by models of cascades of dynamic linear systems and a static nonlinear element. The developed structure identification criterion can be summarized in the following 4 steps:

(1) If:

$B_y(\omega_1, \omega_2)$ is zero for all values of ω_1 and ω_2

then:

the structure is described by a linear model.

(2) If:

$B_y(\omega_1, \omega_2)$ is constant for all values of ω_1 and ω_2

then :

the structure is described by a static nonlinear model.

(3) If :

$B_y(\omega_1, \omega_2)$ is real for all values of ω_1 and ω_2

then :

the structure is described by a Wiener model.

(4) If :

$B_y(\omega_1, \omega_2)$ is complex.

then :

the bicoherence function $b_y(\omega_1, \omega_2)$ given by Eq. (3.24) is used to differentiate between the Hammerstein model and the Wiener-Hammerstein model as follows:

If :

$b_y(\omega_1, \omega_2)$ is constant for all values of ω_1 and ω_2

then :

the structure is described by a Hammerstein model.

else :

it is described by a Wiener-Hammerstein model.

The structure identification criterion described above can be extended to a more general class of nonlinear systems which can be represented by parallel branches of block cascades in parallel with a linear system. Extensive simulation has been carried out for this general model and the results are reported in chapter 5. It has been found that the structure identification criterion described

above is still valid for this model provided that the parallel nonlinear branches are all of the same type.

In order to support the above criterion, several examples were simulated and the results are shown in section 5.2 of chapter 5. The examples were simulated using different types of nonlinearities (i.e., odd and/or even nonlinearities).

CHAPTER 4

FREQUENCY RESPONSE IDENTIFICATION OF PARALLEL BRANCH MODELS WITH LINEAR AND NONLINEAR BLOCKS

4.1 INTRODUCTION

This chapter presents a spectral analysis methodology for analyzing the spectral properties of a nonlinear model with parallel linear and nonlinear systems of arbitrary type. This analysis methodology was recommended by Bendat *[2]*. Measurements of the input and the total output are needed. The methodology is based on decomposing the total output spectral density function into its uncorrelated linear and nonlinear components. By so doing, an equivalent nonlinear model with uncorrelated linear and nonlinear systems can be constructed and analyzed to obtain the spectral properties of the original model. The procedure will be applied in the present work to quadratic and cubic Hammerstein models in parallel with a linear system and to a nonlinear model for sea wave force on structures. Simulation results for these two models are shown in chapter 5.

4.2 ANALYSIS METHODOLOGY

A general physical nonlinear system of a single-input/single-output with parallel linear and nonlinear systems is shown in Fig. 4.1 . As shown in this figure, the total output $y(t)$ due to the input $x(t)$ is the sum of a linear output $y_1(t)$, a nonlinear output $y_2(t)$, and an extraneous noise $n(t)$. Here, $n(t)$ is

assumed to be a zero-mean stationary random noise and uncorrelated with $y_1(t)$ and $y_2(t)$. The input $x(t)$ is assumed to be a zero-mean white Gaussian process.

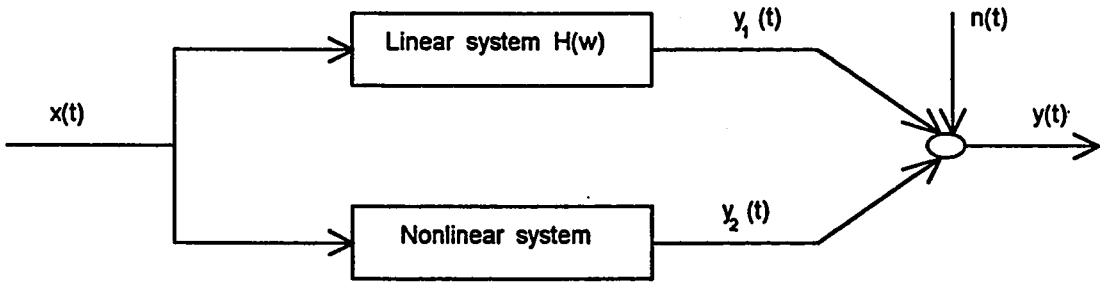

Fig. 4.1 *Nonlinear model with parallel linear and nonlinear systems where outputs can be correlated.*

The output of Fig. 4.1 satisfies the following equation

$$y(t) = y_1(t) + y_2(t) + n(t) \tag{4.1}$$

Although the mean value of the input $x(t)$ is taken to be zero, the total output $y(t)$ may have a non-zero mean value due to the nonlinear output $y_2(t)$. Finite Fourier transforms of the quantities $y(t)$, $y_1(t)$, $y_2(t)$, $n(t)$, and $x(t)$ with non-zero mean values removed are defined as follows *[4]*:

$$Y(\omega) = \int_0^T \{y(t) - \mu_y\} e^{-j\omega t} dt \quad ; \quad Y_1(\omega) = \int_0^T y_1(t) e^{-j\omega t} dt$$

$$Y_2(\omega) = \int_0^T \{y_2(t) - \mu_y\} e^{-j\omega t} dt \quad ; \quad N(\omega) = \int_0^T n(t) e^{-j\omega t} dt$$

$$X(\omega) = \int_0^T x(t) e^{-j\omega t} dt \tag{4.2}$$

where T is the record length and μ_y is the mean value of the total output $y(t)$ which is the same as the mean value of the nonlinear output $y_2(t)$ because the mean value of $y_1(t)$ is zero. Eq. (4.1) can be also written as follows

$$\{y(t) - \mu_y\} = y_1(t) + \{y_2(t) - \mu_y\} + n(t) \tag{4.3}$$

Taking the finite Fourier transform of the above equation gives

$$Y(\omega) = Y_1(\omega) + Y_2(\omega) + N(\omega) \tag{4.4}$$

The autospectral density function of $x(t)$ and the cross spectral density function of $x(t)$ and $\{y(t) - \mu_y\}$ are defined, respectively, as *[2]*

$$S_{xx}(\omega) = \frac{1}{T} E[X^*(\omega) X(\omega)] \tag{4.5}$$

$$S_{xy}(\omega) = \frac{1}{T} E[X^*(\omega) Y(\omega)] \tag{4.6}$$

The autospectral density function of the output $\{y(t) - \mu_y\}$ and the cross-spectral density function between $\{y(t) - \mu_y\}$ and $x(t)$ are found, respectively, from Eq. (4.3) as

$$S_{yy}(\omega) = S_{y_1y_1}(\omega) + S_{y_2y_2}(\omega) + S_{y_1y_2}(\omega) + S_{y_2y_1}(\omega) + S_{nn}(\omega) \tag{4.7}$$

$$\begin{aligned} S_{xy}(\omega) &= S_{xy_1}(\omega) + S_{xy_2}(\omega) \\ &= H(\omega) S_{xx}(\omega) + S_{xy_2}(\omega) \end{aligned} \tag{4.8}$$

As shown from Eq. (4.7), it is difficult to decompose $S_{yy}(\omega)$ into its linear and nonlinear components because the linear output $y_1(t)$ and the nonlinear output $y_2(t)$ are generally correlated. To avoid this problem, Bendat *[2]* recommended to change the nonlinear model of Fig. 4.1 into another equivalent nonlinear model in which the input $x(t)$ produces a different linear output $y_o(t)$ and a different uncorrelated nonlinear output $y_u(t)$ as shown in Fig. 4.2. $H_o(\omega)$ is called the overall optimum linear transfer function because it is chosen in such a way to make the new nonlinear output $y_u(t)$ uncorrelated with $x(t)$.

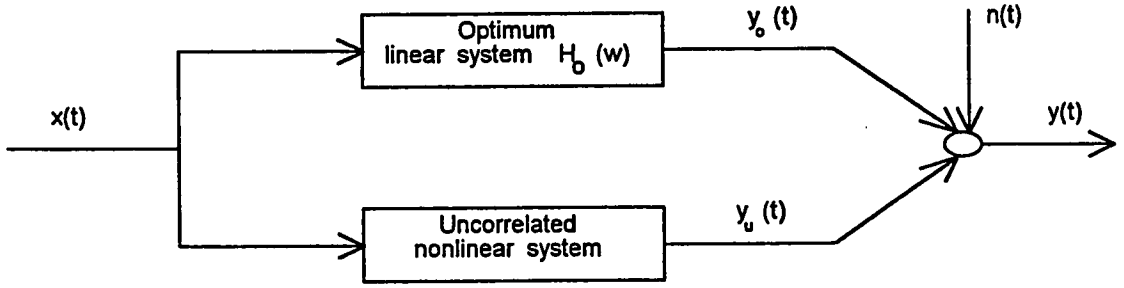

Fig. 4.2 *Equivalent nonlinear model with parallel linear and nonlinear systems where outputs are uncorrelated.*

The overall optimum linear transfer function $H_o(\omega)$ is found from measurements of the input $x(t)$ and the output $y(t)$ by determining the ratio of the cross spectral density function $S_{xy}(\omega)$ to the autospectral density function $S_{xx}(\omega)$ *[2]*. Since

$$y(t) = y_o(t) + y_u(t) + n(t) \tag{4.9}$$

then

$$S_{xy}(\omega) = S_{xy_o}(\omega) = H_o(\omega)S_{xx}(\omega) \tag{4.10}$$

and one can write

$$H_o(\omega) = \frac{S_{xy}(\omega)}{S_{xx}(\omega)} \qquad (4.11)$$

Another expression for $H_o(\omega)$ can be found by substituting Eq. (4.8) into Eq. (4.8) as follows

$$H_o(\omega) = H(\omega) + S_{xy_2}(\omega) / S_{xx}(\omega) \qquad (4.12)$$

By the help of Eq. (4.12), the nonlinear model of Fig. 4.2 can be repictured as shown in Fig. 4.3.

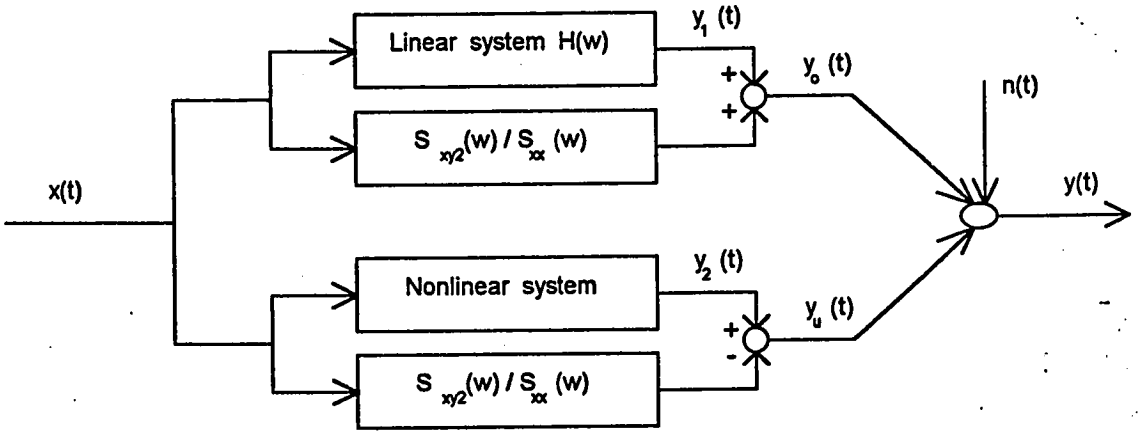

Fig. 4.3 *Equivalent nonlinear model*.

Since the output $y(t)$ is decomposed into uncorrelated components $y_o(t)$, $y_u(t)$ and $n(t)$, then the nonlinear system and the transfer function $\{S_{xy_2}(\omega) / S_{xx}(\omega)\}$ can be identified depending on the type of the nonlinearity

present. Once $\{S_{xy_2}(\omega)/S_{xx}(\omega)\}$ is known, the linear system $H(\omega)$ is identified from Eq. (4.12) as follows

$$H(\omega) = H_o(\omega) - S_{xy_2}(\omega)/S_{xx}(\omega) \qquad (4.13)$$

and the identification problem is solved.

4.3 QUDRATIC AND CUBIC HAMMERSTEIN MODELS IN PARALLEL WITH A LINEAR SYSTEM

To illustrate the idea of section 4.2 consider the nonlinear model shown in Fig. 4.4. An analysis methodology for this model is shown in Bendat *[2]*.

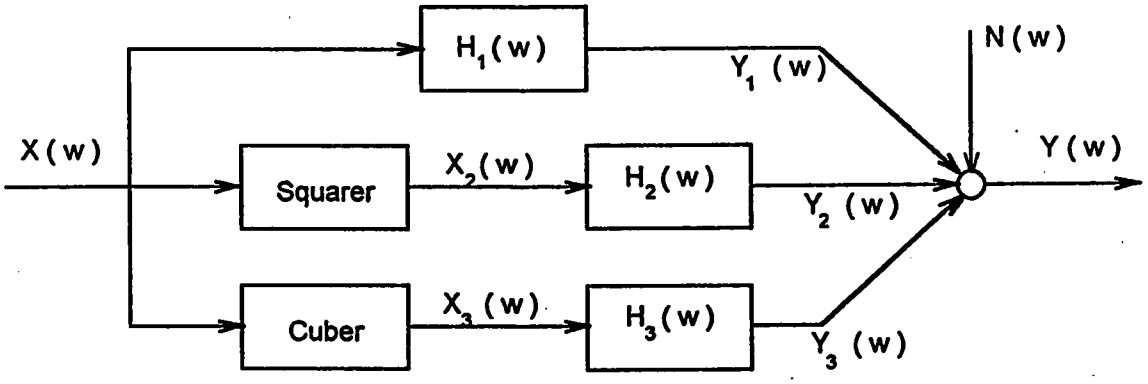

Fig. 4.4 *Qudratic and cubic Hammerstein models in parallel with a linear system.*

The optimum linear system $H_o(\omega)$ is found from the measurements of only the input $x(t)$ and the output $y(t)$ as

$$H_o(\omega)=\frac{S_{xy}(\omega)}{S_{xx}(\omega)} \qquad (4.14)$$

The output $y_2(t)$ is uncorrelated with the input $x(t)$ due to the square-law operation (i.e. $E[x(t)x^2(t)]=0$). Therefore the cross spectral density function $S_{xy}(\omega)$ can be written as

$$\begin{aligned} S_{xy}(\omega) &= S_{xy_1}(\omega)+S_{xy_3}(\omega) \\ &= H_1(\omega)S_{xx}(\omega)+S_{xy_3}(\omega) \end{aligned} \qquad (4.15)$$

The cross spectral density function of a cubic Hammerstein model is given by

$$S_{xy_3}(\omega)=3\sigma_x^{\,2}H_3(\omega)S_{xx}(\omega) \qquad (4.16)$$

where σ_x is the standard deviation of $x(t)$ substituting Eq. (4.16) into Eq. (4.15) yields

$$S_{xy}(\omega)=\{H_1(\omega)+3\sigma_x^{\,2}H_3(\omega)\}S_{xx}(\omega) \qquad (4.17)$$

and therefore the optimum linear system $H_O(\omega)$ is found to be

$$H_o(\omega)=\frac{S_{xy}(\omega)}{S_{xx}(\omega)}=H_1(\omega)+3\sigma_x^{\,2}H_3(\omega) \qquad (4.18)$$

Using the optimum linear transfer function $H_o(\omega)$ defined in Eq. (4.18), the output $Y(\omega)$ can be separated into uncorrelated linear, nonlinear, and noise

components as shown in Fig. 4.5. To identify the linear systems $H_1(\omega)$, $H_2(\omega)$ and $H_3(\omega)$ of Fig. 4.5, one needs to compute the finite Fourier transforms of the inputs to these linear systems with the non-zero mean values removed as follows

$$X(\omega)=F.T.[x(t)]; \qquad Y(\omega)=F.T.[y(t)-\mu_y]$$
$$X_2(\omega)=F.T.[x^2(t)-\mu_{x^2}]; \qquad Z(\omega)=F.T.[x^3(t)-3\sigma_x^2 x(t)] \tag{4.19}$$

where $z(t)=x^3(t)-3\sigma_x^2 x(t)$ is the input to $H_3(\omega)$ in Fig. 4.5.

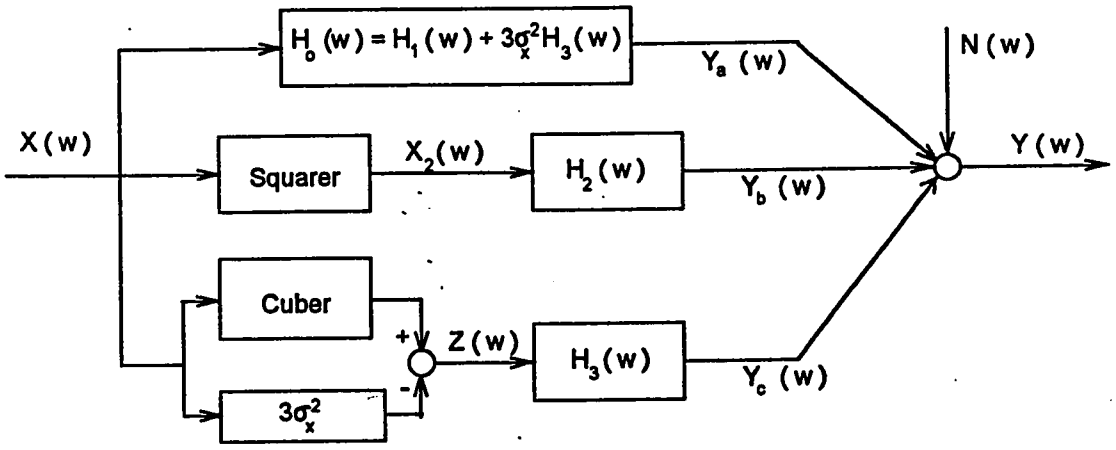

Fig. 4.5 *Equivalent Nonlinear model with uncorrelated outputs.*

Since the outputs $y_a(t)$, $y_c(t)$ and $n(t)$ are uncorrelated with $x_2(t)=x^2(t)$, then the cross spectral density function between $x_2(t)$ and $y(t)$ can be written as

$$S_{x_2y}(\omega)=S_{x_2y_b}(\omega)=H_2(\omega)S_{x_2x_2}(\omega) \tag{4.20}$$

The linear system $H_2(\omega)$ can be determined from the above equation as

$$H_2(\omega)=\frac{S_{x_2y}(\omega)}{S_{x_2x_2}(\omega)} \tag{4.21}$$

where $$S_{x_2x_2}(\omega)=\frac{1}{T}E[X_2^*(\omega)X_2(\omega)] \tag{4.22}$$

and $$S_{x_2y}(\omega)=\frac{1}{T}E[X_2^*(\omega)Y(\omega)] \tag{4.23}$$

The same thing can be done to the linear system $H_3(\omega)$ because the outputs $y_a(t)$, $y_b(t)$ and $n(t)$ are uncorrelated with $z(t)=x^3(t)-3\sigma_x^2x(t)$. Therefore, the cross spectral density function between $z(t)$ and $y(t)$ can be written as

$$S_{zy}(\omega)=S_{zy_c}(\omega)=H_3(\omega)S_{zz}(\omega) \tag{4.24}$$

and hence the linear system $H_3(\omega)$ can be determined from the above equation as

$$H_3(\omega)=\frac{S_{zy}(\omega)}{S_{zz}(\omega)} \tag{4.25}$$

where $$S_{zz}(\omega)=\frac{1}{T}E[Z^*(\omega)Z(\omega)] \;;\; S_{zy}(\omega)=\frac{1}{T}E[Z^*(\omega)Y(\omega)] \tag{4.26}$$

Finally, $H_1(\omega)$ is determined from Eq. (4.18) as

$$H_1(\omega)=H_o(\omega)-3\sigma_x^2H_3(\omega) \tag{4.27}$$

and this complete solving the identification problem of the model shown in Fig. 4.4.

4.4 SEA WAVE FORCE MODEL

An important engineering application is the study of the effect of wave forces on offshore structures. Some examples of offshore structures are vertical piles, bridge supports and oil and gas platforms. Fig. 4.6 shows a cylindrical structure subjected to ocean waves. The input to the structure is the wave velocity $x(t)$ and it is assumed to be a Gaussian stationary random process. This input record at a specified depth produces a wave force $y(t)$ on the structure at the same depth. In this section, the measurable one-sided spectral density $G(\omega)$ will be used in the formulas.

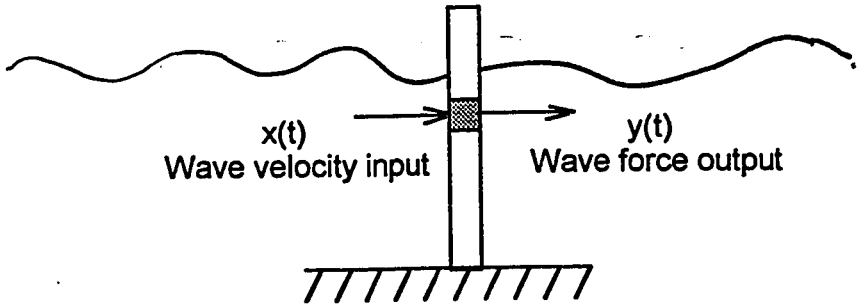

Fig. 4.6 *Illustration of sea wave force problem.*

Morison's equation, as given by Eq. (4.28), is widely used to study such wave forces on offshore structure *[46]*. In this equation, the output wave force $y(t)$ due to an input wave velocity $x(t)$ consists of two main components:

1- A linear inertial force $m(t)$ proportional to the wave acceleration $\dot{x}(t)$.

2- A nonlinear drag force $d(t)$ proportional to $x(t)|x(t)|$ (a squarer with sign).

Therefore, Morison's equation is of the form

$$y(t) = m(t) + d(t) = c_1\dot{x}(t) + c_2x(t)|x(t)| \qquad (4.28)$$

where the coefficients c_1 and c_2 are assumed to be constants.

Based on experimental work , Bendat *[2]* found that the coefficients c_1 and c_2 can vary with frequency and thus he generalized Morison's equation so that linear frequency response functions are used instead of the constants c_1 and c_2. This is illustrated in Fig.4.7. The difficulty in this problem arises because of two main reasons :

1- The drag force has a nonlinear relationship involving a squarer with sign.

2- The drag and inertia forces are correlated.

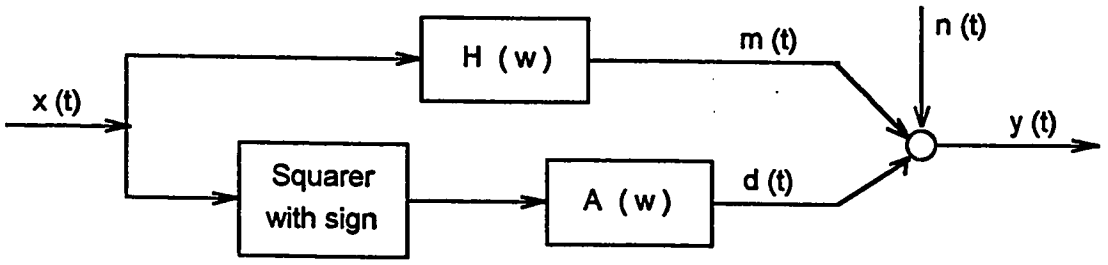

Fig. 4.7 *Nonlinear wave force model with parallel linear and nonlinear systems.*

The above two problems can be avoided by finding an equivalent model to Fig. 4.7. Based on the assumption that *x(t)* is a Gaussian stationary random process with zero mean value, the squarer with sign can be approximated by a zero-memory third-order polynomial least squares approximation having the form

$$x(t)|x(t)| \approx v(t) = 3k\sigma_x^2 x(t) + kx^3(t) \quad ; \quad k = \sqrt{\frac{2}{\pi}}/3\sigma_x \qquad (4.29)$$

where σ_X is the standard deviation of *x(t)*. Therefore, the squarer with sign can

be replaced by the sum of a linear operation plus a cubic operation as shown in Fig. 4.8.

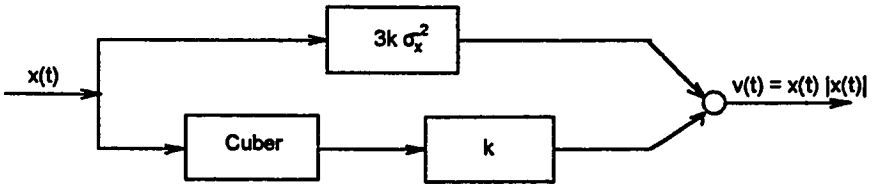

Fig. 4.8 *Zero-memory third-order polynomial nonlinear model for squarer with sign.*

Combining Fig.s 4.8 and 4.7 yields the nonlinear wave force model shown in Fig. 4.9 which can be simplified as in Fig. 4.10.

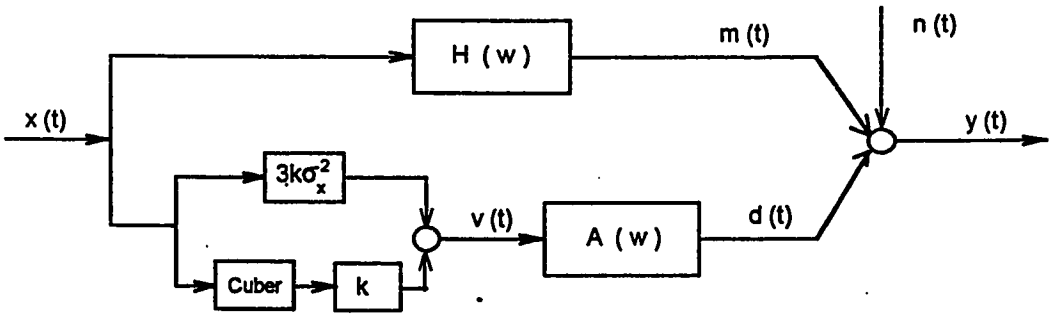

Fig. 4.9 *Nonlinear wave force model approximating Fig. 4.7.*

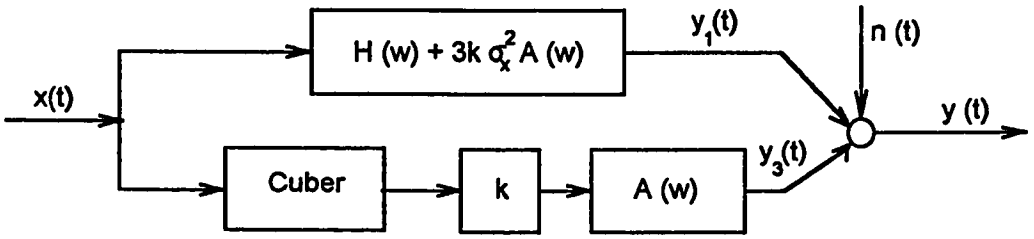

Fig. 4.10 *Nonlinear wave force model with correlated outputs.*

To avoid the second problem (drag and inertia forces correlation), Bendat *[2]* obtained a model equivalent to Fig. 4.10 consisting of an overall optimum linear system in parallel with an uncorrelated revised nonlinear system as shown in Fig. 4.11.

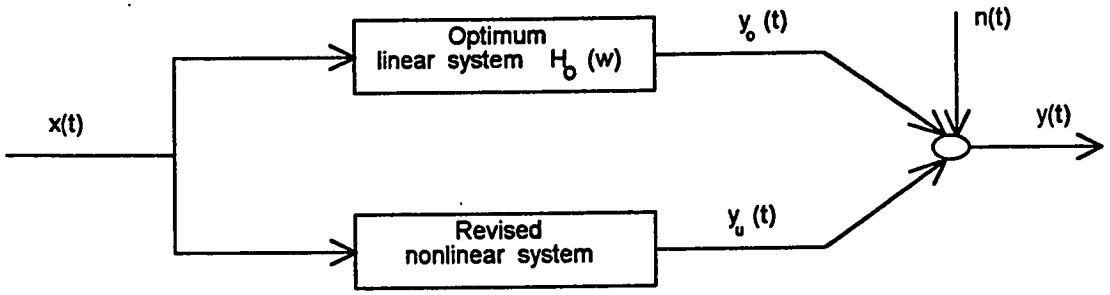

Fig. 4.11 *Nonlinear model with parallel optimum linear system and revised nonlinear system where outputs are uncorrelated.*

Fourier transform relations for Fig. 4.10 are

$$Y(\omega) = Y_1(\omega) + Y_3(\omega) + N(\omega) \tag{4.30}$$

$$Y_1(\omega) = [H(\omega) + 3k\sigma_x^2 A(\omega)]\, X(\omega) \tag{4.31}$$

$$Y_3(\omega) = k\, A(\omega)\, X_3(\omega) \tag{4.32}$$

where $X_3(\omega)$ is the Fourier transform of $x^3(t)$.

The cross-spectral density function between a cubic $(x_3(t)=x^3(t))$ and its input $x(t)$ for $x(t)$ being Gaussian can be obtained as

$$Gxx_3(\omega) = 3\sigma_x^2 Gxx(\omega) \tag{4.33}$$

Substituting Eq.s (4.32) and (4.31) into Eq. (4.30) yields

$$Y(\omega) = [H(\omega) + 3k\sigma_x^2 A(\omega)]\, X(\omega) + k\, A(\omega)\, X_3(\omega) + N(\omega) \qquad (4.34)$$

Using Eq.s (4.33) and (4.34), the cross-spectral density function between $y(t)$ and $x(t)$, assuming $n(t)$ to be uncorrelated with $x(t)$, is found as

$$G_{xy}(\omega) = [H(\omega) + 6k\sigma_x^2 A(\omega)]\, G_{xx}(\omega) \qquad (4.35)$$

The overall optimum linear frequency response function $H_o(\omega)$ is found from Eq.s (4.14) and (4.35) as

$$H_o(\omega) = \frac{G_{xy}(\omega)}{G_{xx}(\omega)} = H(\omega) + 6k\sigma_x^2 A(\omega) \qquad (4.36)$$

Using Eq.(4.36) and Fig. 4.10, the equivalent model of Fig. 4.11 can be finally refigured as shown in Fig. 4.12.

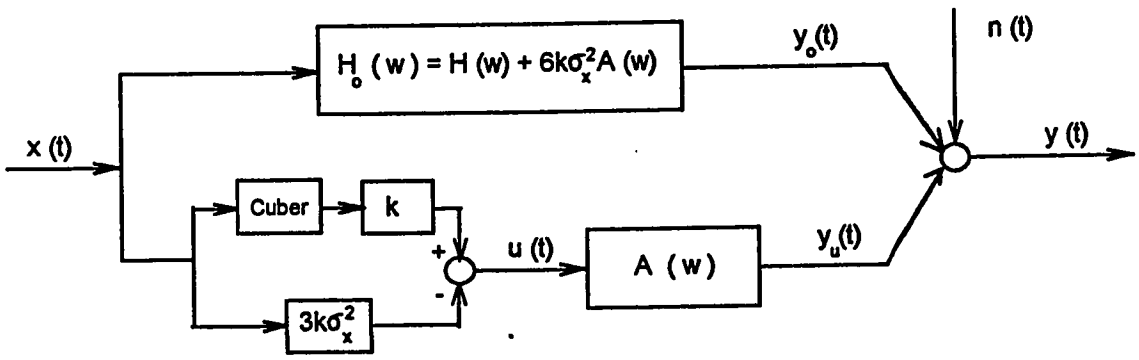

Fig. 4.12 *Nonlinear wave force model with uncorrelated outputs*

Fourier transform relations for Fig. 4.12 are

$$Y(\omega) = Y_o(\omega) + Y_u(\omega) + N(\omega) \qquad (4.37)$$

$$Y_o(\omega) = H_o(\omega)\, X(\omega) \tag{4.38}$$

$$Y_u(\omega) = A(\omega)\, U(\omega) \tag{4.39}$$

$$U(\omega) = k[X_3(\omega) - 3\sigma_x^2 X(\omega)] \tag{4.40}$$

The autospectral density function of $u(t)$ and the cross-spectral density function between $u(t)$ and $y(t)$ can be found from Eq.(4.40), respectively, as

$$Guu(\omega) = k^2[Gx_3x_3(\omega) - 9\sigma_x^4 Gxx(\omega)] \tag{4.41}$$

$$Guy(\omega) = k[Gx_3y(\omega) - 3\sigma_x^2 Gxy(\omega)] \tag{4.42}$$

where

$$G_{x_3y}(\omega) = \frac{2}{T} E[X_3^*(\omega) Y(\omega)] \tag{4.43}$$

and T is the length of the record. Since $u(t)$ is uncorrelated with both $y_o(t)$ and $n(t)$, then

$$G_{uy}(\omega) = G_{uy_o}(\omega) \tag{4.44}$$

Therefore, the frequency response function $A(\omega)$ is found to be

$$A(\omega) = \frac{G_{uy_o}(\omega)}{G_{uu}(\omega)} = \frac{G_{uy}(\omega)}{G_{uu}(\omega)} \tag{4.45}$$

Once $A(\omega)$ is estimated from Eq.s (4.41), (4.42) and (4.45), then $H(\omega)$ can be found from Eq. (4.36)

$$H(\omega) = H_o(\omega) - 6k\sigma_x^2 A(\omega) \qquad (4.46)$$

and the identification problem is completely solved.

For the purpose of supporting the theoretical results, both models of Fig.s 4.4 and 4.7 were simulated using a zero mean stationary white Gaussian process as an input to the models. The results are reported in section 5.4 of chapter 5 and it has been shown that the estimated impulse responses are very close to the theoretical ones.

CHAPTER 5

SIMULATION RESULTS

This chapter presents simulation examples dealing with structure and impulse response identification. Fig. 5.1 represents the class of nonlinear systems considered in chapters 2 and 3. The input $x(t)$ in all examples is taken to be a zero-mean white Gaussian process.

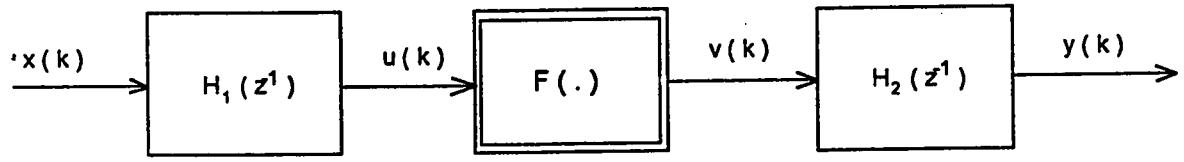

Fig. 5.1 *Wiener-Hammerstein model*

The following linear transfer functions will be used in all examples of sections 5.1 and 5.2.1

$$H_1(z^{-1}) = H_2(z^{-1}) = \frac{0.1813\, z^{-1}}{1 - 0.8187\, z^{-1}}$$

All examples (except Example 5.2) will be simulated using three different types of nonlinearities given by

process 1: General nonlinearity

$$v(k) = F\{u(k)\} = 2 + u(k) + 2u^2(k) + u^3(k) + 3u^4(k)$$

process 2: Odd nonlinearity

$$v(k) = F\{u(k)\} = u(k) + u^3(k)$$

process 3: Even nonlinearity

$$v(k) = F\{u(k)\} = 2 + 2u^2(k) + 3u^4(k)$$

5.1 STRUCTURE IDENTIFICATION VIA CORRELATION FUNCTIONS

This section discusses several simulated examples that supports the structure identification criterion presented in chapter 2. The examples were simulated using a white noise input sequence. The input sequence contains 50 records with each record having a length of 1000 data points. In other words, each model was simulated 50 times with different records of stationary random signals and then the correlation functions were averaged over these 50 runs. All the models that were simulated are subclasses of the Wiener-Hammerstein model shown in Fig. 5.1.

Example 5.1 ***Wiener model:***

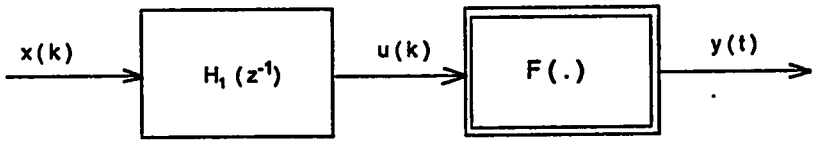

Fig. 5.2 *Wiener model*

Example 5.2 ***Hammerstein model:***

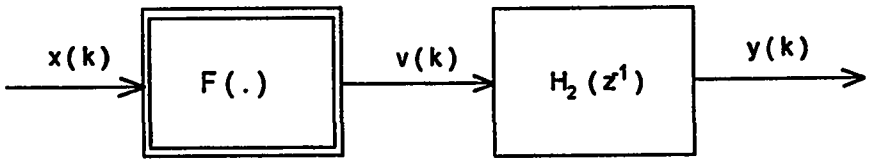

Fig. 5.3 *Hammerstein model*

For this example, the following nonlinearities will be considered

Process 1: *General nonlinearity*

$$v(k) = F_1(x(k)) = 2 + x(k) + 0.5x^2(k)$$

Process 2: *Odd nonlinearity*

$$v(k) = F_2(x(k)) = x(k) + 2x^3(k)$$

Process 3: *Even nonlinearity*

$$v(k) = F_3(x(k)) = 2 + 0.5x^2(k) + 0.5x^4(k)$$

Example 5.3 ***linear model:***

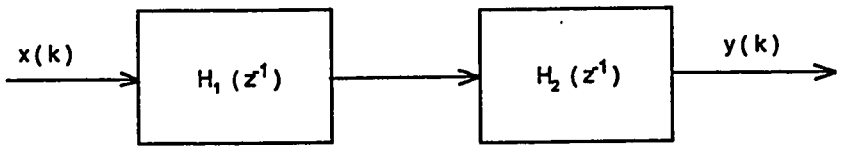

Fig. 5.4 *Linear model*

Example 5.4 ***Static model:***

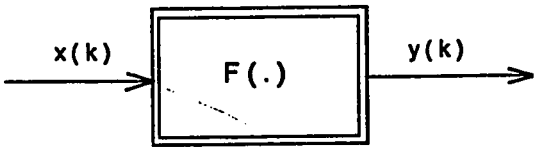

Fig. 5.5 *Static model*

The plots of Fig. 5.6 indicate a Wiener model because the nonlinear cross-correlation function $R_{x^2y}(\tau)$ is proportional to the square of the linear cross-correlation function $R_{xy}(\tau)$. If the nonlinear element has an odd or even nonlinearity only, then the case is different. Fig. 5.7 , for example, shows that for a Wiener model with odd nonlinearity, the nonlinear cross-correlation function $R_{x^2y}(\tau)$ is always zero. When the Wiener model has an even nonlinearity, then the linear cross-correlation function $R_{xy}(\tau)$ is always zero as shown in Fig. 5.8.

The plots of Fig. 5.9 indicate a Hammerstein model because the nonlinear cross-correlation function $R_{x^2y'}(\tau)$ is proportional to the linear cross-correlation function $R_{xy'}(\tau)$. If the nonlinear element has an odd or even nonlinearity only, then the case is different. Fig. 5.10 , for example, shows that for a Hammerstein model with odd nonlinearity, the nonlinear cross-correlation function $R_{x^2y'}(\tau)$ is always zero. When the Hammerstein model has an even nonlinearity, then the linear cross-correlation function $R_{xy'}(\tau)$ is always zero as shown in Fig. 5.11.

The plots of Fig. 5.12 indicate a linear model because the nonlinear cross-correlation function $R_{x^2y'}(\tau)$ is zero for all shifting times.

The plots of Fig. 5.13 indicate a static model with general nonlinearity because both the linear $R_{xy'}(\tau)$ and nonlinear $R_{x^2y'}(\tau)$ cross-correlation functions are always zero except for zero shifting time. As shown in Fig. 5.14 , for a static model with odd nonlinearity, the nonlinear cross-correlation function $R_{x^2y'}(\tau)$ is zero for all shifting times and the linear cross-correlation function $R_{xy'}(\tau)$ is always zero except for zero shifting time. Fig. 5.15 indicates a static model with even nonlinearity because the linear cross-correlation function $R_{xy'}(\tau)$ is zero for all shifting times and the nonlinear cross-correlation function $R_{x^2y'}(\tau)$ is always zero except for zero shifting time.

When the nonlinear element has an odd or even nonlinearity only, then both the Wiener and Hammerstein models will have the same results as obtained in the plots of Examples 5.1 and 5.2 and hence the structure identification using correlation techniques for such models fails. Therefore, a better technique is needed in this respect. To be able to deal with such a situation, a better technique that utilizes the bispectrum will be used in the next section.

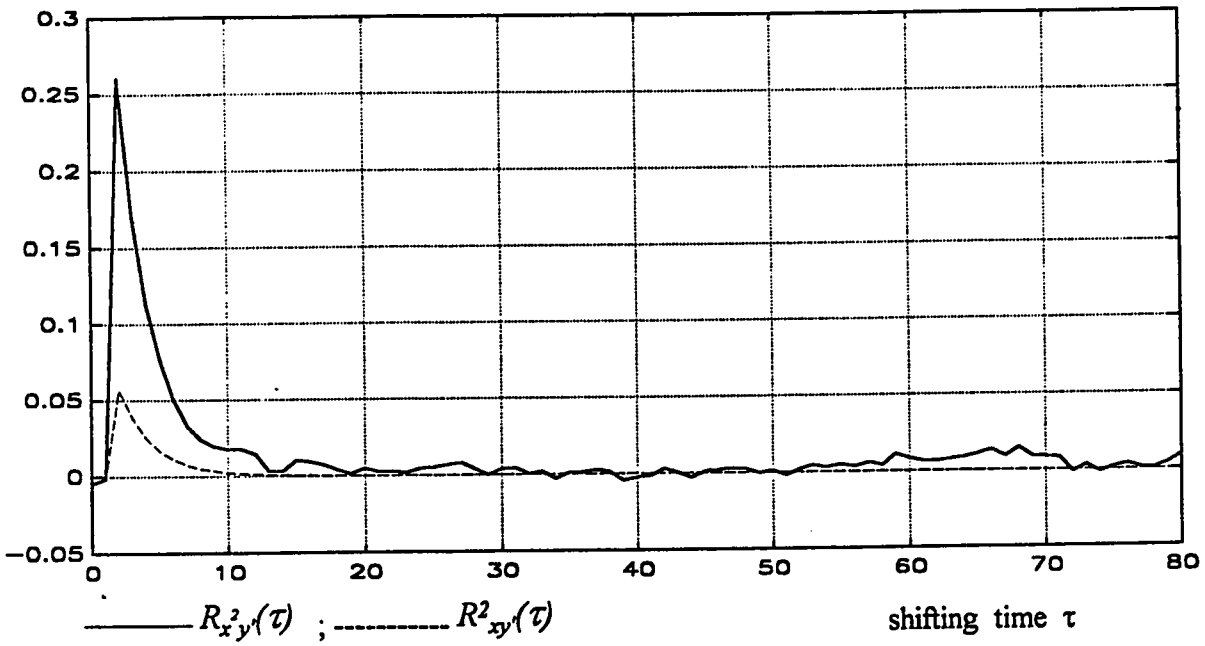

Fig. 5.6 *Wiener model with general nonlinearity (Example 5.1)*

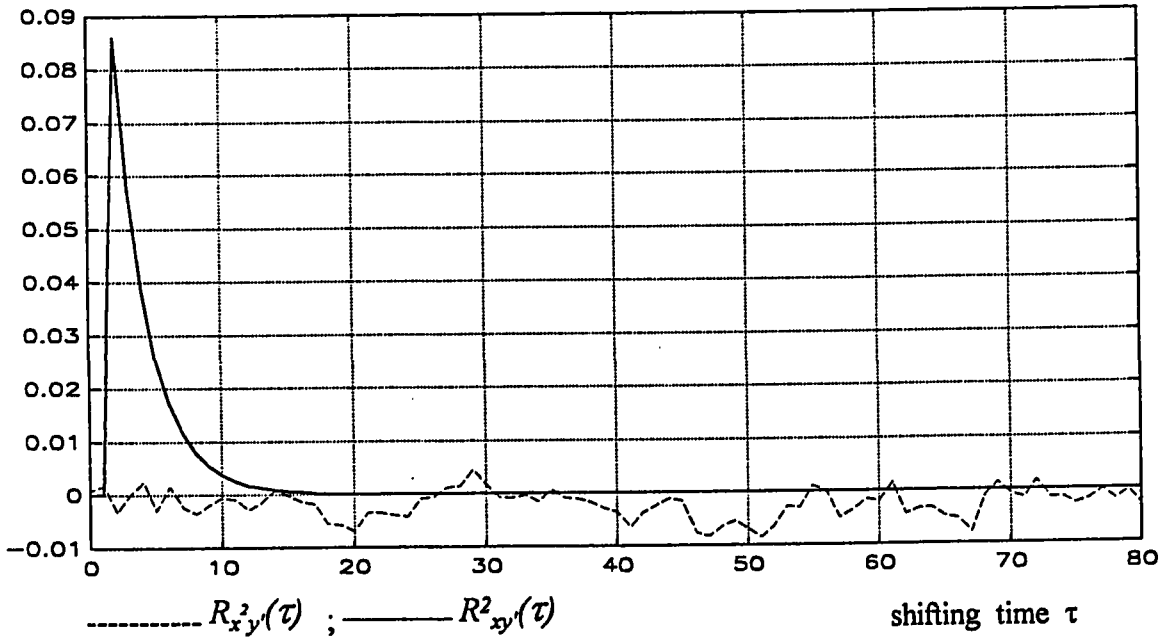

Fig. 5.7 *Wiener model with odd nonlinearity (Example 5.1)*

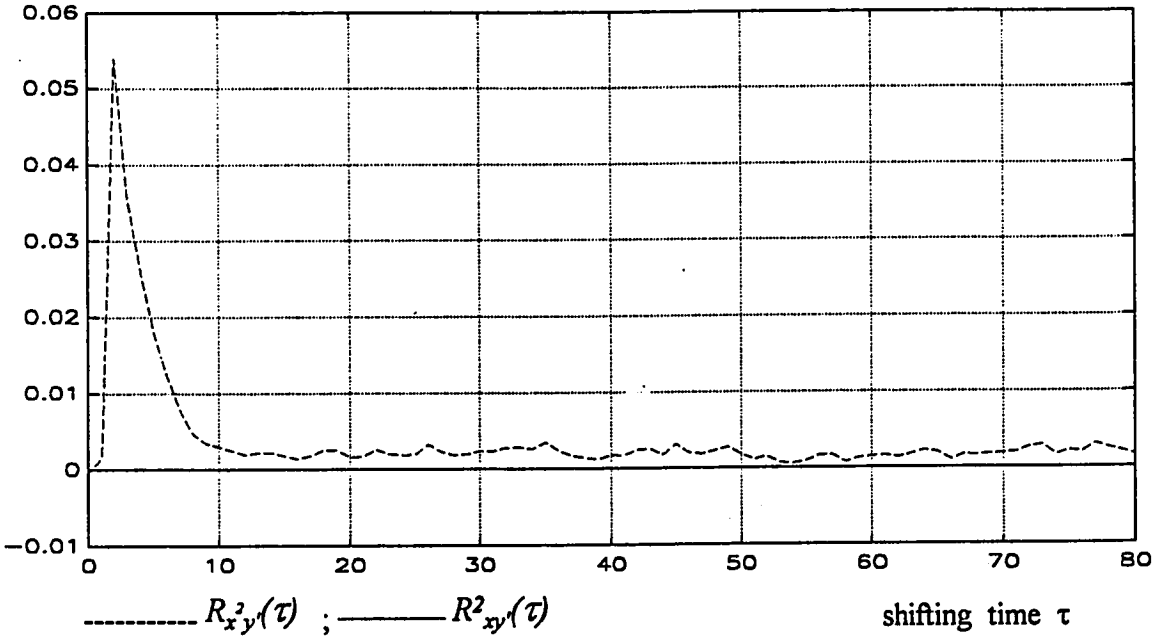

Fig. 5.8 *Wiener model with even nonlinearity (Example 5.1)*

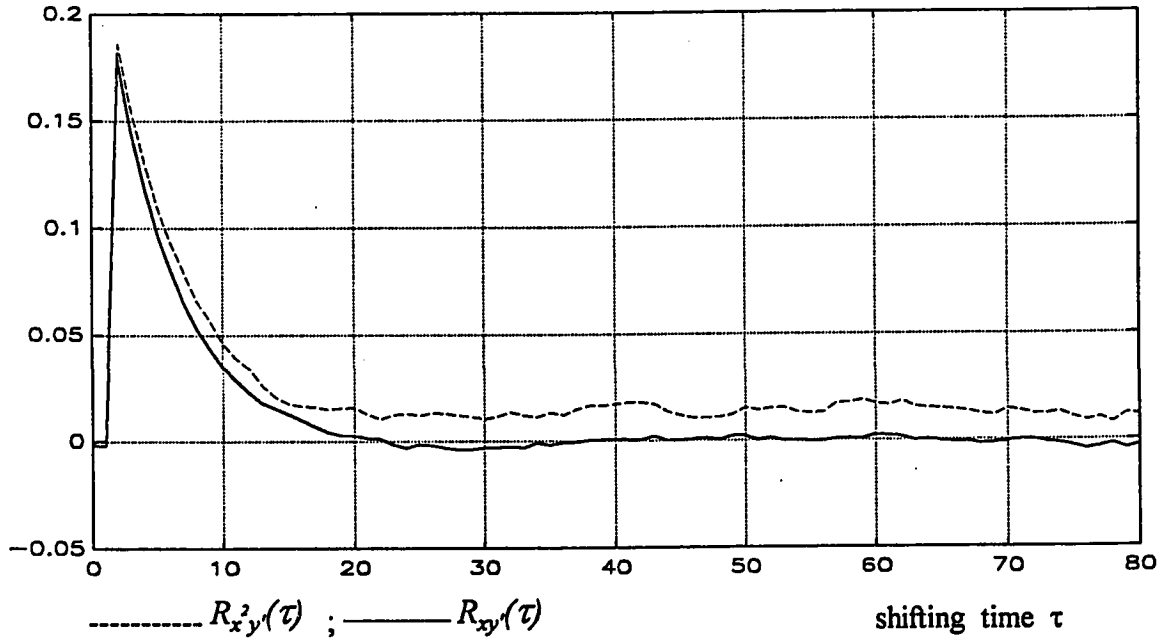

Fig. 5.9 *Hammerstein model with general nonlinearity (Example 5.2)*

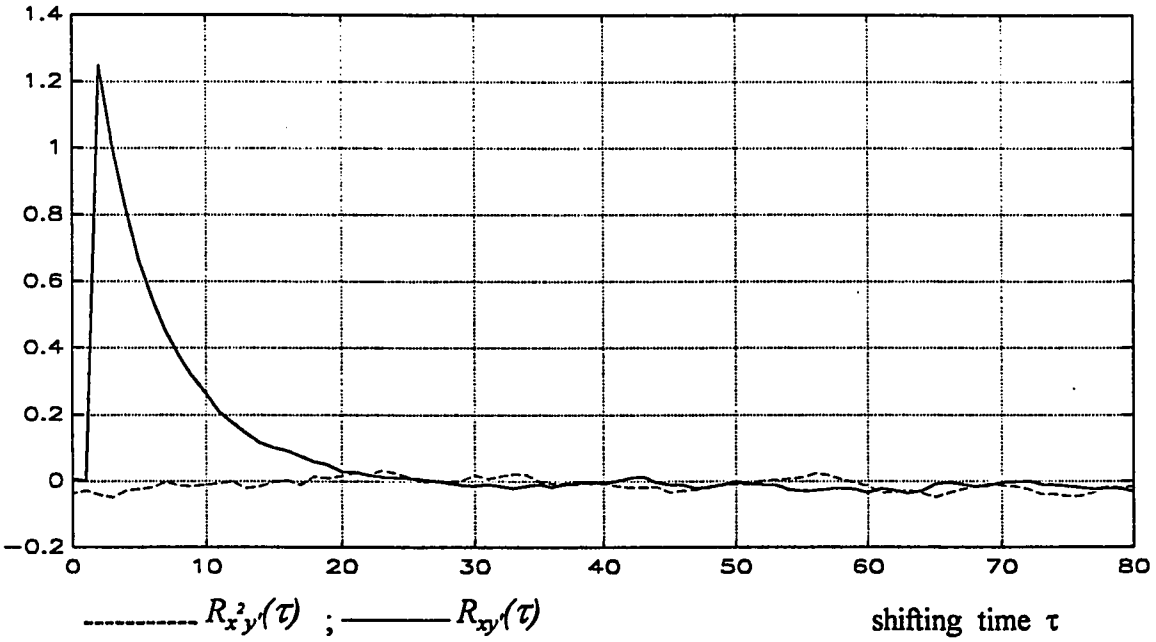

Fig. 5.10 *Hammerstein model with odd nonlinearity (Example 5.2)*

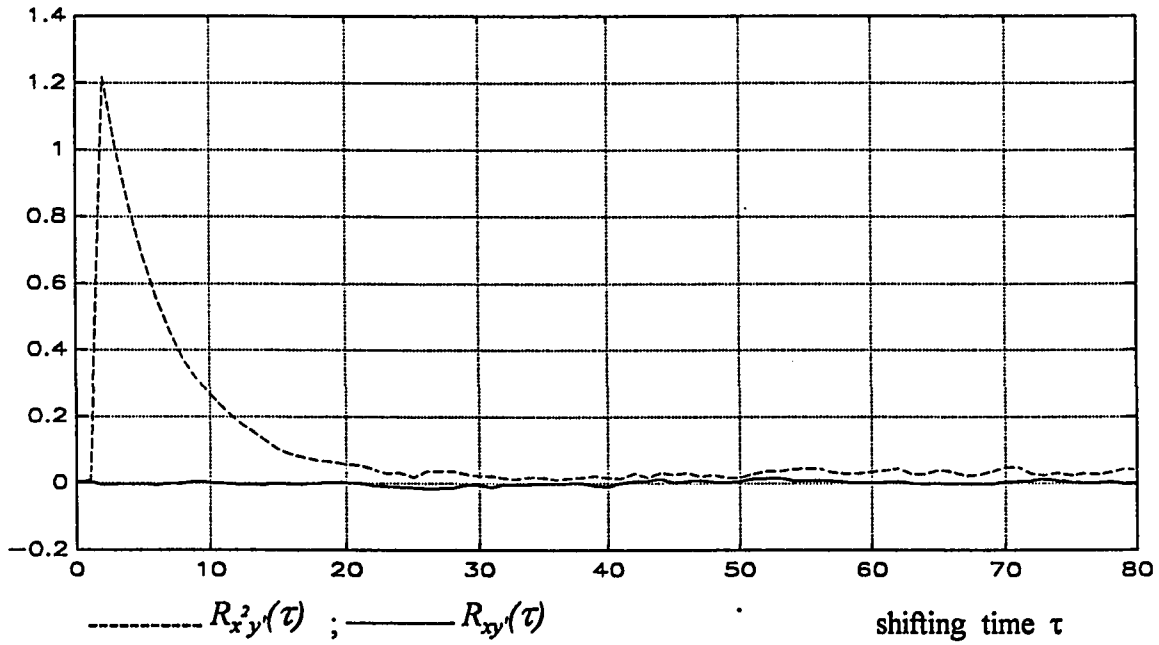

Fig. 5.11 *Hammerstein model with even nonlinearity (Example 5.2)*

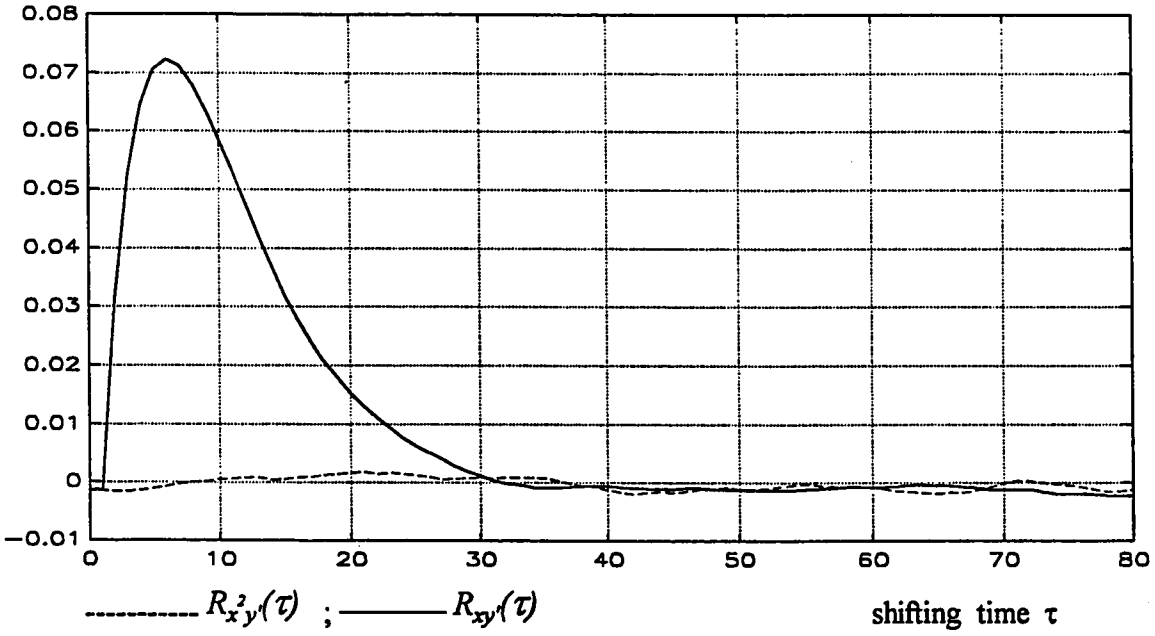

Fig. 5.12 *Linear model (Example 5.3)*

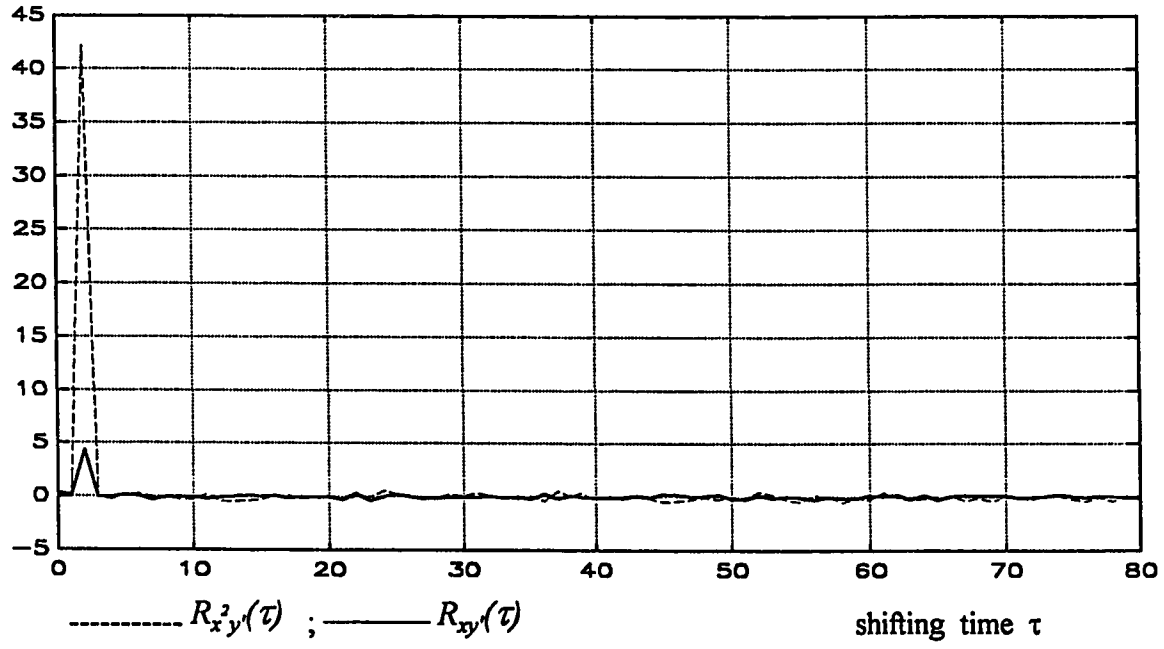

Fig. 5.13 *Static model with general nonlinearity (Example 5.4)*

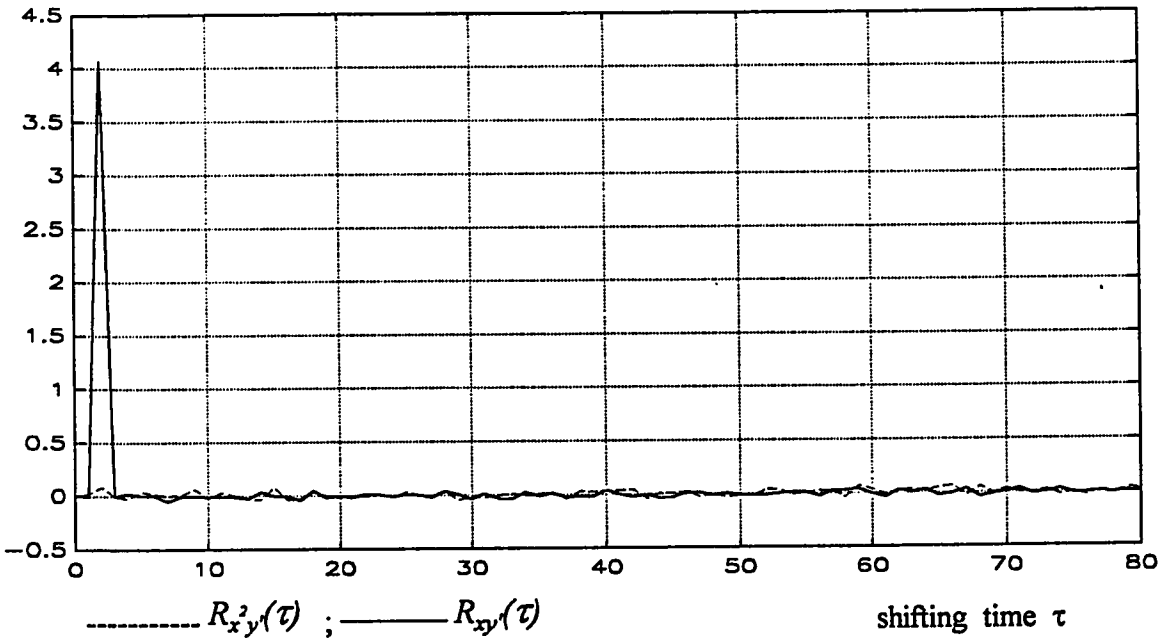

Fig. 5.14 *Static model with odd nonlinearity (Example 5.4)*

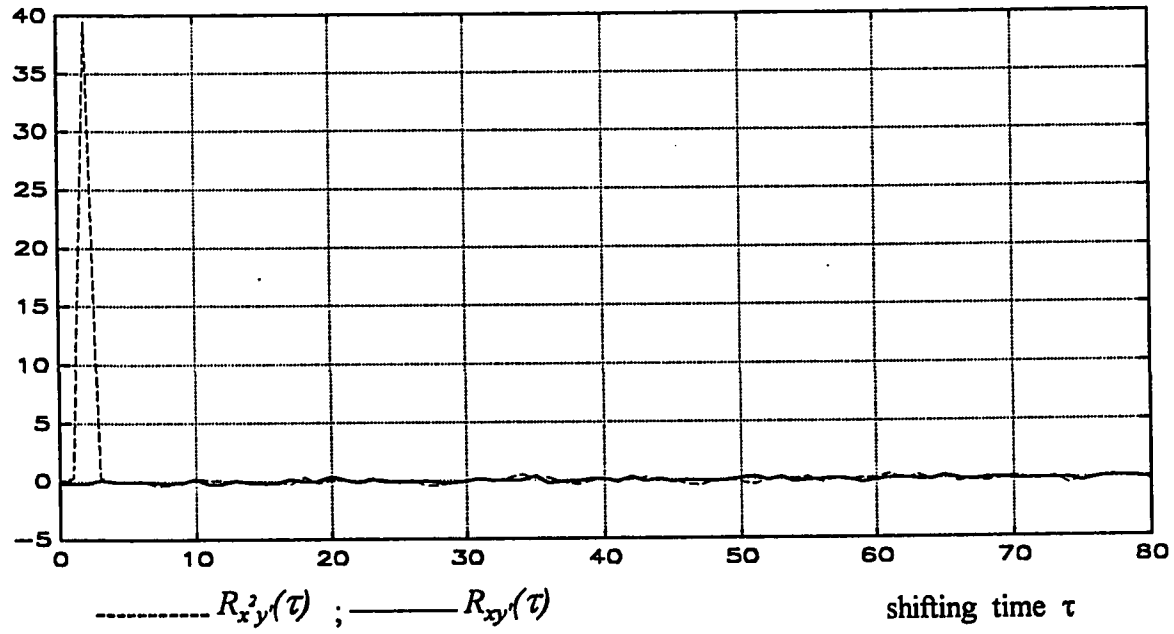

Fig. 5.15 *Static model with even nonlinearity (Example 5.4)*

5.2 STRUCTURE IDENTIFICATION VIA OUTPUT BISPECTRUM

The structure testing criterion outlined in section 3.2.5 will be demonstrated here. The examples considered in this section were simulated using a zero-mean white Gaussian input sequence that has a length of 10240 data points. The bispectrum of the output $By(\omega_1, \omega_2)$ was calculated using the direct method described in Appendix B.

5.2.1 Single-Branch Models

The models considered here are the Wiener model, Hammerstein model and Wiener-Hammerstein model. The cases are discussed in Examples 5.5-5.7 where the results are obtained as the ensemble average over 40 runs.

Example 5.5 ***Wiener model:*** See Fig. 5.2.
Example 5.6 ***Hammerstein model:*** See Fig. 5.3.
Example 5.7 ***Wiener-Hammerstein model:*** See Fig. 5.1.

The plots of Fig. 5.20 indicate a Wiener model because the bispectrum of the output $B_y(\omega_1, \omega_2)$ is almost real for all values of ω_1 and ω_2. For the case of only odd nonlinearities the results show that the structure identification criterion need to be enhanced via, for example, higher order statistics *[e.g., 24]*.

Each of Fig.s 5.23 and 5.24 indicates either a Hammerstein model or a Wiener-Hammerstein model because the bispectrum of the output $B_y(\omega_1, \omega_2)$ is complex as the imaginary part of $B_y(\omega_1, \omega_2)$ is not small as compared to the real part. To differentiate between the Hammerstein and the Wiener Hammerstein models one needs to estimate the bicoherence function $by(\omega_1, \omega_2)$ of the two

models. The bicoherence function for the two models were plotted in Fig. 5.25. This figure shows that one of the bicoherence functions is almost constant while the other one is not. The model with constant bicoherence function corresponds with the Hammerstein model and the other one corresponds with the Wiener-Hammerstein model. It is also clear from Fig.s 5.26-5.29 that when the nonlinearity of the system is odd only then the bispectrum of the output of this system is almost zero compared to that which has even terms. Therefore, the structure identification criterion can be applied only if the nonlinear block has at least one even term.

5.2.2 Parallel-Branch Models

The examples here were carried out by using 50 records. In other words, each model was simulated 50 times with different records of stationary random signals and then the results were averaged over these 50 times. In all simulation examples considered below, the following impulse transfer functions are used to represent various blocks of the simulated models

$$H_1(z^{-1})=\frac{3z^{-1}}{1-0.9z^{-1}}$$

$$H_2(z^{-1})=\frac{z^{-1}-0.5z^{-2}}{1-1.5z^{-1}+0.8z^{-2}}$$

$$H_3(z^{-1})=\frac{2z^{-1}}{1-0.8z^{-1}}$$

Example 5.8 ***Parallel Wiener model:***

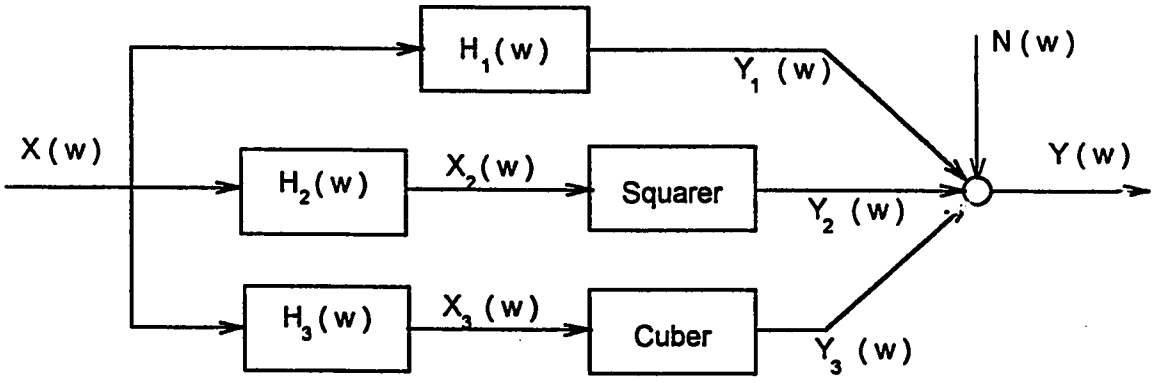

Fig. 5.16 *Parallel Wiener model*

Example 5.9 ***Parallel Hammerstein model:***

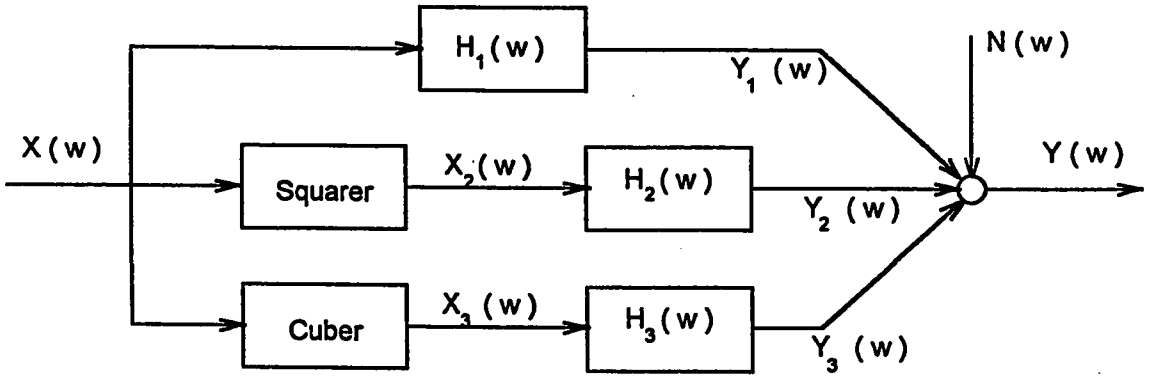

Fig. 5.17 *Qudratic and cubic Hammerstein models in parallel with a linear system.*

Example 5.10 ***Parallel Wiener-Hammerstein model:***

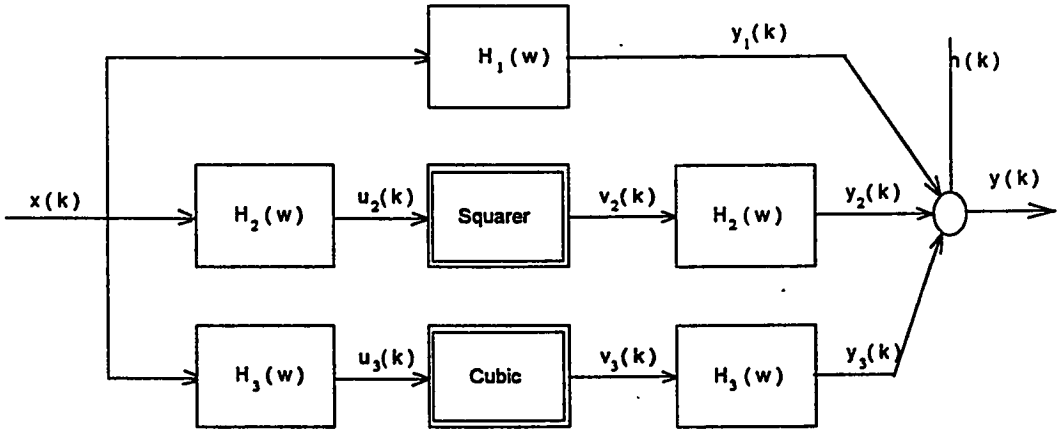

Fig. 5.18 *Parallel Wiener-Hammerstein model.*

Example 5.11 ***Parallel linear static nonlinear blocks:***

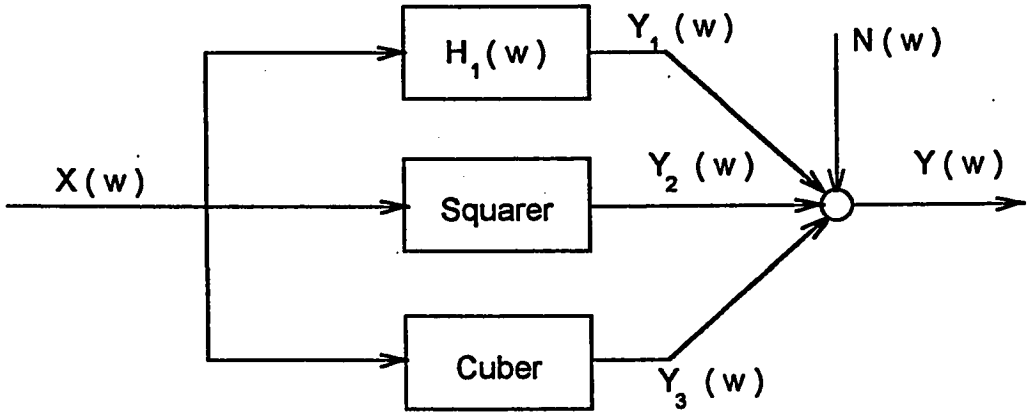

Fig. 5.19 *Parallel linear and static nonlinear blocks.*

The bispectrum of the output sequence of each of the above examples has been estimated and the results are shown in Fig.s 5.30-5.33. It appears from these figures that the obtained results of the structure identification of the considered examples reasonably agree with the structure testing criterion discussed in section 3.2.5. Fig. 5.30 indicates that the corresponding model is more likely of the Wiener type because the bispectrum of the output $B_y(\omega_1, \omega_2)$ is almost real for all values of ω_1 and ω_2.

On the other hand, each of Fig.s 5.31 and 5.32 indicates either a Hammerstein model or a Wiener-Hammerstein model because the imaginary part of $B_y(\omega_1, \omega_2)$ is not small compared to the real part. To differentiate between the two models one needs, as discussed in Examples 5.6 and 5.7, to estimate the bicoherence functions of the two models. The bicoherence function $b_y(\omega_1, \omega_2)$ of the two models were plotted in Fig. 5.33. This figure shows that one of the bicoherence functions is almost constant while the other one varies with ω_1 and ω_2. The model with constant bicoherence function corresponds with the Hammerstein model and the other one corresponds with the Wiener-Hammerstein model. Fig. 5.34 indicates a static model because the bispectrum $B_y(\omega_1, \omega_2)$ is almost constant for all values of ω_1 and ω_2. Examples 5.8-5.11 show that the structure identification criterion developed for single branch can be applied to nonlinear systems of multi parallel branches.

(a) Real and imaginary parts of $B_y(\omega_1, \omega_2)$

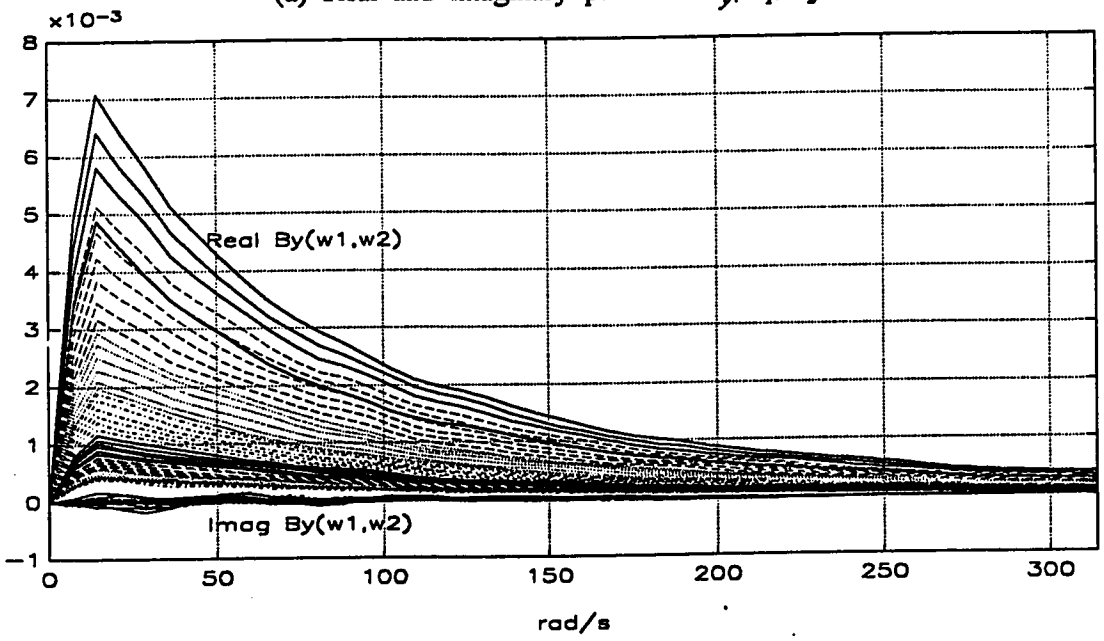

(b) Real $B_y(\omega_1, \omega_2)$

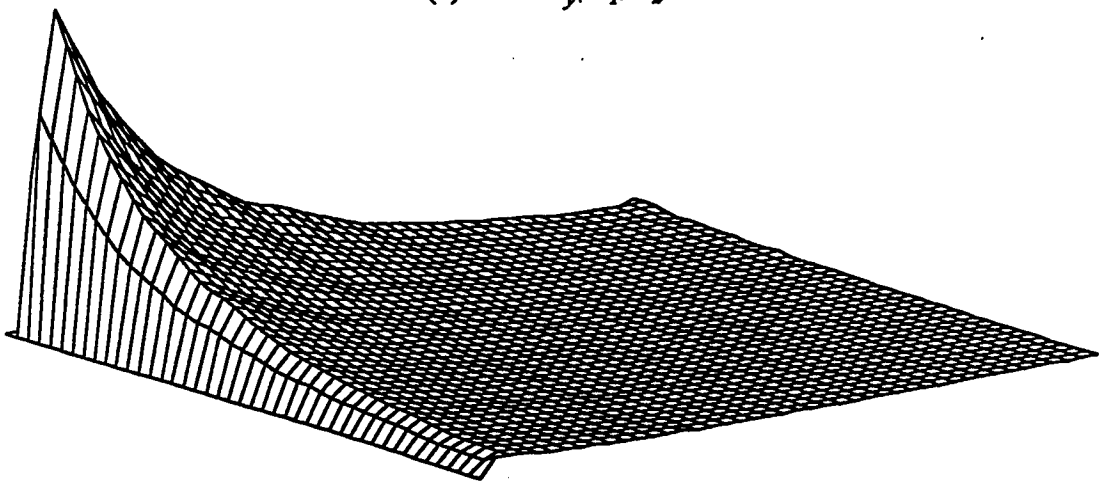

(c) Imag $B_y(\omega_1, \omega_2)$

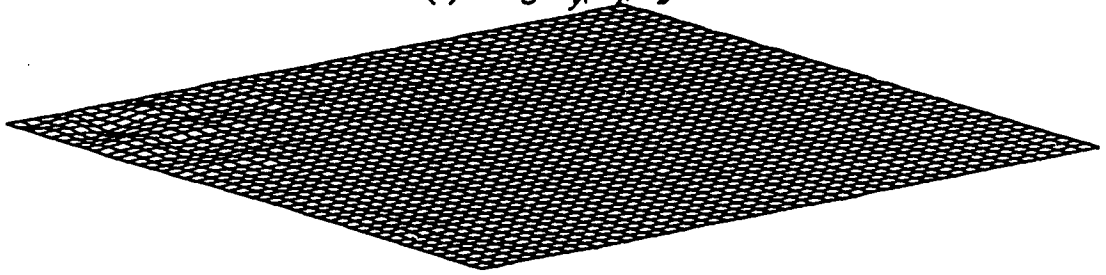

Fig. 5.20 *Bispectrum of the Wiener model of Example 5.5 (process 1)*

(a) Real $B_y(\omega_1, \omega_2)$

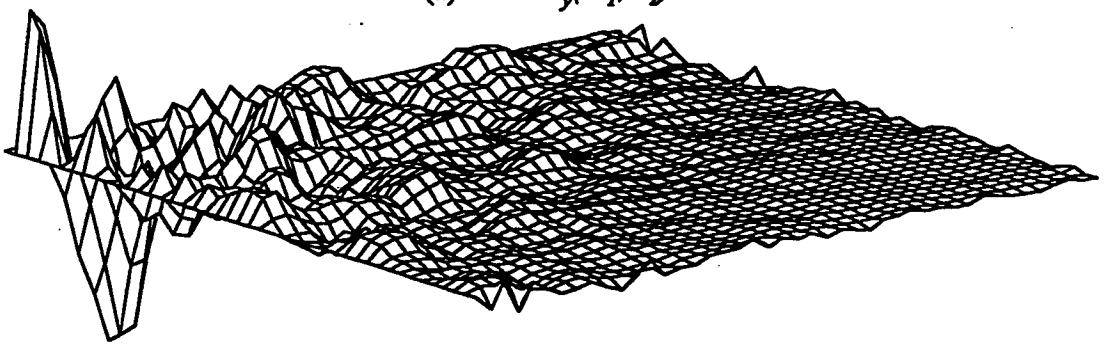

(b) Imag $B_y(\omega_1, \omega_2)$

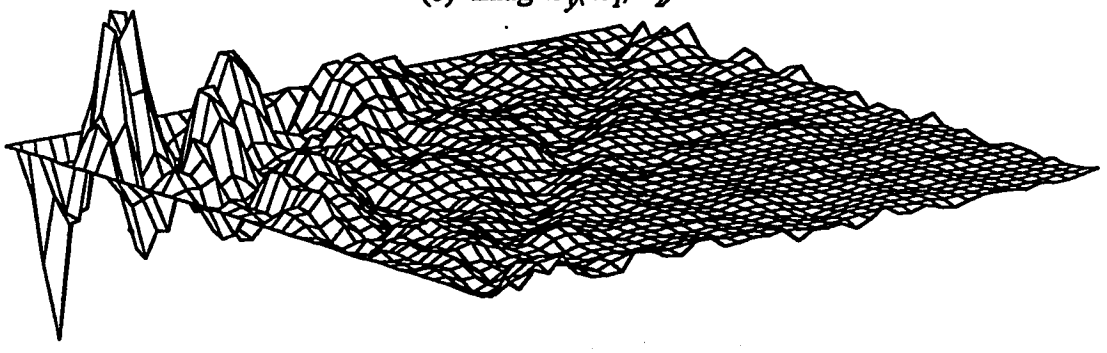

Fig. 5.21 *Bispectrum of the Wiener model of Example 5.5 (process 2)*

(a) Real and imaginary parts of $B_y(\omega_1, \omega_2)$

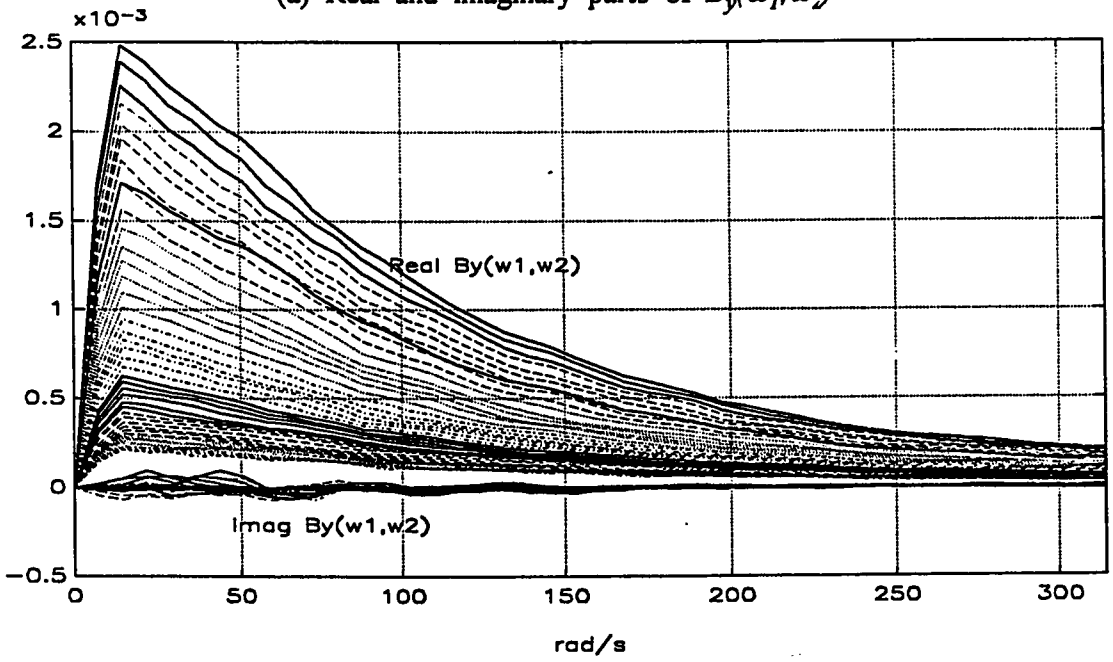

(b) Real $B_y(\omega_1, \omega_2)$

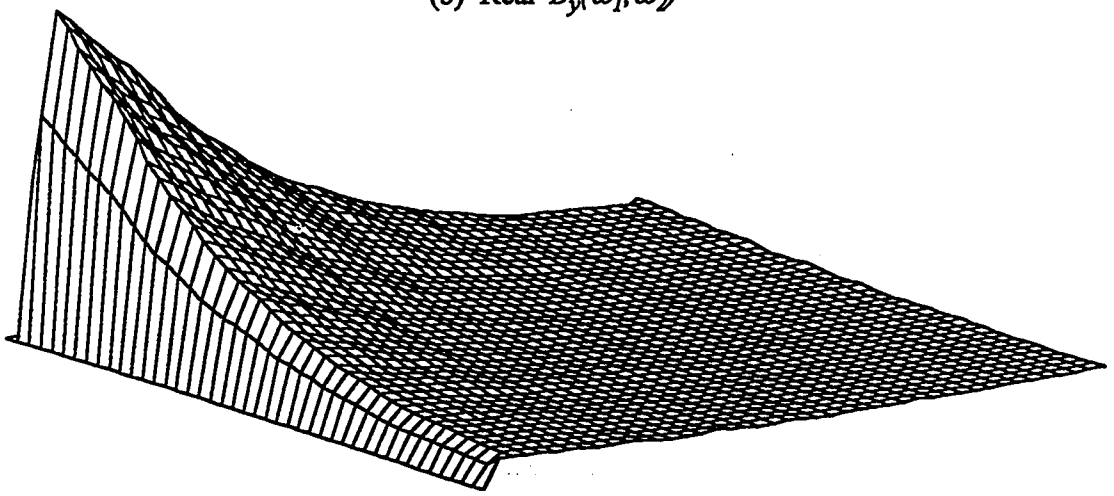

(c) Imag $B_y(\omega_1, \omega_2)$

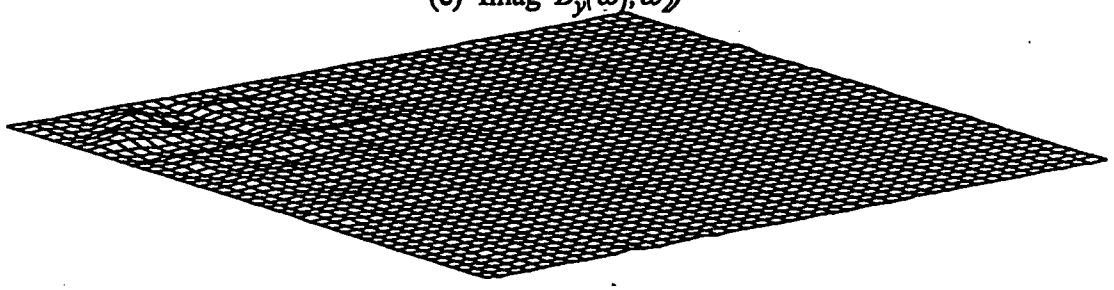

Fig. 5.22 *Bispectrum of the Wiener model of Example 5.5 (process 3)*

(a) Real and imaginary parts of $B_y(\omega_1, \omega_2)$

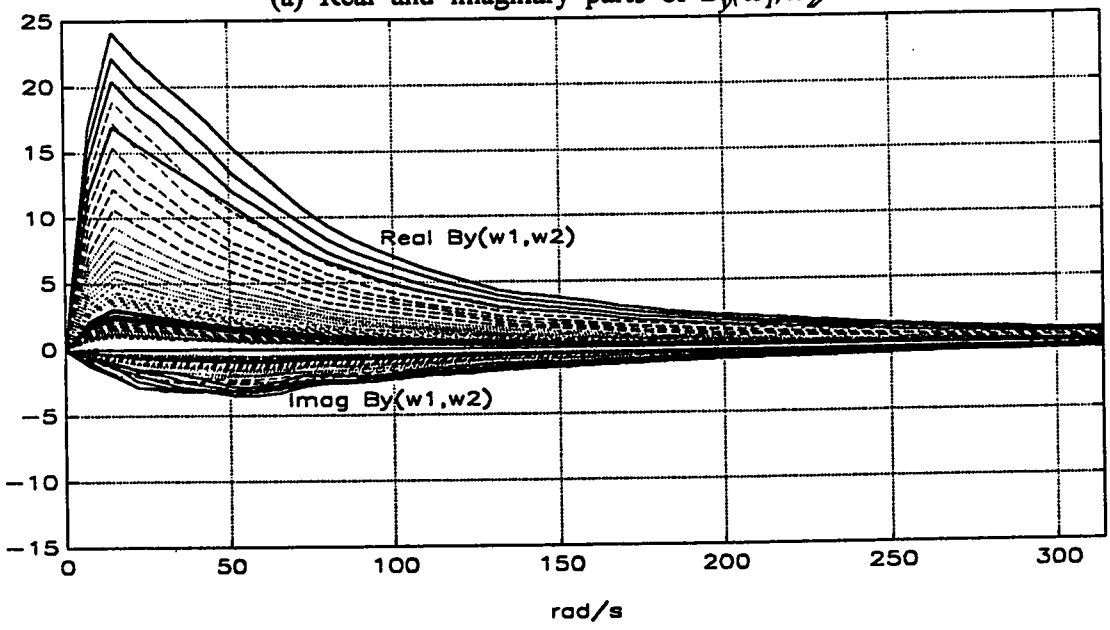

(b) Real $B_y(\omega_1, \omega_2)$

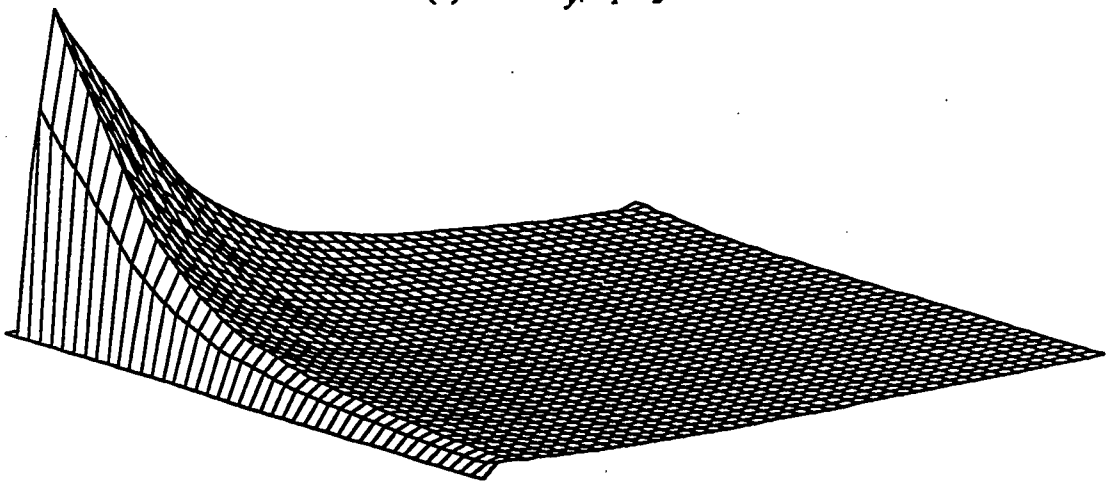

(c) Imag $B_y(\omega_1, \omega_2)$

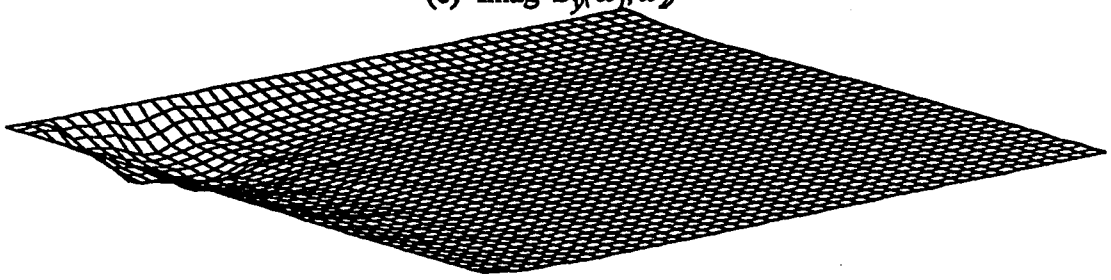

Fig. 5.23 *Bispectrum of the Hammerstein model of Example 5.6 (process 1)*

(a) Real and imaginary parts of $B_y(\omega_1, \omega_2)$

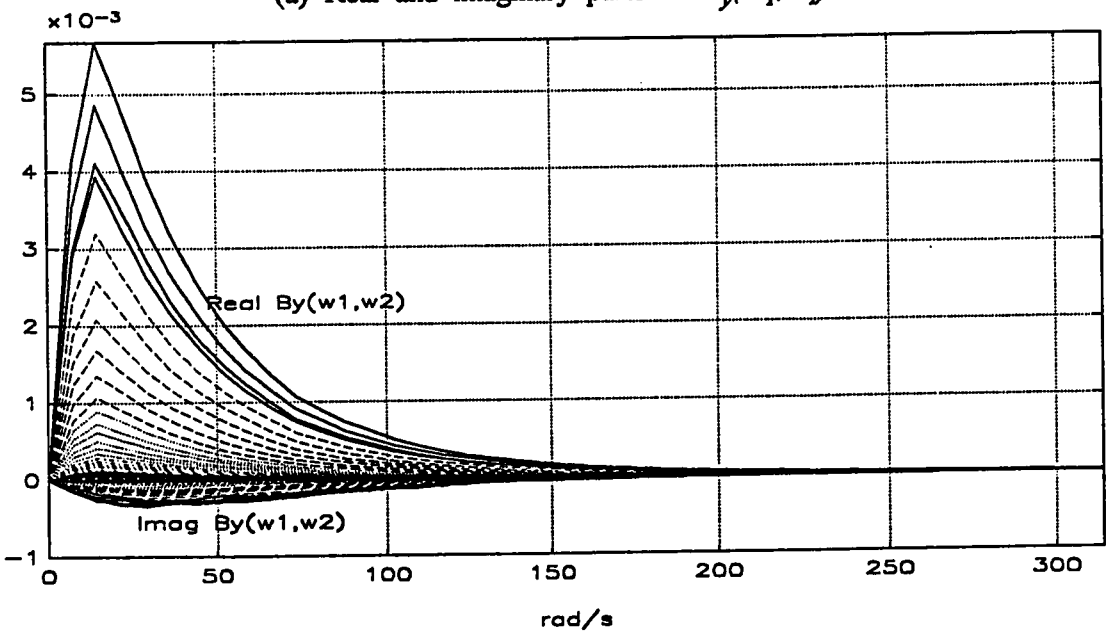

(b) Real $B_y(\omega_1, \omega_2)$

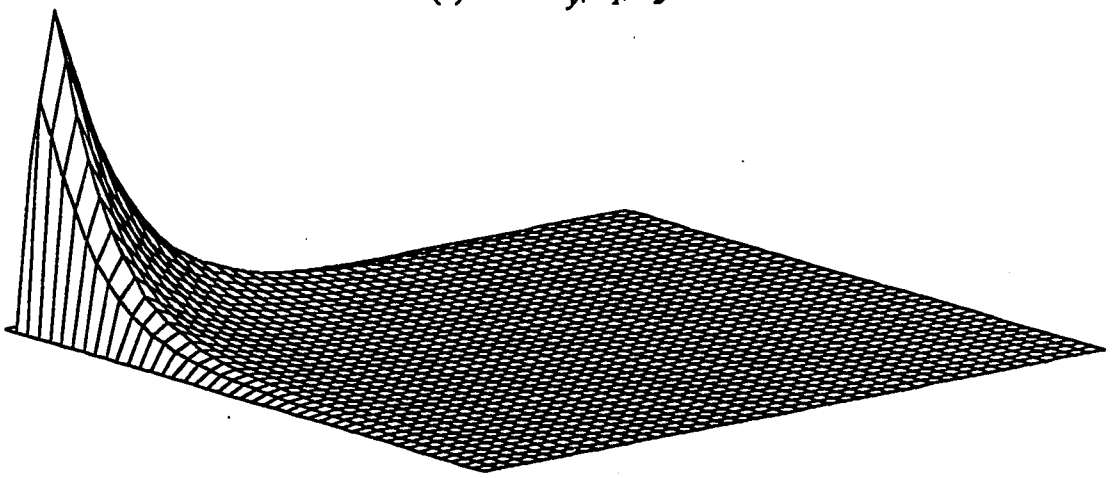

(c) Imag $B_y(\omega_1, \omega_2)$

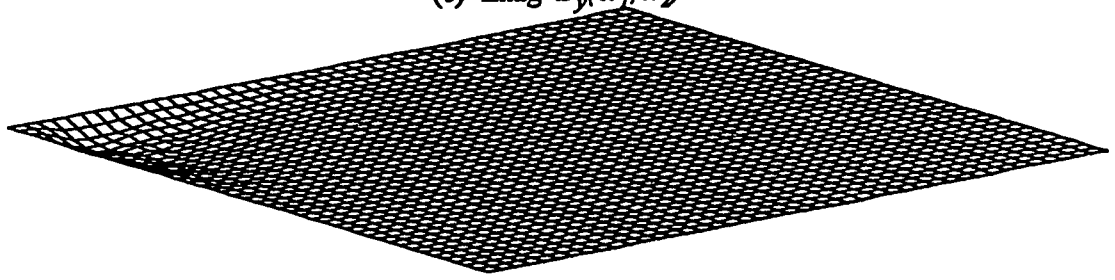

Fig. 5.24 *Bispectrum of the Wiener-Hammerstein model of Example 5.7 (process 1)*

(a) $b_y(\omega_1, \omega_2)$ of Examples 5.6 and 5.7

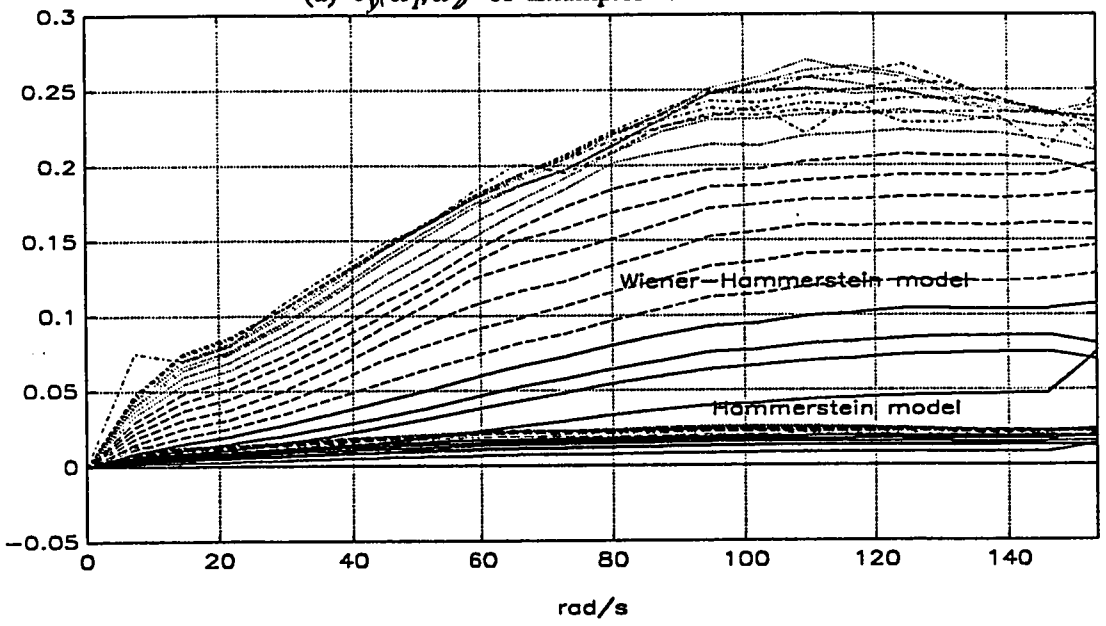

(b) $b_y(\omega_1, \omega_2)$ of the Wiener-Hammerstein model of Example 5.7

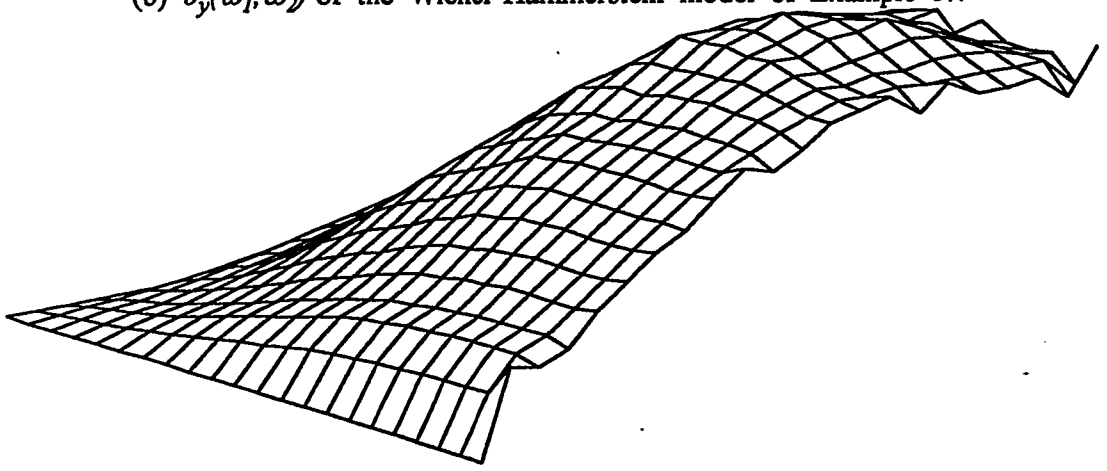

(c) $b_y(\omega_1, \omega_2)$ of the Hammerstein model of Example 5.6

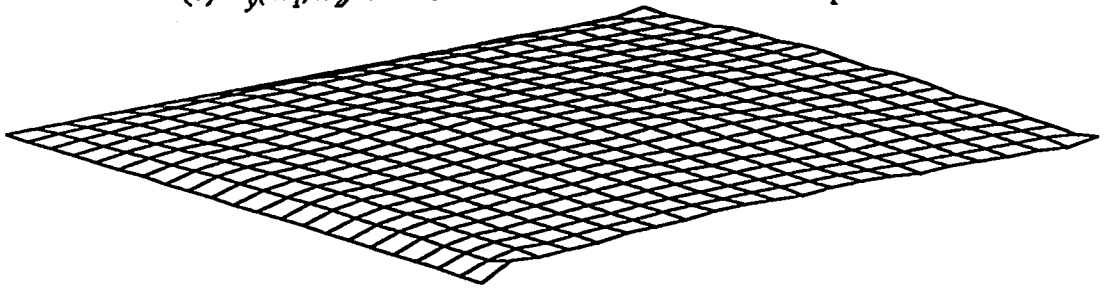

Fig. 5.25 *Bicoherence functions of Examples 5.6 and 5.7 (process 1)*

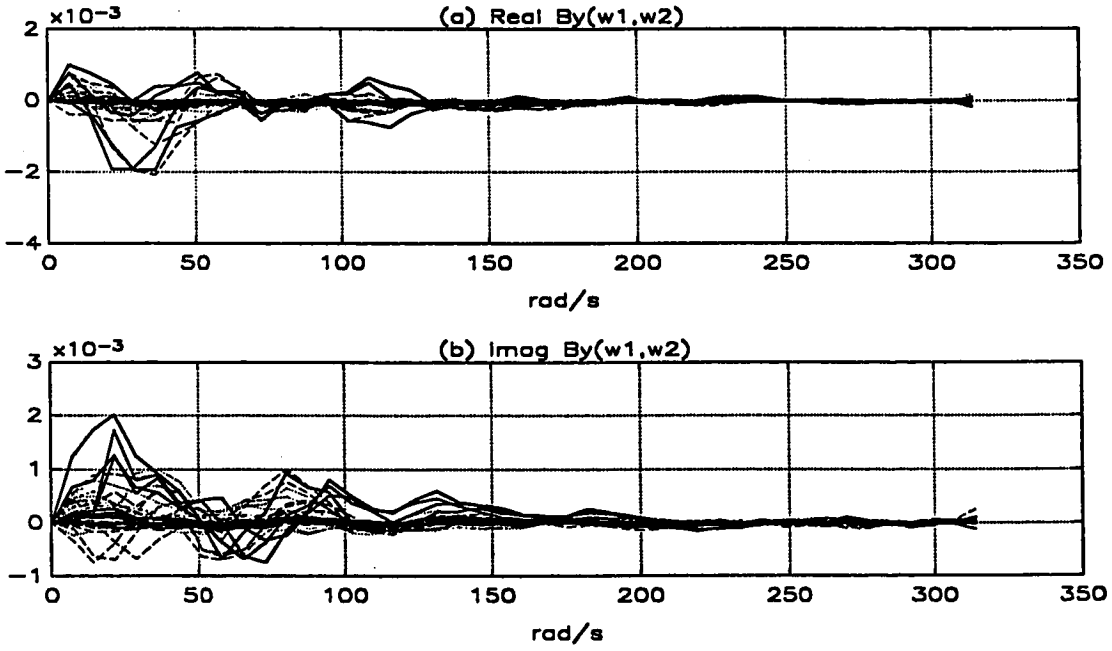

Fig. 5.26 *Bispectrum of the Hammerstein model of Example 5.6 (process 2)*

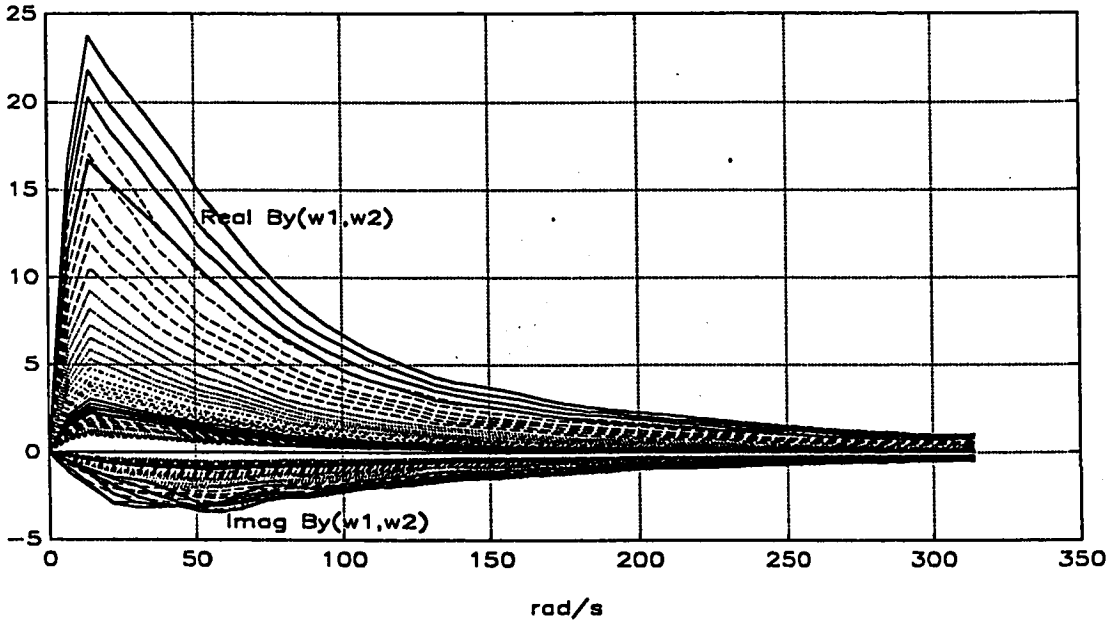

Fig. 5.27 *Bispectrum of the Hammerstein model of Example 5.6 (process 3)*

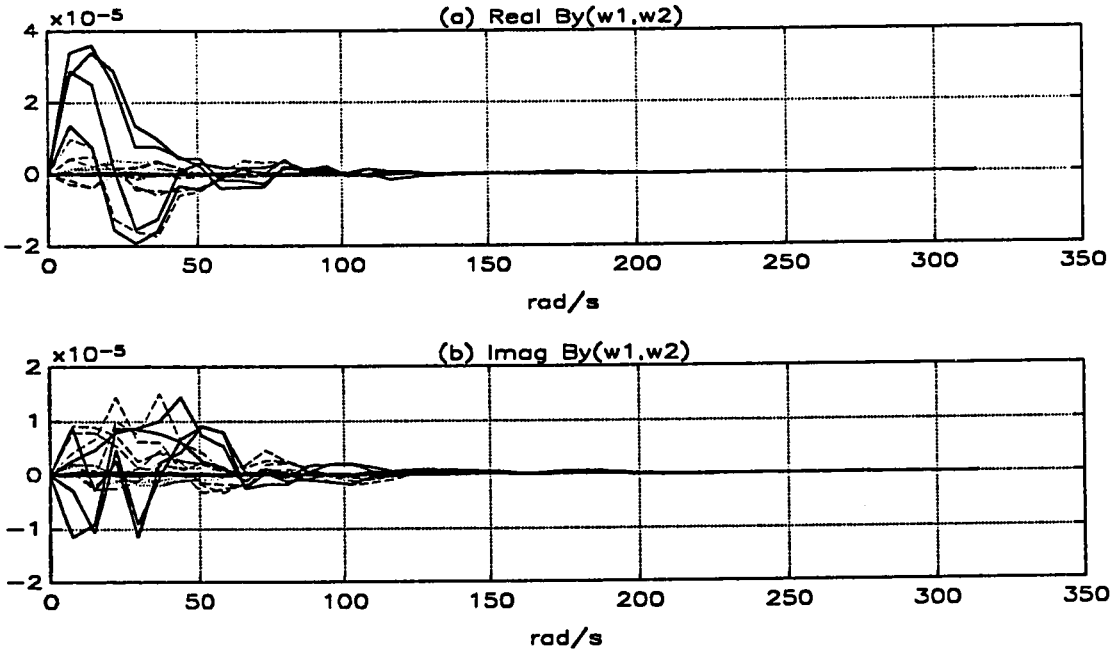

Fig. 5.28 *Bispectrum of the Wiener-Hammerstein model of Example 5.7 (process 2)*

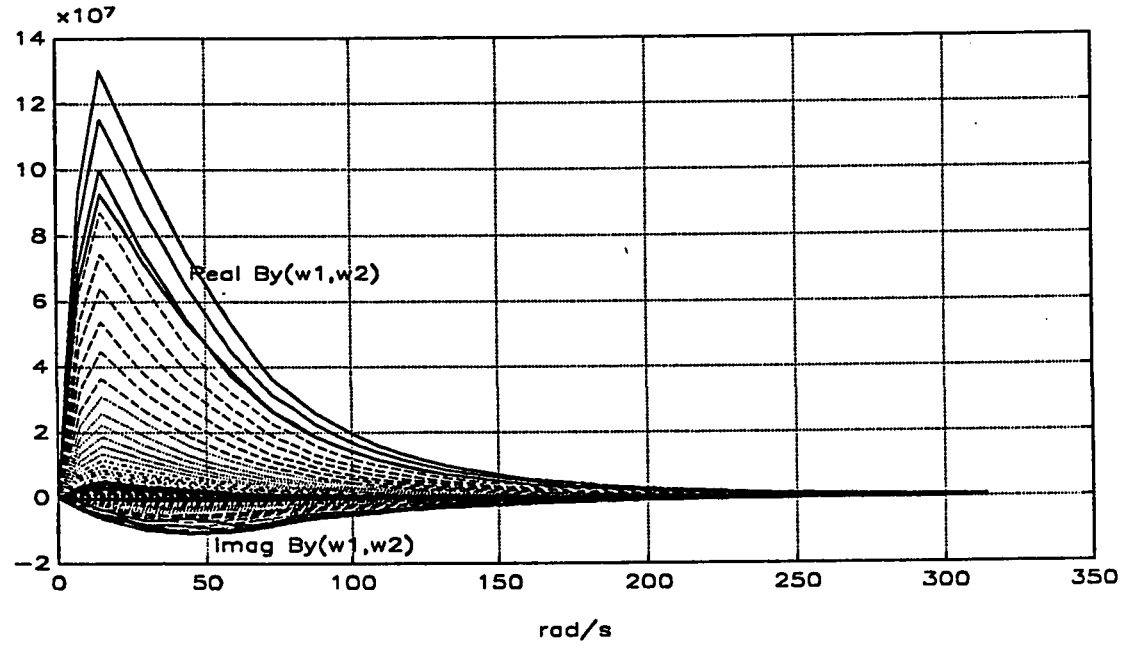

Fig. 5.29 *Bispectrum of the Wiener-Hammerstein model of Example 5.7 (process 3)*

(a) Real and imaginary parts of $B_y(\omega_1, \omega_2)$

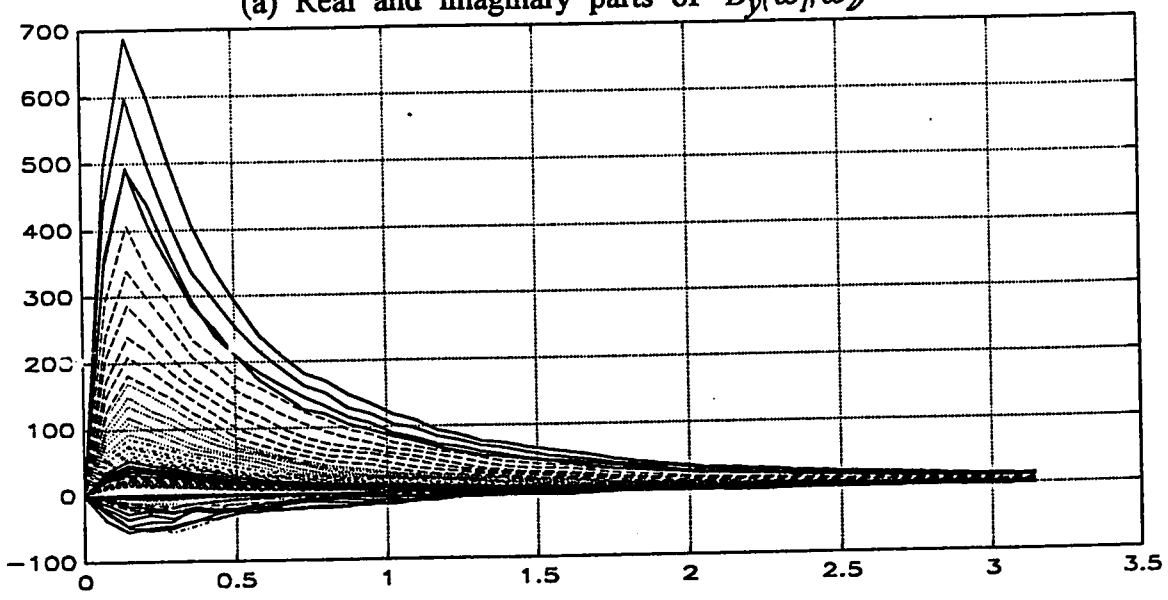

(b) Real By(w1,w2)

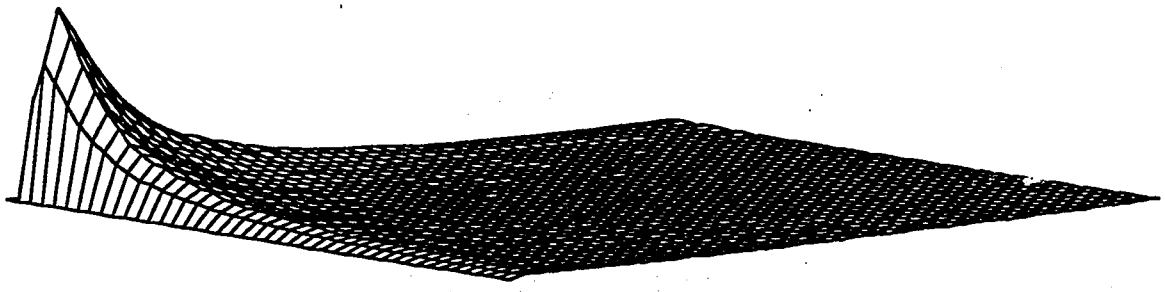

(c) Imag By(w1,w2)

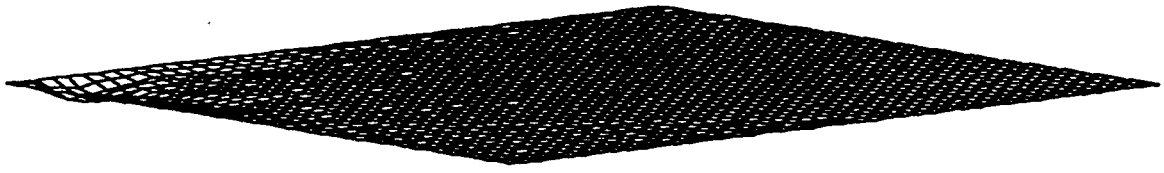

Fig. 5.30 *Parallel Wiener model of Example 5.8*

(a) Real and imaginary parts of $B_y(\omega_1, \omega_2)$

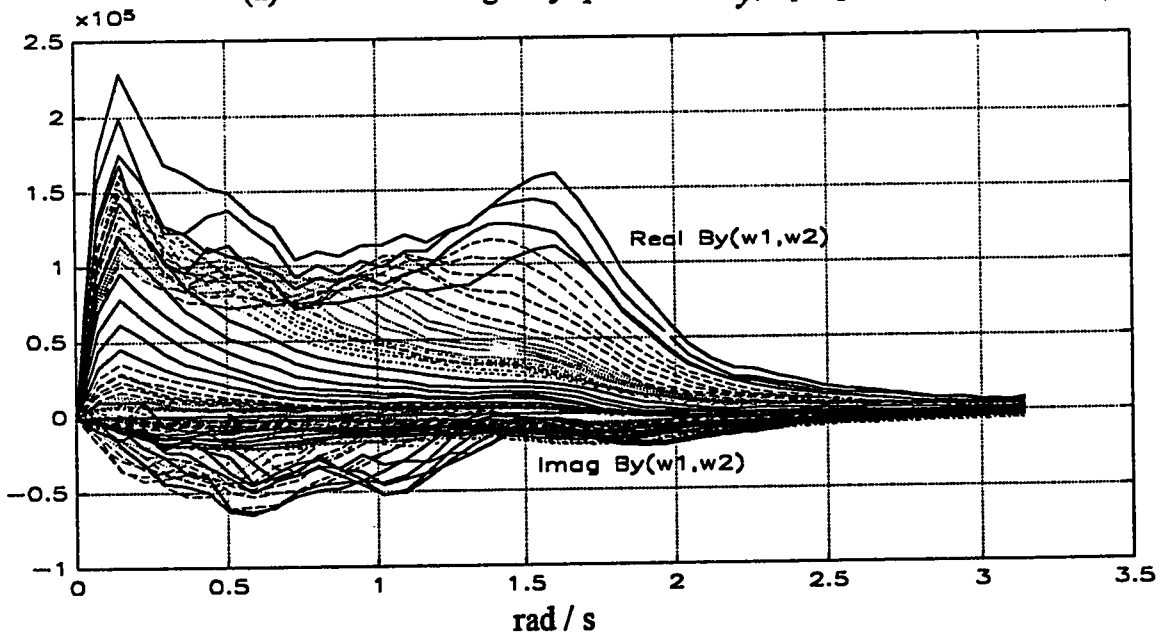

(b) Real $B_y(\omega_1, \omega_2)$

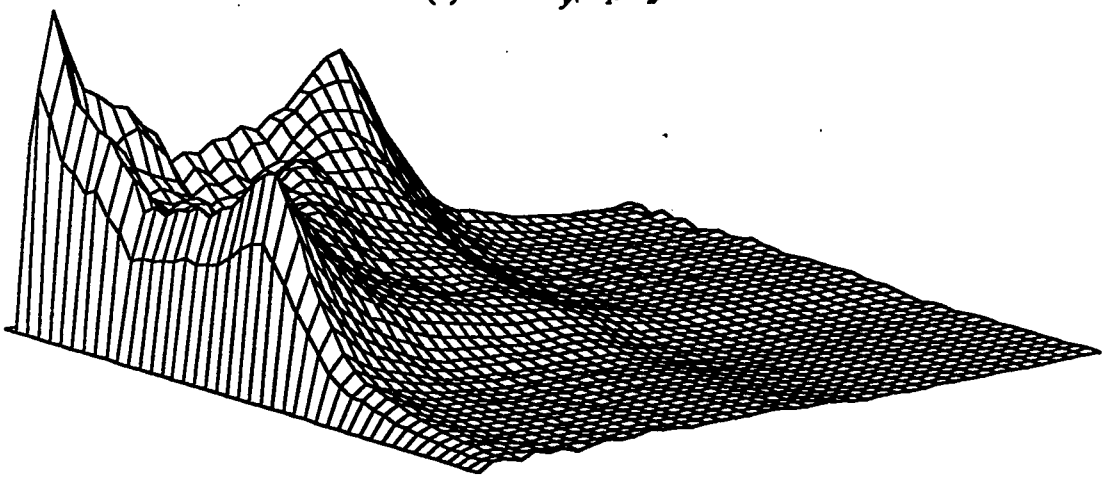

(c) Imag $B_y(\omega_1, \omega_2)$

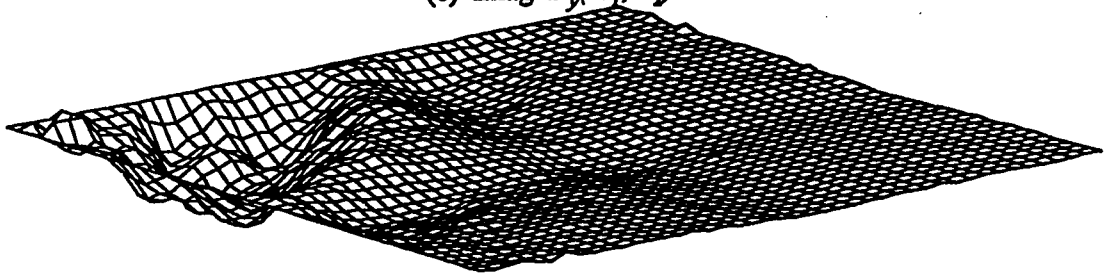

Fig. 5.31 *Parallel Hammerstein model of Example 5.9*

(a) Real and imaginary parts of $B_y(\omega_1, \omega_2)$

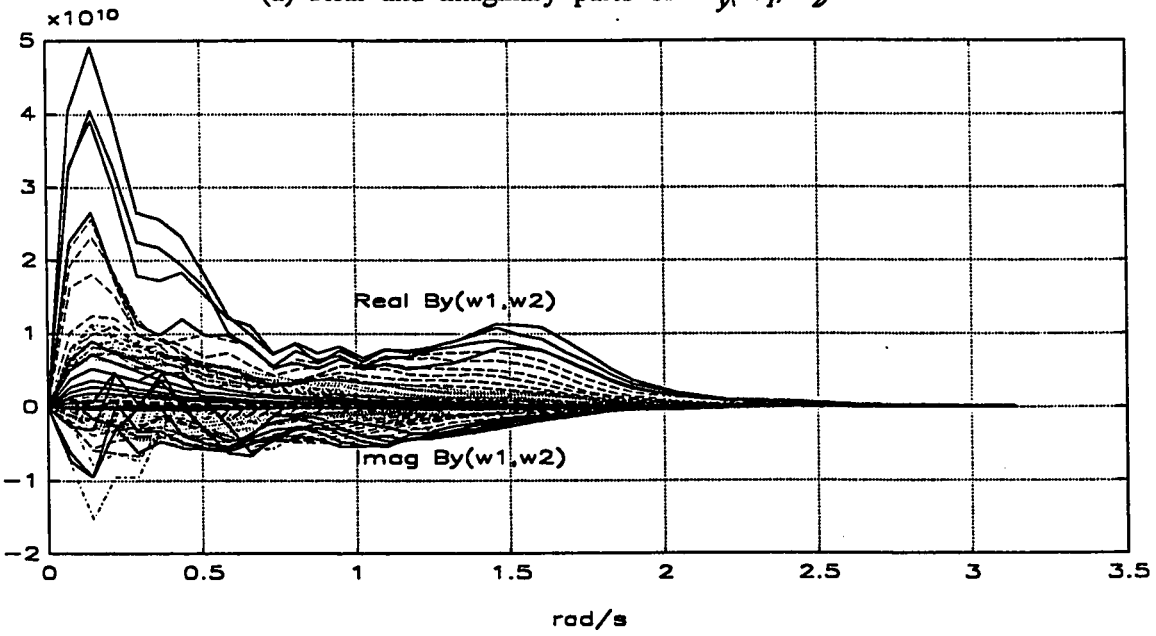

(b) Real $B_y(\omega_1, \omega_2)$

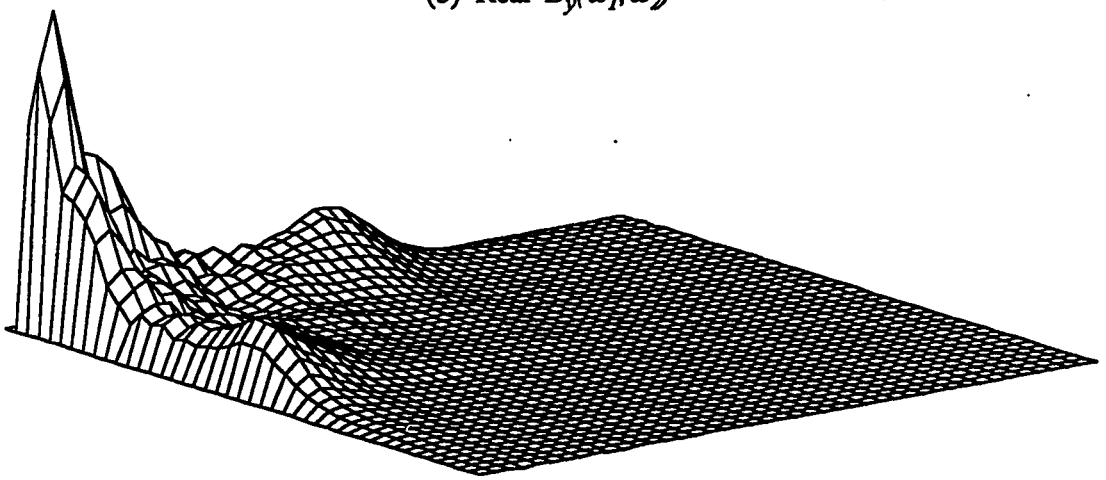

(c) Imag $B_y(\omega_1, \omega_2)$

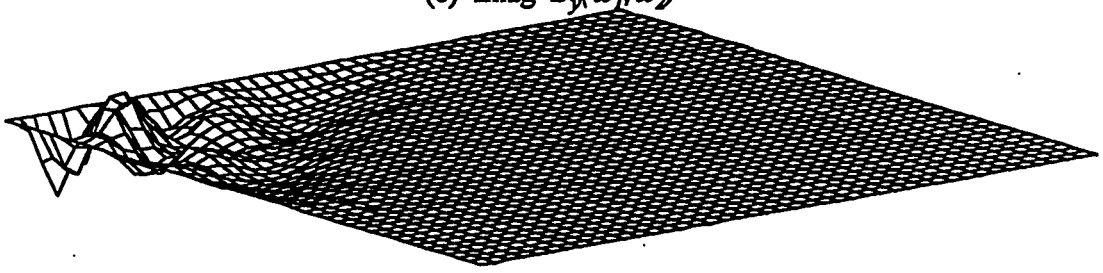

Fig. 5.32 *Parallel Wiener-Hammerstein model of Example 5.10*

(a) Bicoherence functions $b_y(\omega_1, \omega_2)$ of examples 5.9 and 5.10

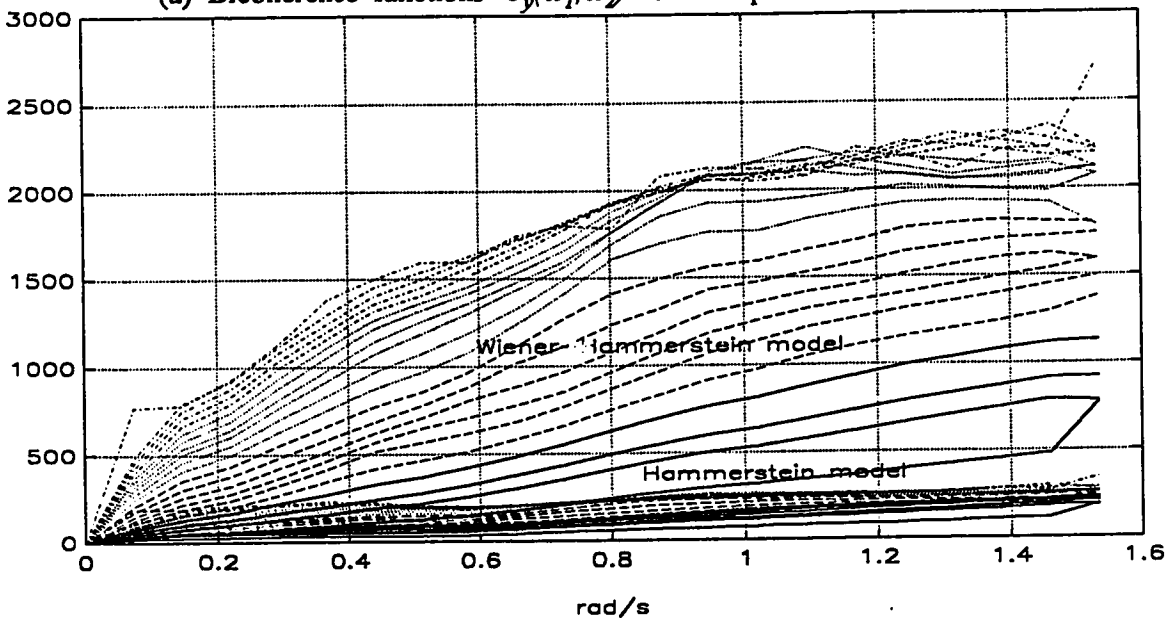

(b) $b_y(\omega_1, \omega_2)$ of the Wiener-Hammerstein model of Example 5.10

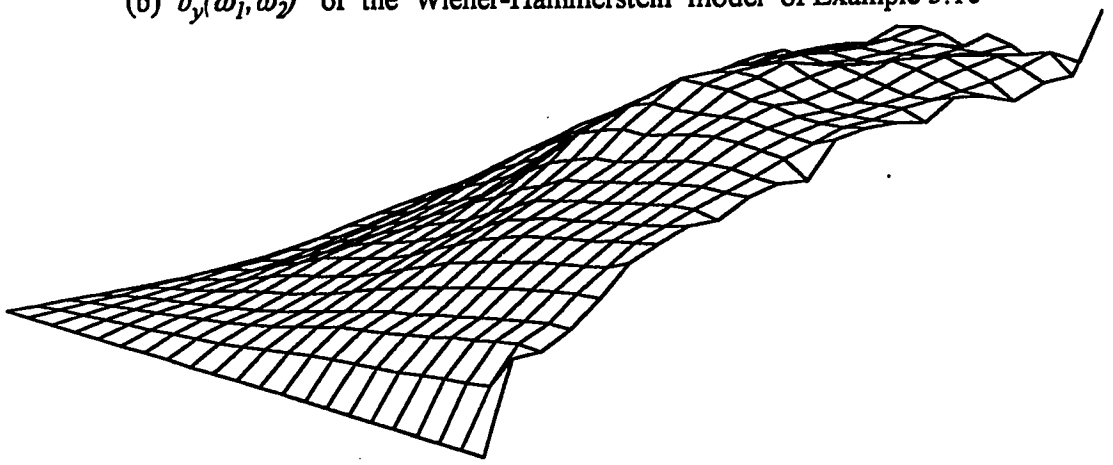

(c) $b_y(\omega_1, \omega_2)$ of the Hammerstein model of Example 5.9

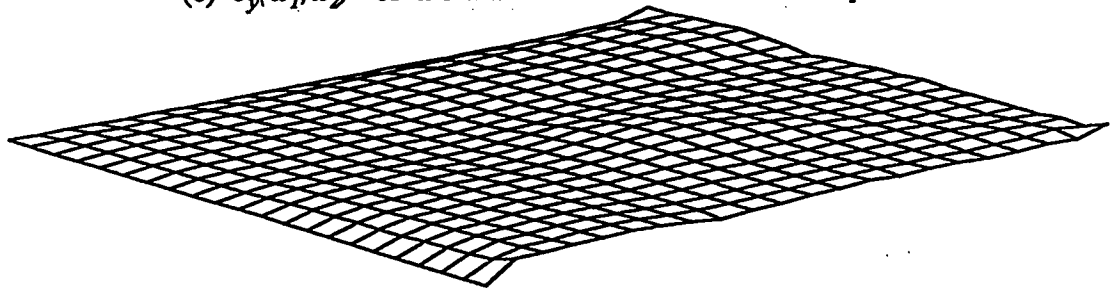

Fig. 5.33 *Bicoherence functions of Example 5.9 and 5.10*

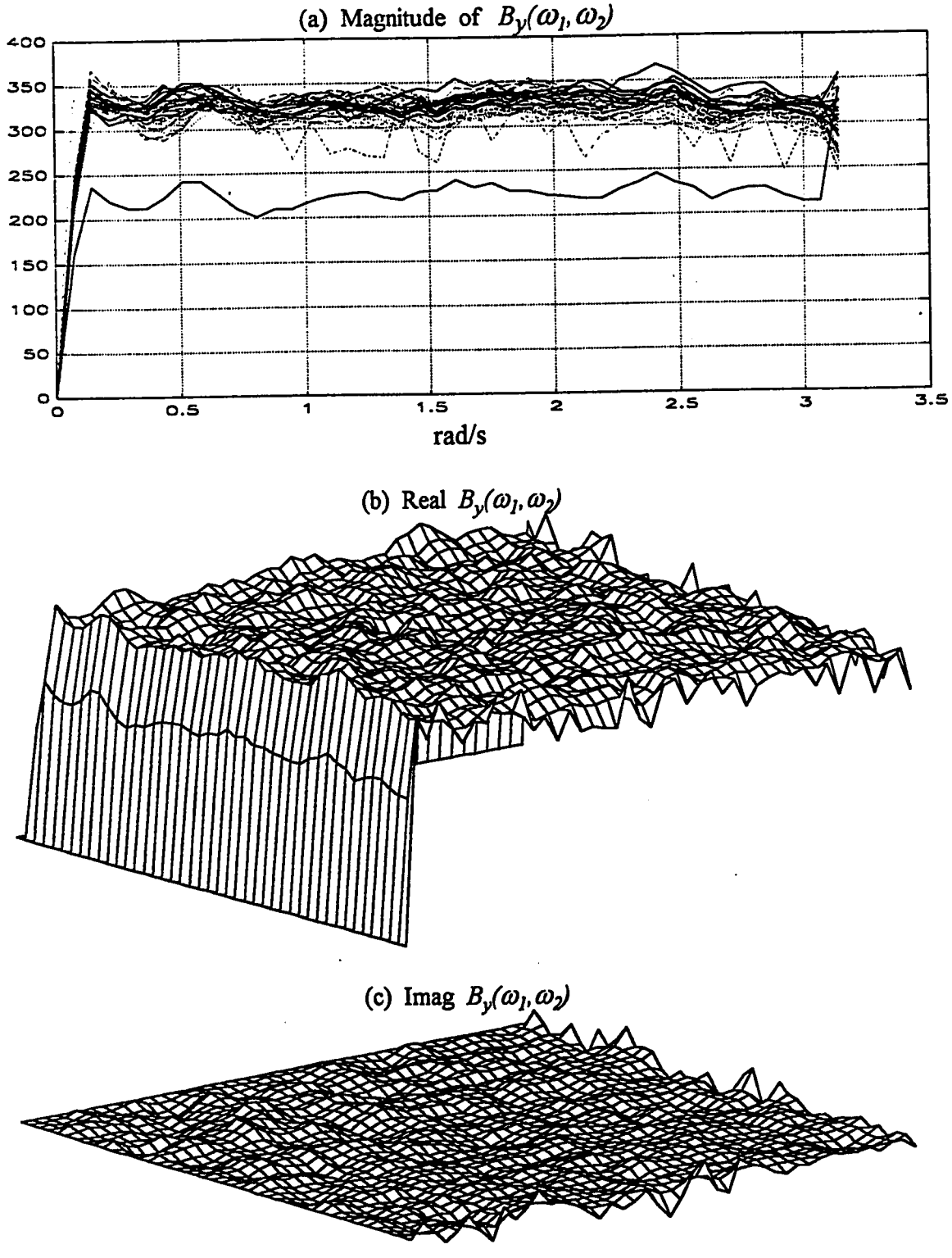

Fig. *5.34 Parallel static model of Example 5.11*

5.3 STATISTICAL TEST FOR CHECKING ESTIMATED VALUES OF BISPECTRUM

The structure identification criteria discussed in this thesis can be implemented with a hypothesis test to check some of the estimated values. The hypothesis can be briefly viewed as follows:

The claimed hypothesis is tested by comparing the estimated values to the critical ones. If the estimated values fall within an acceptance region for a given level of significance, say α, then the claimed hypothesis is accepted. If the estimated values fall outside the acceptance region then the hypothesis is not true and should be rejected according to the level of significance α.

For the case of claiming that the estimated bispectrum $B_y(\omega_1, \omega_2)$ is real, the corresponding null hypothesis for the imaginary part can be tested using, for example, a chi-square distribution as follows:

The deviation of the estimated imaginary part, $\mathrm{Im}(B_y)$, from the zero value is squared and compared to the critical value of the chi-square distribution k_α, for a given level of significance α (α is usually taken as 0.05). If the computed value is within the acceptance region, i.e., if *[3]*

$$(\mathrm{Im}(B_y) - 0)^2 < k_\alpha$$

then the null hypothesis is accepted and the bispectrum can be considered as being real with confidence 95% (when $\alpha=0.05$). Otherwise, it is rejected.

Implementing a statistical test for the structure identification criteria is beyond the work of this thesis. This matter has been recently addressed by Moustafa and

Emara-Shabaik *[44]*. In this paper, a statistical test that depends on two statistics which are functions of the third and fourth order cumulants of the system output has been developed using a chi-square distribution. The test is conducted by comparing these statistics to their 95% confidence limits. It is shown that the system nonlinearity and its type can be detected by comparing the value of test statistics to their critical values for the given level of significance.

5.4 IMPULSE RESPONSE ESTIMATION

This section presents simulation results for the two models described in chapter 4 (i.e., the parallel branch model with quadratic and cubic nonlinearities and the sea wave force model). The two models were simulated using a zero-mean Gaussian white random input sequence that has a length of 1024 data points. A total of 300 data records were used in the simulation and the results were averaged over these 300 records in order to improve accuracy. The following linear subsystems were used in the simulation

$$H_1(z^{-1}) = \frac{3z^{-1}}{1-0.9z^{-1}}$$

$$H_2(z^{-1}) = \frac{z^{-1}-0.5z^{-2}}{1-1.5z^{-1}+0.8z^{-2}}$$

$$H_3(z^{-1}) = \frac{2z^{-1}}{1-0.8z^{-1}}$$

Example 5.12 ***Quadratic and cubic Hammerstein models in parallel with a linear system:***

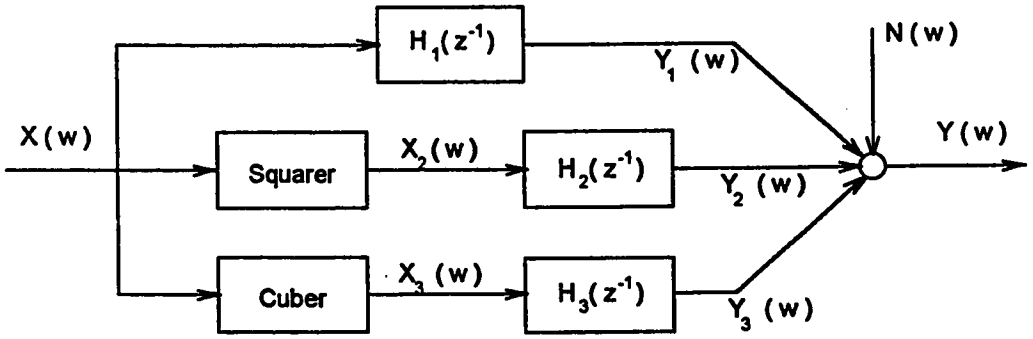

Fig. 5.35 *Quadratic and cubic Hammerstein models in parallel with a linear system.*

Example 5.13 ***Nonlinear wave force model with parallel linear and nonlinear systems:***

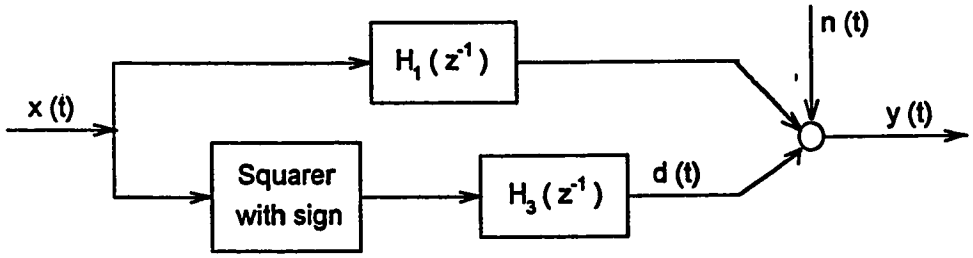

Fig. 5.36 *Nonlinear wave force model with parallel linear and nonlinear systems.*

The individual linear subsystems impulse responses for Examples 5.12 and 5.13 were estimated respectively, using the results described in sections 4.3 and 4.4. Comparisons of the estimated impulse responses and the theoretical weighting sequences of the linear subsystems for Examples 5.12 and 5.13 are illustrated, respectively, in Fig.s 5.37 and 5.38. The figures clearly show that the estimated impulse responses are very close to the theoretical weighting sequences which demonstrates that the identification procedure for such systems is reliable.

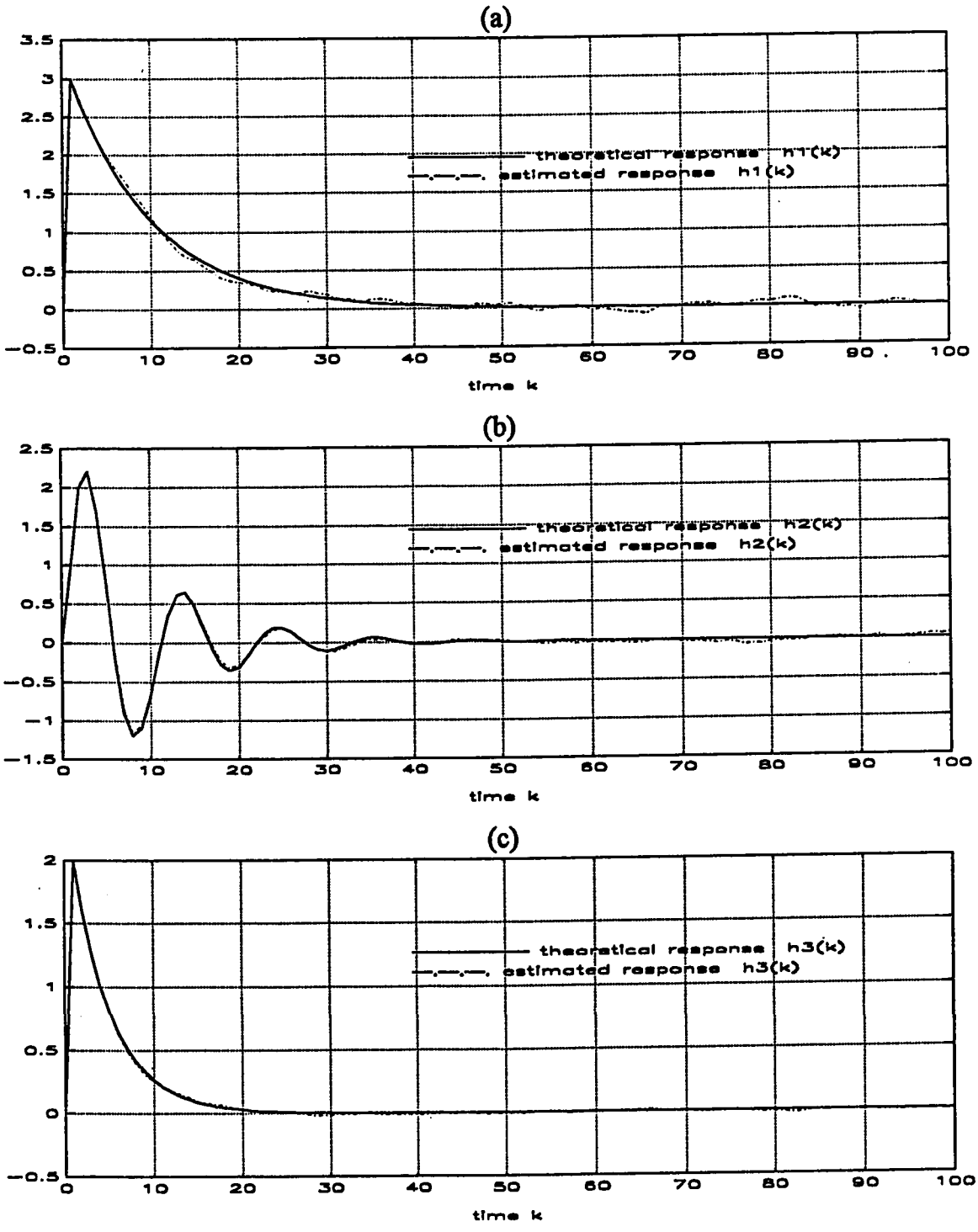

Fig. 5.37 *Comparison of impulse responses for Example 5.12*
(a) $h_1(k)$, (b) $h_2(k)$, (c) $h_3(k)$

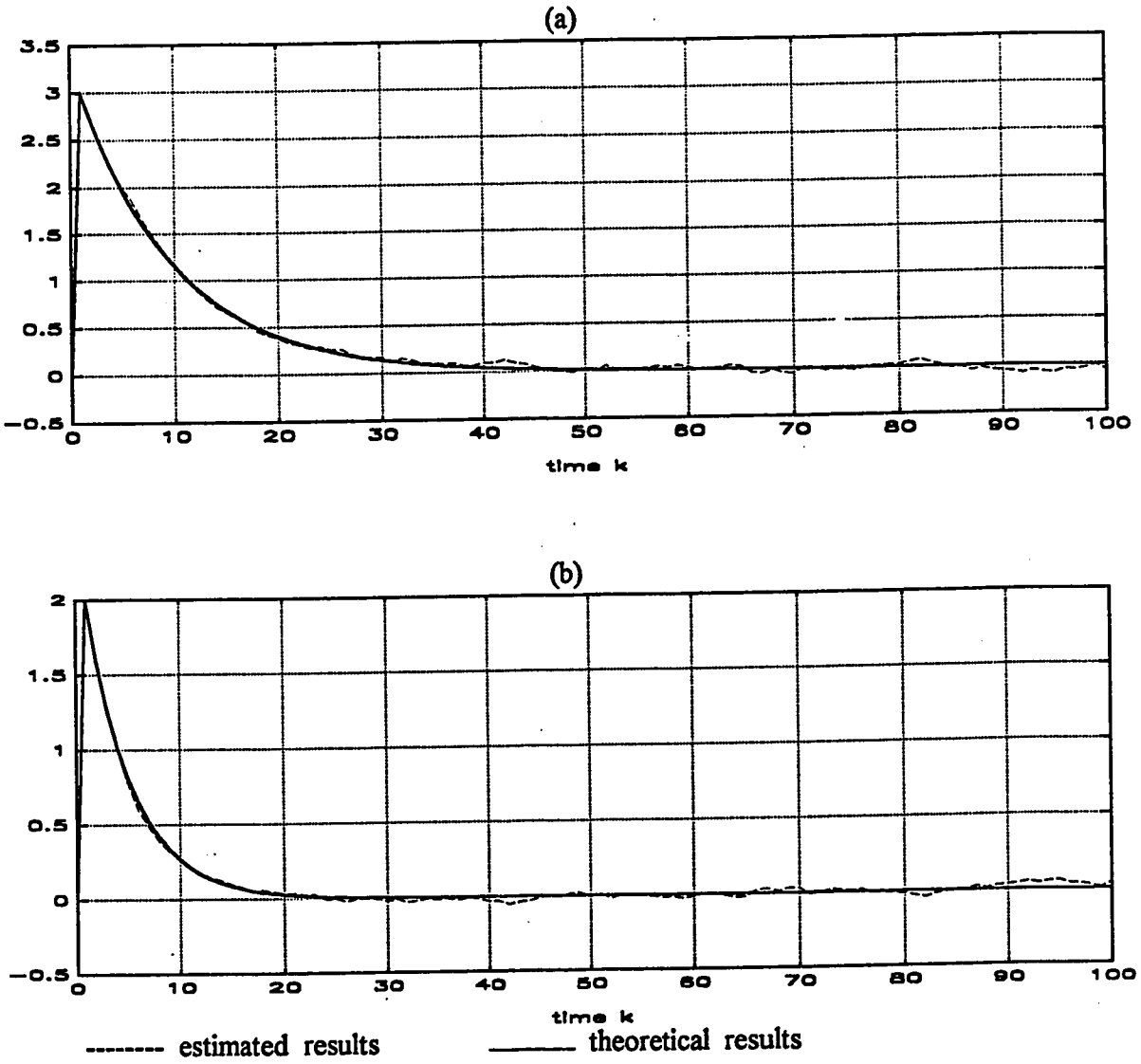

Fig. 5.38 *Comparison of impulse responses for Example 5.13*
(a) $h_1(k)$, (b) $h_3(k)$

CHAPTER 6

CONCLUSIONS AND RECOMMENDATIONS

6.1 CONTRIBUTIONS

As a result of this research three points have been achieved. First, the structure identification criterion developed by Emara-Shabaik and Moustafa *[26]*, which handles a single branch model, has been extended to handle models of parallel branches by simulation. Second, in comparison between the structure identification criterion using the bispectrum approach and the one that uses correlation techniques, it has been found that the criterion that uses correlation techniques applies for nonlinear systems with general nonlinearity only while the other one that uses the bispectrum approach applies only if the nonlinearity has at least one even term. Third, the spectral analysis approach that identifies the impulse responses of the linear blocks of nonlinear systems (Bendat *[2]*) has been demonstrated by simulation.

6.2 CONCLUSIONS

In this thesis, the structure identification of block cascade models composed of linear dynamic and static nonlinear blocks was considered. Two main approaches have been utilized, the structure identification in the time domain and the structure identification in the frequency domain.

In the time domain analysis, discussed in chapter 2, cross-correlation techniques have been used for the structure identification when the input to the system is a white Gaussian signal. The nonlinear systems considered in this part are those that can be described by a model consisting of a linear dynamic block in cascade with a nonlinear element followed by another linear dynamic block. This model is refered to as a Wiener-Hammerstein model. Linear and nonlinear cross-correlation functions were used to identify the structure of this model. From these two functions, a structure identification criterion that covers all the

subclasses of the Wiener-Hammerstein model has been presented. It has been found that this structure identification criterion fails to distinguish between the Wiener model and the Hammerstein model when the nonlinearity of the nonlinear element is odd or even only.

In the frequency domain, the structure identification of the Wiener-Hammerstein model has been performed utilizing the bispectrum of the system output. Using a zero-mean stationary white Gaussian process as an input to this model, a structure identification criterion based on the bispectrum of the output sequence *[26]* has been presented in chapter 3 of this thesis.

The structure identification criterion *[26]* has been applied to a wider class of nonlinear systems which can be represented by parallel branches of block cascades in parallel with a linear system. It has been found from the simulation results that the structure identification criterion is still valid for this model provided that the parallel nonlinear branches are all of the same type. Also it has been noticed that when the nonlinear block of a Wiener-Hammerstein model has odd nonlinearity only, the structure identification criterion will have difficulty distinguishing the model structure. In this case, a statistical test could be employed to significantly enhance the detection procedure. The structure identification criterion discussed here needs measurements of the output sequence only and does not require measurements of the input sequence, assuming the input to be a zero mean Gaussian signal. It is also important to notice that it is difficult to achieve a zero mean Gaussian process and therefore averaging is done to improve accuracy.

6.3 RECOMMENDATIONS FOR FUTURE WORK

An area which may be considered for future research is the structure identification of nonlinear systems when the input is Non-Gaussian process. Also a way to enhance the implementation of the structure identification criterion, for example via a statistical test, will improve the detection resolution.

REFERENCES

[1] Astrom, K. J. and Eykhoff, P., "System Identification - A Survey", *Automatica,* vol. 7, pp. 123-162, 1971.

[2] Bendat, Julius S., "Nonlinear System Analysis and Identification from Random Data", *John Wiley & Sons, Inc.,* 1990.

[3] Bendat, Julius S. and Piersol, Allan G., "Random Data: Analysis and Measurement procedures", *John Wiley & Sons, Inc.,* 1986.

[4] Bendat, Julius S. and Piersol, Allan G., "Spectral Analysis of Nonlinear Systems involving Square-Law operations", *Journal of Sound and Vibration,* vol. 81, no. 2, pp. 199-213, 1982 .

[5] Bendat, Julius S. and Piersol, Allan G., "Decomposition of Wave Forces into Linear and Nonlinear Components", *Journal of Sound and Vibration,* vol. 81, no. 2, pp. 199-213, 1986.

[6] Billings, S. A. and Fakhouri, S. Y., "Identification of a Class of Nonlinear Systems Using Correlation Analysis", *Proc. IEE,* vol. 125, Pt. D, pp. 691-697, 1978a.

[7] Billings, S. A. and Fakhouri, S. Y., "Theory of Separable Processes With Application to the Identification of Nonlinear Systems", *Proc. IEE,* vol. 125, Pt. D, pp. 1051-1058, 1978b.

[8] Billings, S. A. and Fakhouri, S. Y., "Nonlinear System Identification Using the Hammerstein Model", *Int. J. Systems Sci.*, vol. 10, p. 567, 1979a.

[9] Billings, S. A. and Fakhouri, S. Y., "Identification of Nonlinear S_m Systems", *Ibid.*, vol. 10, p. 1401, 1979b.

[10] Billings, S. A., "Identification of Nonlinear Systems - A Survey", *Proc. Instn. elect. Engrs (IEE)*, Pt D., vol. 127, p. 272, 1980.

[11] Billings, S. A. and Fakhouri, S. Y., "Identification of Systems Containing Linear Dynamic and Static Nonlinear Elements", *Automatica*, vol. 18, p. 15, 1982.

[12] Chang, F. H. I. and Luss, R., "A Noniterative Method for Identification Using Hammerstein Model", *IEEE Trans. Automat. Contr.*, pp. 464-468, Oct. 1971.

[13] Daist, N. D., Chang, F. H. I. and Luss, R., "Nonlinear Identification in the Presence of Correlated Noise Using a Hammerstein Model", *IEEE Trans. Automat. Contr.*, pp. 552-555, 1973.

[14] Falkner, A. H., "Identification of the System Comprising Parallel Hammerstein Branches", *Int. J. Systems Sci.*, vol. 22, no. 11, pp.2079-2087, 1991.

[15] Haber, R., "Parametric Identification of Nonlinear Dynamic Systems Based on Correlation Functions", *5th IFAC Symposium on Identification, Darmstadt, FRG*, pp. 515-522, 1979.

[16] Haber, R., "Parametric Identification of Nonlinear Dynamic Systems Based on Nonlinear Crosscorrelation Functions", *Proc. IEE.*, vol. 135, Pt. D, no. 6, pp. 405-420, Nov. 1988.

[17] Haber, R., "Structure Identification of Block-oriented Models Based on the Volterra Series", *7th IFAC/IFIP Symp. on Identification and System Parameter Estimation,* York, UK, in the Appendix, 1985.

[18] Haber, R., "Structural Identification of Quadratic Block-Oriented Models Bsed on Volterra Kernels", *Int. J. Systems Sci.*, vol. 20, no. 8, pp. 1355-1380, 1989.

[19] Haber, R. and Keviczky, "Identification of Nonlinear Dynamic Systems-- A Survey Paper", *Preprints IFAC Symp. on Identification and System Parameter Estimation,* Tbilisi, U.S.S.R., pp. 62-112, 1978.

[20] Haber, R. and Unbehauen, H., "Structure Identification of Nonlinear Dynamic Systems-- A Survey on Input/Output Approaaches", *Automatica,* vol. 26, no. 4, pp. 651-677, 1990.

[21] Hsia, T. C., "Least Square Method for Nonlinear Discrete System Identification", in *Conf. Rec., 2nd Asilomar Conf. Circuits and Systems,* pp. 423-426, 1968.

[22] Hsia, T. C., "System Identification - Least Square Methods", *Lexington Books, Mass,* 1977.

[23] Isermann, R.,"Identification of Dynamic Systems (in German)", (Springer Verlag, Berlin, 1988).

[24] Hosam E. Emara-Shabaik and Kamal A.F. Moustafa, "Characterization of Dynamic System Nonlinearities Via Probabibistic Approach", to appear, *Int. J. Systems Science*, 1994.

[25] Kamal A.F. Moustafa and Hosam E. Emara-Shabaik, "Non-linearity Detection of Weakly Non-linear Dynamic Systems Using Cumulants", *Int. J. Systems Science*, vol. 23, no.7, pp. 1167-1177, 1992.

[26] Hosam E. Emara-Shabaik and Kamal A. F. Moustafa, "Structure Identification Criteria of Nonlinear Systems Via Bispectrum", to appear, *Arab Journal for Science and Engineering (AJSE)*, 1994.

[27] Korenberg, M. J., "A Rapid and Accurate Method for Estimating the Kernels of a Nonlinear System with Lengthy Memory", *15th Biennial Symp. Communications, Queen's Unversity, Kingston, Canada*, pp. 57-60, June 1990.

[28] Kornberg, M. J. "Functional Expansions, Parallel Cascades and Nonlinear Difference Equations", *Los Angeles: USC Biomedical Simulation Resource*, vol. 1, pp. 221-240, 1987.

[29] Korenberg, M. J., "Parallel Cascade Identification and Kernel Estimation for Nonlinear Systems", *Ann. Biomed. Eng.*, vol. 19, pp. 429-455, 1991.

[30] Korenberg, M. J., "Statistical Identification of Prallel Cascades of Linear and Nonlinear Systems", *IFAC Symp. Iden. Sys. Param. Est.*, vol. 1, pp. 580-585, 1982.

[31] Menedel, Jerry M.,"Tutorial on Higher-Order Statistics (Spectrea) in Signal Processing and System theory: Theoretical Results and Some Applications", Proceedings of the *IEEE*, vol. 79, No. 3, pp. 277-305, March 1991.

[32] Narendra, K. S. and Gallman, P. G., "An Iterative Method for the Identification of Nonlinear Systems Using a Hammerstein Model", *IEEE Trans. Automat. Contr.*, vol. AC-11, pp. 546-550, July 1986.

[33] Nikias, C. L. and Raghuveer, M. R., "Bispectrum Estimation: A Digital Signal Processing Framework", Proceedings of the *IEEE*, vol. 75, No. 7, pp. 869-891, July 1987.

[34] Nikias, C. L. and Mendel, J. M., "Signal Processing with Higher-Order Spectra", *IEEE Signal Processing Magazine*, pp. 10-37, July 1993.

[35] Norton, J. P., "An Introduction to Identification", *Acadimic Press*, 1986.

[36] Palm, G., " On the Representation and Approximation of Nonlinear Systems", *Biol. Cybern.*, vol. 31, pp. 119-124, 1978.

[37] Palm, G., "On the Representation and Approximation of Nonlinear Systems. Part II: Discrete Time", *Biol. Cybern.*, vol. 34, pp. 49-52, 1979.

[38] Palm, G. and Poggio, "The Volterra Representation and the Wiener Expansion: Validity and Pitfalls", *SIAM J. APPL. MATH.*, vol. 33, no. 2, Sept. 1977.

[39] Schetzen, Martin, "The Volterra and Wiener Theories of Nonlinear Systems", *John Wiley & Sons, Inc.*, 1980.

[40] Shi, J. and Sun, H., "Nonlinear System Identification Via Parallel Cascaded Structure", *Proc. 12th Annual International Conference of the IEEE Engineering in Medicine and Biology Society*, vol. 12, no. 4, pp. 1897-1898, 1990.

[41] Shi, J. and Sun, H., "Nonlinear System Identification for Cascaded Block Model: An Application to electrode Polarization Impedance", *IEEE Trans. Biomed. Eng.*, vol. 37, no. 6, pp. 574-587, Jun,1990.

[42] Sodertrom, T. and Stoica, P., "System Identification", *Prentice-Hall*, 1989.

[43] Hosam E. Emara-Shabaik, Kamal A.F. Moustafa and Jaleel H. S. Talaq, "On Identification of Parallel Block-cascade Nonlinear Models", submitted, *Int. J. Systems Science*, 1994.

[44] Kamal A.F. Moustafa and Hosam E. Emara-Shabaik, "A Statistical Test for Detecting System Nonlinearity and Distinguishing its Type", *Proc. 10th IFAC Symb. on Systems Identification*, Copenhagen, Denmark, paper SYSID-No. 100, July 1994.

[45] Wlodzimier Greblicki and Miroslaw Pawlak, "Cascade Non-linear System Identification by a Non-parametric Method", *Int. J. Systems Science*, vol. 25, no. 1, pp. 129-153, 1994.

[46] Vugts, J. H., and Bouquet, A. G., "A Nonlinear Frequency Domain Description of Wave Forces on an Element of a Vertical Pile", *Proc. Behavior of Offshore Structures*, BOSS '85, Delft, Netherlands, 239 (1985).

[47] Hosam E. Emara-Shabaik, Kamal A.F. Moustafa and Jaleel H. S. Talaq, "On Identification of Parallel Wiener-Hammerstein Models", to appear, *Proc. 3rd IEEE Conference on Control Applications, Glasgow, U.K.*, 1994.

APPENDIX A

PRELIMINARIES AND DEFINITIONS

This Appendix lists some basic definitions and properties of random data *[4]*.

A.1 CLASSIFICATIONS OF RANDOM DATA

A.1.1 Random Process

A random process (Stochastic process) is a collection of all time-history records (sample records or ensemble) that the random phenomenon might have produced. Random processes may be either stationary or nonstationary.

A.1.2 Sample Record

A sample record is a single time history record, observed over a finite time interval, which is a possible realization of the random phenomenon.

A.1.3 Stationary Random Process

A stationary random process is a process that has statistical properties which are invariant with respect to translations in time. To explain this, consider for example the random process $\{x(t)\}$ illustrated in Fig. A.1. The mean value (first moment) $\mu_x(t_1)$ and the autocorrelation function (second moment) $R_{xx}(t_1,t_1+\tau)$ of the random process at some time t_1 , are given by

$$\mu_x(t_1)= \lim_{N\to\infty} \frac{1}{N}\sum_{k=1}^{N} x_k(t_1) \qquad (A.1)$$

$$R_{xx}(t_1,t_1+\tau)=\lim_{N\to\infty}\frac{1}{N}\sum_{k=1}^{N}x_k(t_1)x_k(t_1+\tau) \qquad (A.2)$$

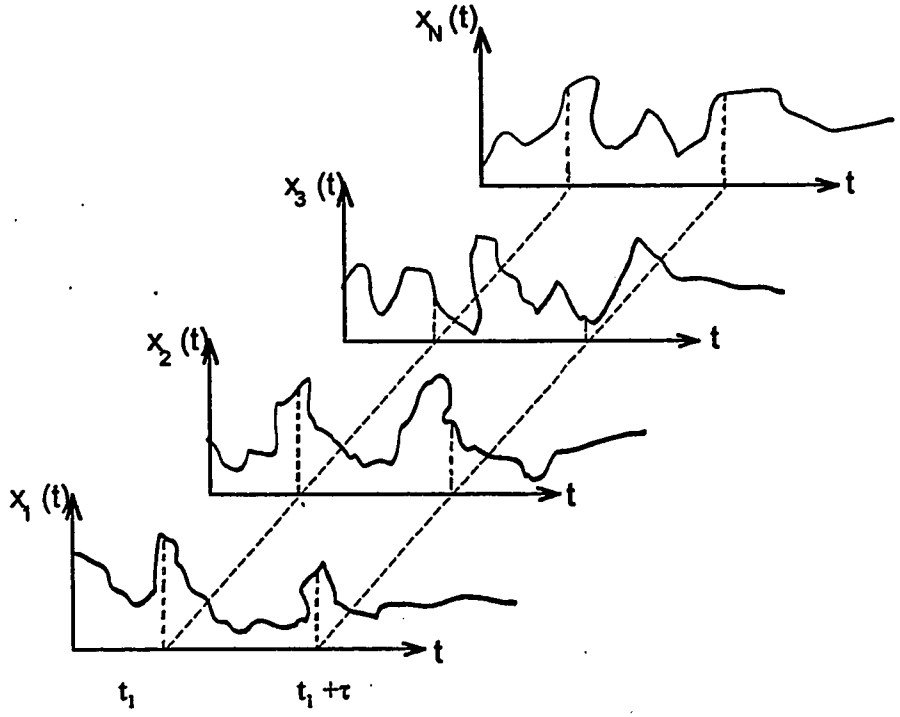

Fig. A.1 *Ensemble of time-history records defining a random process.*

When $\mu_x(t_1)$ and $R_{xx}(t_1,t_1+\tau)$ do not vary as time t_1 varies, then the random process is said to be stationary. That is, for a stationary random process , the mean value is constant $(\mu_x(t_1)=\mu_x)$ and the autocorrelation function is dependent only on the time shift τ $(R_{xx}(t_1,t_1+\tau)=R_{xx}(\tau))$. Stationary random processes may be either ergodic or nonergodic.

A.1.4 Ergodic Process

An Ergodic process is a stationary random process where time averages on any collection of time-history records of this process are the same for every time-history record. That is, ensemble averages and averages on any arbitrary

time-history record are equivalent. This can be explained mathematically for the first and second moments as

$$\mu_x = \frac{1}{N}\sum_{k=1}^{N}\lim_{T\to\infty}\frac{1}{T}\int_0^T x_k(t)dt \qquad ,for\ any\ k\ or\ N \tag{A.3}$$

$$R_{xx}(\tau) = \frac{1}{N}\sum_{k=1}^{N}\lim_{T\to\infty}\frac{1}{T}\int_0^T x_k(t_1)x_k(t_1+\tau)dt \qquad ,for\ any\ k\ or\ N \tag{A.4}$$

A.2 GAUSSIAN VARIABLE

A random variable $x(t)$ is said to be Gaussian (or normal) when its probability density function at any time t is given by

$$p(x) = \frac{1}{\sigma_x\sqrt{2\pi}}e^{\left[\frac{-(x-\mu_x)^2}{2\sigma_x^2}\right]} \tag{A.5}$$

where μ_x and σ_x are , respectively , the mean value and the standard deviation of the random variable $x(t)$ given by

$$\mu_x = E[x(t)] = \int_{-\infty}^{\infty} xp(x)dx \approx \frac{1}{T}\int_0^T x(t)dt \tag{A.6}$$

$$\sigma_x^2 = E[x^2(t)] - \mu_x^2 \tag{A.7}$$

where $E[.]$ stands for the expected value.

Higher-order moments of Gaussian random variables with zero mean values can be expressed in terms of the second-order moments of the variables. The n-th dimensional correlation function is given by *[6]*.

$$E[x_1, x_2, \ldots, x_n] = \begin{cases} 0 & \text{for } n \text{ odd} \\ \sum_{n-1} \prod_{i \neq j} E[x_i x_j] & \text{for } n \text{ even} \end{cases} \qquad (A.8)$$

for example , the fourth and sixth dimensional correlation function are given, respectively, by

$$E[x_1x_2x_3x_4] = E[x_1x_2]E[x_3x_4] + E[x_1x_3]E[x_2x_4] + E[x_1x_4]E[x_2x_3] \qquad (A.9)$$

$$\begin{aligned} E[x_1x_2x_3x_4x_5x_6] = {} & E[x_1x_2]\{E[x_3x_4]E[x_5x_6] + E[x_3x_5]E[x_4x_6] + E[x_3x_6]E[x_4x_5]\} \\ & + E[x_1x_3]\{E[x_2x_4]E[x_5x_6] + E[x_2x_5]E[x_4x_6] + E[x_2x_6]E[x_4x_5]\} \\ & + E[x_1x_4]\{E[x_2x_3]E[x_5x_6] + E[x_2x_5]E[x_3x_6] + E[x_2x_6]E[x_3x_5]\} \\ & + E[x_1x_5]\{E[x_2x_3]E[x_4x_6] + E[x_2x_4]E[x_3x_6] + E[x_2x_6]E[x_3x_4]\} \\ & + E[x_1x_6]\{E[x_2x_3]E[x_4x_5] + E[x_2x_4]E[x_3x_5] + E[x_2x_5]E[x_3x_4]\} \end{aligned} \qquad (A.10)$$

A.3 WHITE NOISE

White noise is a stationary random process with a constant autospectral density function given by

$$G_{xx}(\omega) = \begin{cases} 2a & \text{for } \omega \geq 0 \\ 0 & \text{for } \omega < 0 \end{cases} \qquad (A.11)$$

or $S_{xx}(\omega)=a$; for all ω *(A.12)*

The autocorrelation function of a white noise is given by

$$R_{xx}(\tau)=a\delta(\tau) \qquad (A.13)$$

where $\delta(\tau)$ is the delta function.

A.4 CORRELATION FUNCTIONS

A.4.1 Autocorrelation Function

The autocorrelation function $R_{xx}(\tau)$ of a random process $x(t)$ is the average of the product of $x(t)$ and $x(t+\tau)$ for reasonably large averaging time T. That is

$$R_{xx}(\tau)=E[x(t)x(t+\tau)]=\frac{1}{T}\int_0^T x(t)x(t+\tau)dt \qquad A.14)$$

For a discrete sample record $x(k)$, the autocorrelation function $R_{xx}(\tau)$ is given by

$$R_{xx}(\tau)=E[x(k)x(k+\tau)]=\frac{1}{N-\tau}\sum_{k=1}^{N-\tau}x(k)x(k+\tau) \qquad (A.15)$$

where N is the length of the record.

A.4.2 Cross-Correlation Function

The cross-correlation function $R_{xy}(\tau)$ of two random processes $x(t)$ and $y(t)$ is the average of the product of $x(t)$ and $y(t+\tau)$ for a reasonably large averaging time T.

$$R_{xy}(\tau) = E[x(t)y(t+\tau)] = \frac{1}{T}\int_0^T x(t)y(t+\tau)dt \qquad (A.16)$$

In discrete from, $R_{xy}(\tau)$ is given by

$$R_{xy}(\tau) = E[x(t)y(k+\tau)] = \frac{1}{N-\tau}\sum_{k=1}^{N-\tau} x(k)y(k+\tau) \qquad (A.17)$$

A.5 FOURIER TRANSFORM

The Fourier transform of the process $x(t)$ indicates the frequency distribution of the signal and is defined as

$$X(\omega) = \int_{-\infty}^{\infty} x(t)e^{-j\omega t}dt \qquad (A.18)$$

$X(\omega)$ is also called the Fourier spectrum. Since in practice $x(t)$ is of finite length T, then $X(\omega)$ is estimated using the finite Fourier transform defined by

$$X(\omega) = \int_0^T x(t)e^{-j\omega t}dt \qquad (A.19)$$

A.6 SPECTRAL DENSITY FUNCTIONS

A.6.1 Autospectral Density Function

The autospectral (power spectral) density function $G_{xx}(\omega)$ is defined by finite Fourier transform techniques as

$$G_{xx}(\omega) = \begin{cases} \frac{2}{T}E[|X(\omega)|^2] & for\ \omega \geq 0 \\ 0 & for\ \omega < 0 \end{cases} \qquad (A.20)$$

where $E[\,]$ is an ensemble average for fixed ω over the available sample records of the ensemble. $X(\omega)$ is a finite Fourier transform of $x(t)$ of length T. $G_{xx}(\omega)$ is also called a one-sided autospectral density function because it is defined for positive frequency only. A two-sided autospectral density function $S_{xx}(\omega)$ used for theoretical studies is defined for all ω as

$$S_{xx}(\omega) = \frac{1}{2} G_{xx}(|\omega|) \qquad (A.21)$$

$S_{xx}(\omega)$ can also be written as the Fourier transform of the autocorrelation function

$$S_{xx}(\omega) = \int_{-\infty}^{\infty} R_{xx}(\tau) e^{-j\omega\tau} d\tau \qquad (A.22)$$

A.6.2 Cross-Spectral Density Function

The cross-spectral density function $G_{xy}(\omega)$ is defined by finite Fourier transform techniques as

$$G_{xy}(\omega) = \begin{cases} \frac{2}{T} E[X^*(\omega) Y(\omega)] & \text{for } \omega \geq 0 \\ 0 & \text{for } \omega < 0 \end{cases} \qquad (A.23)$$

Similar relations to Eq.s (A.21) and (A.22) can be written as follows

$$S_{xy}(\omega) = \frac{1}{2} G_{xy}(|\omega|) \qquad (A.24)$$

$$S_{xy}(\omega) = \int_{-\infty}^{\infty} R_{xy}(\tau) e^{-j\omega\tau} d\tau \qquad (A.25)$$

A.7 POLYSPECTRA

The second and the third order cumulants of a zero mean random signal $x(k)$ are defined ,respectively, as *[31,33]*

$$C_2(\tau) = E[x(k)x(k+\tau)] \qquad (A.26)$$

$$C_3(\tau_1, \tau_2) = E[x(k)x(k+\tau_1)x(k+\tau_2)] \qquad (A.27)$$

Polyspectra are defined as the Fourier transforms of cumulants *[31,33,34]*. The Fourier transforms of Eq.s (A.26) and (A.27) give ,respectively, the power spectrum and the bispectrum of the signal $x(k)$ as

$$P(\omega) = \sum_{\tau=-\infty}^{\infty} C_2(\tau)\, e^{-j\omega\tau} \qquad (A.28)$$

$$B(\omega_1, \omega_2) = \sum_{\tau_1=-\infty}^{\infty} \sum_{\tau_2=-\infty}^{\infty} C_3(\tau_1, \tau_2)\, e^{-j(\omega_1\tau_1+\omega_2\tau_2)} \qquad (A.29)$$

A.8 LINEAR SYSTEM

A system is said to be linear if the characteristics of its output are additive and homogeneous with respect to its input. If $y(x)$ is the output of a linear system excited by an input $x(t)$, then the additive and homogeneous properties are defined respectively as

$$y(x_1+x_2) = y(x_1) + y(x_2) \;; \qquad \textit{additive property} \qquad (A.30)$$

$$y(cx) = cy(x) \qquad ; \qquad \textit{homogeneous property} \qquad (A.31)$$

where c is a constant.

If $h(\tau)$ is the weighting function (also called the unit impulse response function) of a linear system, then the system output $y(t)$ for an arbitrary input $x(t)$ is given by the well-known convolution integral

$$y(t) = \int_0^\infty h(\tau)x(t-\tau)d\tau \qquad (A.32)$$

The above relation can be written in the frequency domain as follows

$$Y(\omega) = H(\omega)X(\omega) \qquad (A.33)$$

The cross-spectral density function $S_{xy}(\omega)$ and the output spectrum $S_{yy}(\omega)$ can be written in terms of the input spectrum $S_{xx}(\omega)$ as follows

$$S_{xy}(\omega) = H(\omega)S_{xx}(\omega) \qquad (A.34)$$

$$S_{yy}(\omega) = |H(\omega)|^2 S_{xx}(\omega) \qquad (A.35)$$

A.9 NONLINEAR SYSTEM

A system is said to be nonlinear if it is either not additive (Eq.(A.30)) and/or not homogeneous (Eq.(A.31)). A nonlinear system is called a zero-memory nonlinear system if the output of this system depends on the instantaneous input

only. If the zero-memory nonlinear system is followed and/or preceded by a linear system, then the whole system is called a finite-memory nonlinear system.

A.10 STABILITY

A linear system is said to be stable if the system output $y(t)$ is bounded for any bounded input $x(t)$. In other words, for a stable linear system the absolute value of the weighting function $|h(\tau)|$ should be integrable. That is

$$\int_0^\infty |h(\tau)| d\tau < \infty \qquad (A.36)$$

APPENDIX B

COMPUTATION OF BISPECTRUM

This appendix presents a direct method for computing the bispectrum estimate of a process $x(k)$ as follows *[33]*:

Let $\{x(1),x(2),...,x(N)\}$ be the available set of observations for the process $x(k)$. If f_s is the sampling frequency and N_0 is the total number of frequency samples, then the required spacing is given by $\Delta_0=f_s/N_0$. The following 4 steps are to be followed:

a) Segment the data into K segments of M samples each (i.e., $N=KM$) and subtract from each segment its mean value. If necessary, add zeros at each segment to obtain a convenient length M for the FFT.

b) Assuming that $\{X^{(i)}(k), k=0,1,2,...,M-1\}$ are the data of segment $\{i\}$, generate the DFT coefficients

$$Y^{(i)}(\lambda)=\frac{1}{M}\sum_{k=0}^{M-1}x^{(i)}(k)\exp(-j2\pi k\lambda/M) \qquad \lambda= 0,1,...,M/2$$

$$i = 1,2,...,K.$$

c) In general $M=M_1*N_0$, where M_1 is assumed to be a positive odd integer $(M_1=2L_1+1)$. Since M is even and M_1 is odd, it should be compromised over the value of N_0 (closest over the triangular region $0\le\lambda_2\le\lambda_1$, $\lambda_1+\lambda_2\le N_0/2$).

$$b_i(\lambda_1,\lambda_2)=\frac{1}{\Delta_0{}^2}\sum_{k_1=-L_1}^{L_1}\sum_{k_2=-L_1}^{L_1}Y^{(i)}(\lambda_1+k_1)Y^{(i)}(\lambda_2+k_2)Y^{(i)*}(\lambda_1+\lambda_2+k_1+k_2)$$

For the special case where no averaging is performed in the bispectrum domain, $M_1=1$, $L=0$ and therefore

$$b_i(\lambda_1,\lambda_2)=\frac{1}{\Delta_0^{\,2}}Y^{(i)}(\lambda_1)Y^{(i)}(\lambda_2)Y^{(i)*}(\lambda_1+\lambda_2)$$

d) The bispectrum estimate of the given data is the average of the K pieces

$$B_D(\omega_1,\omega_2)=\frac{1}{K}\sum_{i=1}^{K}b_i(\omega_1,\omega_2)$$

where

$$\omega_1=\left(\frac{2\pi f_s}{N_0}\right)\lambda_1 \quad \textit{and} \quad \omega_2=\left(\frac{2\pi f_s}{N_0}\right)\lambda_2$$